INFORMATION TO USERS

This manuscript has been reproduced from the microfilm master. UMI films the text directly from the original or copy submitted. Thus, some thesis and dissertation copies are in typewriter face, while others may be from any type of computer printer.

The quality of this reproduction is dependent upon the quality of the copy submitted. Broken or indistinct print, colored or poor quality illustrations and photographs, print bleedthrough, substandard margins, and improper alignment can adversely affect reproduction.

In the unlikely event that the author did not send UMI a complete manuscript and there are missing pages, these will be noted. Also, if unauthorized copyright material had to be removed, a note will indicate the deletion.

Oversize materials (e.g., maps, drawings, charts) are reproduced by sectioning the original, beginning at the upper left-hand corner and continuing from left to right in equal sections with small overlaps. Each original is also photographed in one exposure and is included in reduced form at the back of the book.

Photographs included in the original manuscript have been reproduced xerographically in this copy. Higher quality 6" x 9" black and white photographic prints are available for any photographs or illustrations appearing in this copy for an additional charge. Contact UMI directly to order.

UMI®

Bell & Howell Information and Learning
300 North Zeeb Road, Ann Arbor, MI 48106-1346 USA
800-521-0600

Wind-Induced Dispersion of Building Exhaust in an Urban Environment: a Full-Scale and Wind-Tunnel Study

Wei Xuan

A Thesis

In

The Department

of

Building, Civil and Environmental Engineering

Presented in Partial Fulfillment of the Requirements

for the Degree of Master of Applied Science at

Concordia University

Montreal, Quebec, Canada

March 1999

National Library
of Canada

Acquisitions and
Bibliographic Services

395 Wellington Street
Ottawa ON K1A 0N4
Canada

Bibliothèque nationale
du Canada

Acquisitions et
services bibliographiques

395, rue Wellington
Ottawa ON K1A 0N4
Canada

Your file Votre référence

Our file Notre référence

0-612-39097-7

Canada

ABSTRACT

Wind-Induced Dispersion of Building Exhaust in an Urban Environment: a Full-Scale and Wind-Tunnel Study

Wei Xuan

The reingestion of toxic or odorous gases exhausted from rooftop stacks may be a cause of indoor air quality problems of a building. In order to avoid such problems, certain precautions should be taken during the design period. One of the current engineering practices is to evaluate the exhaust dispersion using ASHRAE dispersion models. As another alternative, a wind tunnel study can be carried out to predict peak concentrations at critical locations.

However, neither ASHRAE models nor wind tunnel modeling have been thoroughly validated with full-scale data. For the purpose of evaluating empirical formulas and wind tunnel modeling techniques, four field tests on the roof of the Hall Building of Concordia University and a wind tunnel study have been carried out. The influence of various parameters on the dispersion process were investigated. These included the exhaust momentum ratio, stack location, stack height and building shape. Flow visualization was performed as well to determine the flow pattern around buildings.

Several results were drawn from the current study: 1) the ASHRAE models generally provide reasonable prediction of minimum dilution (D_{min}) with some notable exceptions. 2) In general, wind tunnel results compared well with the full-scale data; however, for receptors close to the stack, the wind tunnel overestimates D_{min}. 3) Both wind tunnel and field results indicate that D_{min} is significantly affected by the exhaust momentum ratio (M); wind tunnel tests with the isolated building do not show this dependence on M. 4) Roof level concentration can be reduced by increasing the stack height. 5) Building shape has a considerable influence on rooftop flow patterns.

ACKNOWLEDGEMENTS

The author would like to gratefully acknowledge the contribution of:

Dr. T. Stathopoulos and Dr. P.J. Saathoff, for their thorough and patient guidance on performing experiments and composing the thesis, their valuable advice on life and providing financial support through-out the research period;

Dr. H. Wu, for his helpful and kindly guidance at the beginning of the research;

Mr. J. Zilkha, Mr. J. Hrib and Mr. J. Payer for setting up the experimental facilities, constructing the models and other assistance through-out the project.

TABLE OF CONTENTS

LIST OF FIGURES

LIST OF SYMBOLS

A_e	cross-section area of the vent
B_0	empirical constant for initial dilution
B_1	air entrainment parameter
C	contaminant mass concentration at receptor
C_e	contaminant mass concentration in exhaust
C_r	contaminant concentration at roof level on the plume axis
D	i) dilution factor
	ii) dimension of the upwind face
D_0	initial dilution
D_{crit}	critical dilution factor at roof level for uncapped vertical exhaust at critical wind speed U_{crit} for given distance S and stack height h_s
$D_{crit.0}$	critical dilution factor at roof level for uncapped vertical exhaust with zero stack height at critical wind speed $U_{crit.0}$ for given distance S
D_{min}	minimum dilution factor D at given wind velocity for all exhaust locations at same distance S from intake
Fr	Froude number
H	building height
H_c	maximum recirculation cavity height
I_u	turbulence intensity

L	cube along-wind dimension
L_c	recirculation cavity length
M	exhaust momentum ratio
Q	contaminant volumetric release rate
Q_0	initial entrainment at the source
Q_e	total exhaust volumetric flow rate
R	i) scaling length ii) radius of exhaust plume with uniform concentration profile
R_0	effective initial plume radius
R_e	radius of the exhaust
Ri	Richardon number
Re_b	building Reynolds number
Re_s	stack Reynolds number
S	stretched string distance
T	absolute temperature
U	mean wind velocity
U_{crit}	critical wind speed that produces smallest minimum dilution factor D_{crit}
$U_{crit.0}$	critical wind speed that produces smallest minimum dilution factor $D_{crit.0}$ for flush vent
U_H	wind speed at building height

U_g	gradient wind speed
W_e	stack emission velocity
W	width of the building
Y	height-to-spread parameter
Z	height above the ground-level
Z_g	gradient height
d	effective exhaust stack diameter
g	gravitational acceleration
h	plume height from centerline
h_s	stack height
Δh	the height of plume rise
Δh_f	the height of final plume rise
u, v, w	denote wind speed components on x, y and z directions
v_a	entrainment velocity of ambient air into the exhaust plume
x, y, z	denote cartesian coordinates
z_0	roughness length
α	i) power law exponent
	ii) building shape parameter (Halitsky)
	iii) entrainment constant

β	i) capping factor
	ii) entrainment constant for internal self-generated turbulence
δ	boundary layer depth
θ	wind incidence angle
μ	dynamic viscosity of the air
ν	kinematic viscosity of the air
ρ_a	ambient air density
ρ_e	exhaust gas density
σ	standard deviation
σ_u	standard deviation of the mean wind speed
σ_s	standard deviation of the plume width in x direction
σ_y	standard deviation of the plume width in y direction
	standard deviation of the plume width in z direction
σ_θ	standard deviation of wind direction and fluctuations in y direction
σ_ϕ	standard deviation of wind direction and fluctuations in z direction

CHAPTER 1

INTRODUCTION

1.1 General

Wind-induced dispersion of pollutants around buildings can have a significant impact on both indoor and outdoor air quality. Building exhaust vents may release hazardous or odorous gases and, under certain wind conditions, contaminate fresh air intakes of the building or surrounding buildings. The reingestion of the building exhaust can cause serious indoor air quality problems, particularly for industrial facilities and institutional laboratories, which tend to have many emission sources. Thus, it is important to take certain precautions when designing the building air inlets and exhaust vents. In this regard, a thorough understanding of atmospheric dispersion can be beneficial in reducing the probability of reingestion of building exhaust.

One of the basic considerations when designing the building exhaust system is that exhausted gases should not be reingested through fresh air intakes. For example, the Quebec regulation regarding the work environment quality stipulates that fresh air intakes must be located so that no air already evacuated from an establishment is reintroduced [S-2.1, r.15 (1994)]. Similarly, another design consideration is that exhaust gases should not adversely affect air quality in areas of public access.

A large number of parameters that affect the atmospheric dispersion around buildings must be taken into account, in order to ensure the satisfaction of the above design criteria.

Some parameters, like stack height and location, emission velocity, intake location and building configuration, are controllable, to some extent. On the other hand, other parameters, such as wind speed, wind direction, atmospheric stratification and upstream topography, are uncontrollable. Moreover, it should be noted that wind conditions obtained at a nearby meteorological station might not correctly represent the real wind climate in the vicinity of the building of interest.

As has been proved by previous studies, a high stack can significantly reduce pollutant concentrations at roof and ground level. However, due to aesthetic considerations, mini-chimneys and flush vents are still widely adopted by designers, especially in an urban environment. As a consequence, a number of problems may result, such as the reentry of odorous or hazardous pollutants and the blackening or deterioration of building facades. Tremendous effort has been made by many researchers to cope with such problems. The dilution of building exhaust from rooftop stacks has been extensively studied for about 30 years. In general, three methods are considered feasible for estimating the concentration at roof level and in the near wake region from a rooftop stack.

First, the maximum concentration value can be acquired using semi-empirical diffusion equations recommended by American Society of Heating, Refrigerating and Air Conditioning Engineers [ASHRAE (1997)]. These models estimate the minimum dilution, D_{min}, (i.e. the ratio of the emission concentration to the maximum concentration at a receptor) as a function of the shortest distance from a stack or vent, taking into account the parameters of wind speed, exhaust velocity, exhaust face area and building generated turbulence. For general dilution estimation, ASHRAE models can be considered as the most economical and simplest approach. However, for buildings with

complex upstream geometry, the equations may not produce accurate estimates of D_{min}. The ASHRAE formulas are presented in detail in section 2.3 and application results are discussed in Chapter 4.

The second method for evaluating the dispersion of building exhaust is the full-scale investigation, which can be carried out to obtain accurate dilution data at specific locations. Although this method reveals the actual dispersion processes best, it has many serious difficulties, such as varying wind conditions and high cost due to the use of significant amount of labor, material and time. This explains why relatively few field studies have been performed. Previously full-scale tests are reviewed in Chapter 2 and detailed field test procedures and the results of the current study can be found in Chapter 3 and Chapter 4, respectively.

The third alternative for investigating building exhaust dispersion is the wind tunnel study. Generally, if most of the modeling criteria are satisfied, this method is expected to give relatively accurate predictions of exhaust dilutions around the building. This approach is especially preferred when the upstream topography may have a significant influence on the flow patterns around the building of interest. The advantages of a wind tunnel study are obvious: 1) it is not affected by exterior weather conditions; 2) the same experiment can be repeated easily; 3) it is convenient to test and compare several design alternatives. It should be noted, however, that the validity of wind tunnel results, in terms of dispersion of exhaust from buildings, has not been thoroughly proved with full-scale data yet.

In the future, it may be possible to numerically compute the building exhaust diffusion using Computational Fluid Dynamics (CFD) methods. Many research works have been done to establish and improve the models used in the CFD methods. Presently, CFD methods based on a k-ε turbulence model are widely accepted [Selvam and Huber (1995) and Kot (1989)]. The stochastic models can manipulate inhomogeneous turbulence and unsteadiness, but more powerful computers and extra statistical information are necessary [Kot (1989)]. No matter what model is used in the numerical simulation, the results need to be validated by comparing with either wind tunnel or field data.

1.2 Purpose of the study

Compared with full-scale studies, ASHRAE models and wind tunnel studies are more economical methods for dilution estimation of building exhaust. However, neither of these two methods has been validated with full-scale data. Some case studies have been carried out to compare the ASHRAE formulas' predictions with wind tunnel measurements. However, the results of the assessments have been contradictory. For instance, Petersen and Wilson (1989) found that ASHRAE models tend to underestimate the dilution value when the exhaust velocity is high or the exhaust face area is large. On the other hand, Perera et al (1991) and Schuyler and Turner (1989) have found that the ASHRAE equations may provide unconservative dilution estimates in some cases. Therefore, the first purpose of current study is to evaluate both ASHRAE models and wind tunnel modeling techniques with field study results.

Secondly, previous studies have shown that building shape significantly affects the flow pattern around the building. The ASHRAE formulas are largely based on wind tunnel tests carried out with low-rise buildings of various shapes [Wilson and Winkel (1982) and Wilson and Chui (1985)]. Although cubical models were included in these studies, the results obtained with this shape generally do not compare well with the results obtained with other shapes. For cubical buildings, the flow separation region covers the entire roof [Wilson (1979)] and consequently, the plume emitted from a rooftop flush vent or short stack is trapped in this region. The dispersion process, in this case, is very complicated. As a result, the applicability of ASHRAE models for cubical buildings is questionable. It is expected that the results of current study may answer part of the question.

The last purpose of the present study is to provide guidelines for minimizing the risk of reentry of building exhaust, especially for the cubical building configuration. Numerous wind tunnel experiments have been performed in the current study to investigate the influence of exhaust momentum ratio, stack height and stack location. These wind tunnel data could be used as a valuable reference for determining stack parameters when designing ventilation systems.

1.3 Thesis Organization

In the present study, results of four full-scale tests performed on the roof of the Hall Building of Concordia University in downtown Montreal have been analyzed. These tests were later simulated in the boundary layer wind tunnel at the Building

Aerodynamics Lab in the Centre for Building Studies of Concordia University. The effects of exhaust momentum ratio, stack height, stack location and building configuration were examined by measuring the dilution value at selected tappings. In order to reveal the influence of upstream buildings on the flow pattern around the object building, flow visualization was conducted for two model assemblies—with and without upstream buildings.

The present study is presented as follows:

Chapter 2 reviews the basic theories, ASHRAE models and previous research associated with the current study.

Chapter 3 introduces the experimental methodology used in the field and wind tunnel tests.

Chapter 4 presents the experimental results of both full-scale and wind tunnel tests and discusses the comparison of full-scale data with ASHRAE predictions and wind tunnel measurements.

Chapter 5 draws the conclusions of the current study. It provides guidelines for stack design for the particular case of a cubical building and gives recommendations for future research.

CHAPTER 2

LITERATURE REVIEW

2.1 General

Wind-induced dispersion of building exhaust has been extensively studied for over 30 years. Although several mathematical formulas exist for estimating the diffusion downstream the source, the complexity of real airflow around buildings brings out new questions constantly concerning the results provided by those formulas. A number of full-scale tests as well as wind tunnel studies were carried out for the purpose of establishing or improving the atmospheric dispersion models. Based on the experimental results, a few dispersion models have been developed. Three of the models, which are widely used in today's engineering practice, will be discussed in detail hereafter and related experimental works will be reviewed as well.

2.2 Gas diffusion theory

Atmospheric diffusion is caused by turbulence. Pasquill (1962) defines turbulence as "that quality which is manifested in the random character of the velocity of a fluid (say at a fixed point as a function of time), in contrast to the constancy of such a velocity in steady stream-lined flow, or to the recognizable periodicity of a wave motion".

2.2.1 Methods of turbulence analysis

The turbulent diffusion can be described in two basic ways: Eulerian approach and Lagrangian approach. In an Eulerian system, the velocities at all locations within a fixed coordinate system at a given instant are taken into account. The mass conservation is the basis on which the concentration equation is derived by Eulerian approach. In a Lagrangian system, the motion of a specific particle or element is considered as the basis for the concentration equation. The mean concentration at a certain position is given by the sum of a group of particles' probability densities. Nevertheless, the exact solution for concentration calculation in turbulent flow is not available by using either of above approaches. Thus, more effort on other theoretical or empirical methods is needed in order to solve the diffusion problem.

2.2.2 Gaussian model for dispersion estimation

The Gaussian plume model is one of the most commonly used methods for estimating the plume dispersion downstream a continuous source. The major reasons for using the Gaussian model are that it well represents the random nature of the turbulence and the solution can be acquired easily by mathematically operations.

Considering a continuous source with volume flow rate Q at effective height H, as shown in Figure 2-1, the concentration C at a certain location (x, y, z) within the coordinate system is given by

$$C(x,y,z;H)=\frac{Q}{2\pi u\sigma_y\sigma_z}\exp\left[-\frac{y^2}{2\sigma_y^2}\right]\left\{\exp\left[-\frac{(H-z)^2}{2\sigma_z^2}\right]+\exp\left[-\frac{(H+z)^2}{2\sigma_z^2}\right]\right\} \qquad (2.1)$$

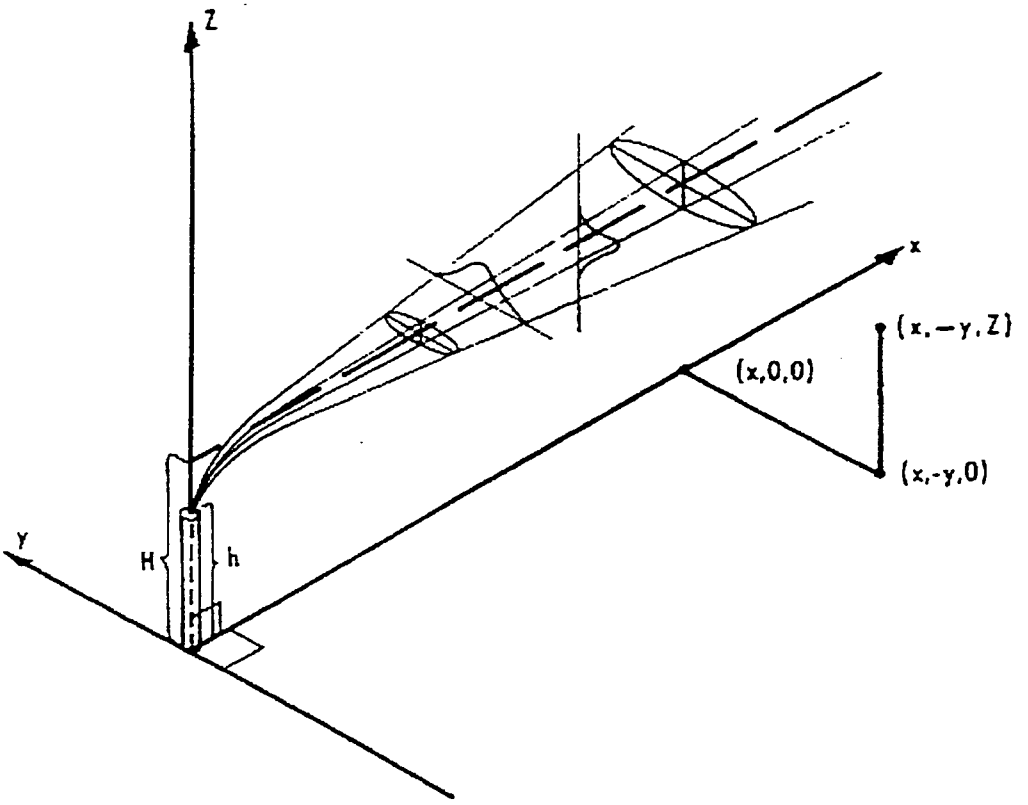

Figure 2-1 Coordinate system of Gaussian model [Turner (1994)]

where u is the mean wind speed at release point, σ_y and σ_z are the standard deviation of the concentration distribution in the crosswind direction and vertical direction respectively at the downwind distance x.

Several constraints should be satisfied when using the Gaussian model [Turner (1994)]:

1) Wind conditions must be stationary (i.e. mean wind speed and mean wind direction are constant);

2) The turbulence must be isotropic and homogeneous;

3) The mass is conserved within the plume;

4) The concentration profiles in both crosswind and vertical directions are well described by the Gaussian distribution.

Huber (1982) suggested that the Gaussian model is generally appropriate for dispersion estimation around buildings based on the wind tunnel results. However, the real airflow around buildings is so complicated that most of above assumptions are violated.

2.3 Dilution estimation models

The concentration of a pollutant in a plume can be expressed in terms of the dilution factor: $D=C_e/C$, where C_e is the contaminant concentration in the exhaust and C is the contaminant concentration at a receptor. Several semi-empirical models have been developed to estimate the minimum dilution in a plume as a function of downwind

distance and the exhaust parameter. The minimum dilution factor D_{min} has been employed as the quantity that shows the reduction in concentration between exhaust source and any receptor or given point around the building. It is defined as:

$$D_{min} = C_e / C_{max} \qquad (2.2)$$

where C_{max} is the maximum contaminant concentration at a receptor.

When determining the minimum dilution, two important factors should be taken into account: stretched string distance S and effective stack height h_s. The stretched string distance is defined as the shortest distance between building exhaust and intake location. The effective stack height is referred to as the stack height above any large roof barrier, such as a penthouse. However, since the following models only considered short stacks or flush vents with zero stack height, h_s was not used as a parameter in either of three models that will be discussed hereafter.

2.3.1 Halitsky model

Halitsky (1963) conducted a series of wind tunnel experiments in the New York University and developed the following model on the basis of his experimental results:

$$D_{min} = [\alpha + 0.11(1 + 0.2\alpha)\, S/A_e^{0.5}]^2 \qquad (2.3)$$

where S is the stretched string distance, A_e is the exhaust area and α is a parameter related to building shape, wind direction and exhaust momentum ratio. Along the plume centerline, where the minimum dilution occurs, $\alpha = 1$ is assumed to be appropriate. A

buoyant emission or high stack may increase the dilution on building surfaces, where $2<\alpha<20$ is recommended.

Since this model was developed based on wind tunnel studies that were only carried out on isolated block-shape buildings and with a non-turbulent flow, its applicability on buildings in a complex surrounding environment and high atmospheric turbulence has been questioned.

2.3.2 Wilson-Chui model

Wilson and Chui (1985, 1987) investigated the influence of changing wind direction on dilution and modified the previous minimum dilution model developed by Wilson (1983). The Wilson-Chui model was expressed as:

$$D_{min} = \left[D_0^{0.5} + \alpha \left(\frac{\pi}{2} \right)^{0.5} \left[\frac{U_H S^2}{Q_e} \right]^{0.5} \right]^2 \qquad (2.4)$$

where D_0 is the initial dilution, U_H is the wind speed at exhaust height, S is the stretched string distance, Q_e is the total exhaust volume flow rate and α is the entrainment constant.

One of the important contributions of the Wilson-Chui model is that it introduced "the concept of initial dilution" [Wilson and Chui (1985)]. Since the traditional Gaussian plume model only considered plume rise, it gives unrealistically high dilution near the vent. In the new theory for initial dilution, instead of accounting for plume rise, the initial dilution model accounted for an initial entrainment Q_0 at the source. As shown in Figure 2-2, the plume from a surface vent is rapidly bent over by the wind and a large

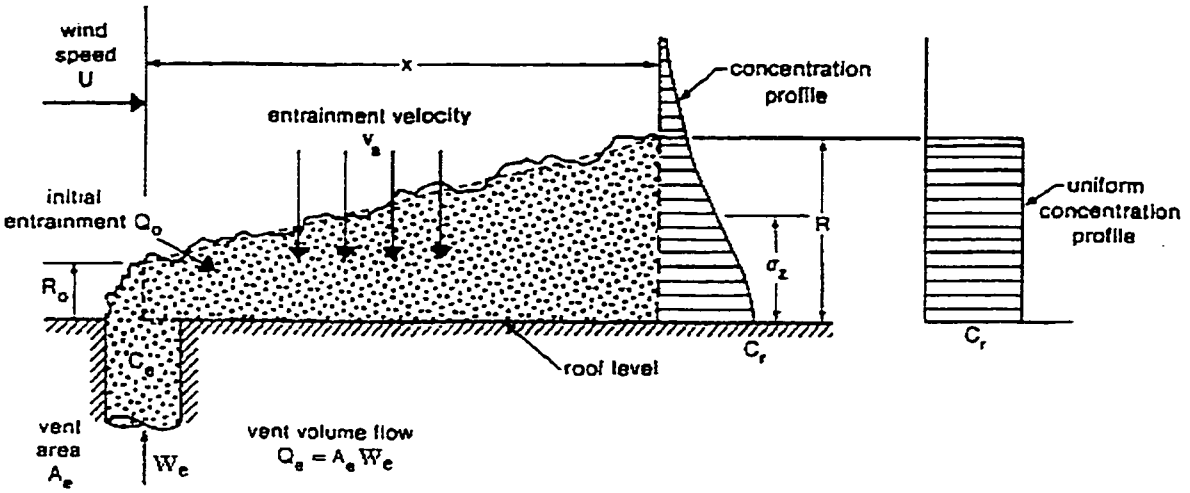

Figure 2-2 Dilution of exhaust from a flush vent [Wilson and Chui (1985)]

amount of ambient air is entrained at the same time. Wind tunnel results showed that the initial dilution model, by considering the added initial entrainment, produced much more accurate estimation of dilution near source than the Gaussian model did [Wilson and Chui (1985)]. The initial dilution D_0 is given by

$$D_0 = 1 + Q_0 / Q_e = 1 + B_0 M^2 \qquad (2.5)$$

where B_0 is the empirical constant for initial dilution and M is the exhaust momentum ratio and is defined as

$$M = (\rho_e / \rho_a)^{0.5} W_e / U_H \qquad (2.6)$$

If the exhaust gas density ρ_e could be assumed to be the same as ambient air density, the M would simply be the ratio of exhaust velocity W_e to the approaching wind speed U_H at stack height.

According to the wind tunnel data of Wilson and Chui (1985), $\alpha = 0.2$ and $B_0 = 7$ were recommended as the appropriate values for the minimum dilution equation. One constraint regarding the initial dilution that ought to be noticed is that equations 2.4 and 2.5 should be only used when $S>10\sqrt{A_e}$, where A_e is the effective area of exhaust. This is because the initial dilution occurs over a distance of several stack diameters, but not immediately at the stack exit. Based on the wind tunnel measurements, Wilson and Chui (1985) suggested the above constraint.

2.3.3 Wilson-Lamb model

Wilson-Lamb (1994), using field data of Lamb and Cronn (1986), revised the Wilson-Chui model. The basic formulation of the Wilson-Lamb model is the same as the Wilson-Chui model, which is given by

$$D_{min} = \left(D_0^{0.5} + D_d^{0.5}\right)^2 \qquad (2.7)$$

where initial dilution D_0 and distance dilution D_d can be obtained by

$$D_0 = 1 + Q_0 / Q_e \qquad (2.8)$$

$$D_d = B_1 \frac{U_H S^2}{Q_e} \qquad (2.9)$$

Wilson and Lamb (1994) proposed two major modifications for the minimum dilution model. First, a revised equation for initial dilution was suggested, which is

$$D_0 = 1 + 13\ M \qquad (2.10)$$

Since the previous empirical formula $D_0 = 1 + 7\ M^2$ was based on wind tunnel data with a range of M-values from 0.1 to 2.0 and with roof-level intakes, it may not provide an accurate prediction for M>2.0 or different level intake locations. By using the standard entrainment assumption that $v_a=\beta d(\Delta h)/dz$, where β is the internal self-generated turbulent entrainment constant and Δh is the height of the plume rise, the volume flow of a fully bent-over plume at its final rise height Δh_f is $Q_0=\pi U_H(\beta\Delta h_f)^2$. As the exhaust volume flux is $Q_e=\pi W_e R_e^2$, where R_e is the radius of the exhaust stack, the original initial dilution equation can be written as

$$D_0 = 1 + \frac{U_H}{W_e}\left(\frac{\beta \Delta h_f}{R_e}\right)^2 \qquad (2.11)$$

With β=0.6 and Δh_f=6.0$R_e W_e/U_H$ from Briggs (1975), equation (2.10) is obtained.

Values of D_0 obtained with equation 2.10 are significantly lower than those obtained with the Wilson-Chui model, when the M-value is higher than 2. This is not surprising, since the Wilson-Chui formula takes the "apparent dilution" due to plume rise into account while the Wilson-Lamb formula only considers the actual dilution due to air entrainment. Nevertheless, Wilson and Lamb (1994) suggest that equation 2.10 may underestimate D_0, based on field and wind tunnel data.

The other major change to the Wilson-Chui minimum dilution model suggested by Wilson and Lamb (1994) concerns the distance dilution parameter B_1, which is related with the entrainment constant α by

$$B_1 = \pi \alpha^2 / 2 \qquad (2.12)$$

By using the Gaussian plume model, equation (2.12) can be theoretically converted into

$$B_1 = \pi \frac{v}{U_H}\frac{w}{U_H} \approx \pi \sigma_\theta \sigma_\phi \qquad (2.13)$$

where v and w are the turbulence velocity components in the crosswind and vertical directions, σ_θ and σ_ϕ are the standard deviations of the horizontal and vertical wind directions.

Equation 2.13 takes into account both horizontal and vertical wind direction standard deviations. Wilson and Lamb (1994) analysed results of previous wind tunnel studies by Wilson and Chui (1985) and the field study by Lamb and Cronn (1986) and concluded that the distance dilution is mainly dominated by upstream atmospheric turbulence (t_a). They suggest that t_a accounts for about 60% of total distance dilution, the remainder being caused by building-generated turbulence (t_b).

Saathoff and Stathopoulos (1997) have questioned the methodology of the Wilson-Lamb study. They contend that the influence of atmospheric turbulence on dilution cannot be determine accurately using the Lamb and Cronn field data because of the significant influence of other factors, such as stack height and momentum ratio.

Nevertheless, Wilson and Lamb (1994) and Wilson (1997) show that the Wilson-Lamb model predictions of D_{min} compare reasonably well with the field data of Lamb and Cronn (1986). Likewise, Ramsdell and Fosmire (1997) found that the Wilson-Lamb model provided an acceptable lower bound to field dilution measurements obtained at a number of nuclear reactor facilities.

2.3.4 Critical dilution estimation with zero stack height

Building exhaust dispersion is critically affected by the wind. If the wind speed is very low and the exhaust speed is high, the plume rise will be large, causing a high dilution at roof level, especially near the stack. Likewise, if the wind speed is very high, the exhaust plume will be stretched longitudinally, resulting in relatively high dilution at roof level. Between these two extremes exists a critical wind speed, U_{crit} that produces the minimum dilution at a particular location. Note that U_{crit} will vary with distance from the stack. By

finding the absolute minimum dilution in formulas 2.7-2.10, the critical wind speed for a flush vent can be given by:

$$U_{crit,0} = \frac{3.6\,W_e}{S}\left(\frac{A_e}{B_1}\right)^{0.5} \qquad (2.14)$$

The critical dilution at this wind speed and distance, S, is given by: [ASHRAE (1997)]

$$D_{crit,0} = \frac{(1+26\,W_e/U_{crit,0})^2}{1+13\,W_e/U_{crit,0}} \qquad (2.15)$$

Note that the subscript 0 of D_{crit} and U_{crit} denotes a flush vent. In the present study, a comparison of field data with the critical dilution curve has been made and results are presented in Chapter 4.

2.3.5 Critical dilution estimation for stack design

ASHRAE (1997) recommends a model for estimating the effect of stack height on critical dilution, D_{crit}. This model can be used during the design process to determine the optimum stack height, if the worst-case dilution (i.e. critical dilution) factor can be specified based on health limits or odor thresholds.

Based on the Gaussian model, ASHRAE (1997) suggests the following formula for the standard deviation of a 10-minute averaged vertical plume spread: σ_z=0.093S, where S is the distance from the source. A height-to-spread parameter, Y, is defined as

$$Y = 28.9\,h_s^2/S^2 \qquad (2.16)$$

The critical wind speed at which the critical dilution is observed is given by

$$U_{crit} = U_{crit,0} / [(Y+1)^{0.5} - Y^{0.5}] \qquad (2.17)$$

where $U_{crit,0}$ is the critical wind speed for a flush vent (i.e. zero stack height) given by equation 2.14. As a consequence, the critical dilution for a particular stack height is given by

$$D_{crit} = \frac{D_{crit,0}\ U_{crit}}{U_{crit,0}} \exp\left[Y + Y^{0.5}(Y+1)^{0.5}\right] \qquad (2.18)$$

Note that equation 2.18 assumes an averaging time of 10-minutes, as in the minimum dilution formulas. The predictions of this model compare well with field data of Wilson and Lamb (1994) [ASHRAE (1997)]. In the present study, the effect of stack height was examined by carrying out wind tunnel experiments and the data were compared to D_{crit} values obtained with equation 2.18. These results are presented in Chapter 4.

2.4 Flow pattern studies

2.4.1 Flow patterns around a rectangular shaped building

The flow around even the simplest building shape tends to be 3-dimensional in nature and consequently very complex. Further complications arise due to the presence of other structures. Although most buildings are located near other buildings, most of the fundamental knowledge about building aerodynamics has been obtained with isolated buildings.

The flow around cubical buildings has been extensively studied in a number of wind tunnel and field studies, such as Castro and Robins (1977), Hunt et al. (1978), Wilson (1979) and Ogawa et al (1983).

As drawn schematically in Figure 2-3, the approaching wind profile is a shear flow. There is a stagnation zone at about two thirds of the building height above ground. As the wind hits the windward face, part of the flow goes over the downwind surfaces (i.e. both sides and roof surface) while part of the flow moves downward and generates a vortex at the lower part of the windward face. If the alongwind length L of the building is long enough, the flow may reattach on the roof and sides. Recirculating streamlines can be found in separation zones, as shown in Figure 2-3. Behind the building is a cavity zone of negative pressure, where the separation streamline reattaches to the ground surface.

2.4.2 Estimation of recirculation zone dimensions

As introduced previously, dilution models are very useful in predicting the critical dilution values likely to occur at a particular location. However, detailed information regarding the wind climate, the exhaust gas composition and flow rate is necessary when applying these methods for design purposes. As an alternative approach, particularly when the wind data and exhaust specifications are difficult to obtain, Wilson (1979) proposed a relatively simple method to estimate the dimensions of the high turbulence regions above a building roof. With this method, stacks and intakes can be located at appropriate places to avoid the effect of high atmospheric turbulence.

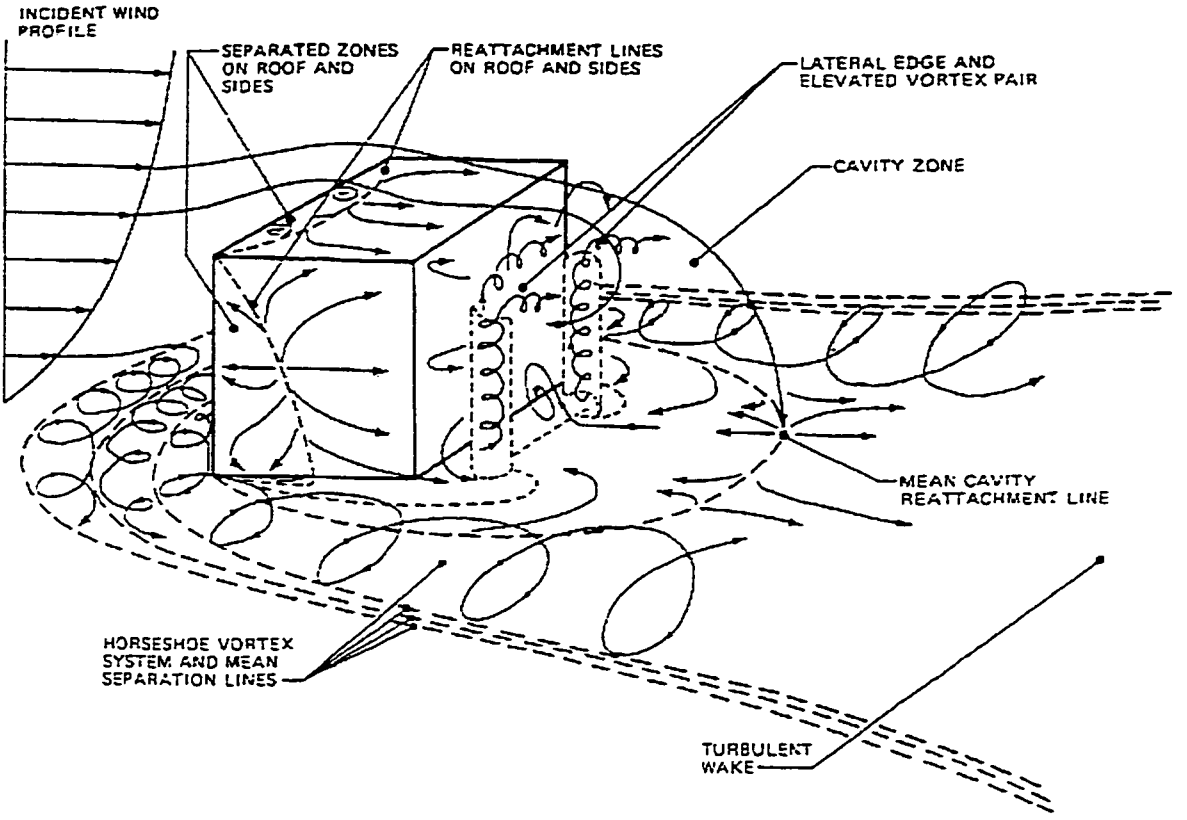

Figure 2-3 Flow patterns around a rectangular building model [Hosker (1979)]

Figure 2-4 illustrates the cross-section of different flow zones with the wind normal to the upwind surface. Due to the separation of the approaching wind at the upwind edge, a cavity is created and a reverse flow can be found in this region. If the downwind roof dimension is long enough, the separation flow reattaches the roof surface and generates a closed region called recirculation zone. The turbulence level in this region is very high and if the exhaust gas is emitted within the recirculation zone, a uniform high concentration will be detected. The boundaries of zone II and zone III are somewhat subjective. Generally, the turbulence levels decrease and downwash flows become insignificant as the measurement location moves towards outside zones.

Wilson (1979) found that both the building height and the upwind face width has an effect on the size of the recirculation zone. He suggested a scaling length, R, which takes into account the height and length of the separation zone, be defined as:

$$R = D_{small}^{0.67} \cdot D_{large}^{0.33} \qquad (2.19)$$

where D is the dimensions of the upwind face. Consequently, the recirculation cavity length, L_c, and maximum cavity height, H_c, is given by:

$$L_c = 0.9\ R,\ \ H_c = 0.5\ R \qquad (2.20)$$

This method provides a simple and quick estimation of the rooftop flow pattern, which is beneficial in the preliminary design stage.

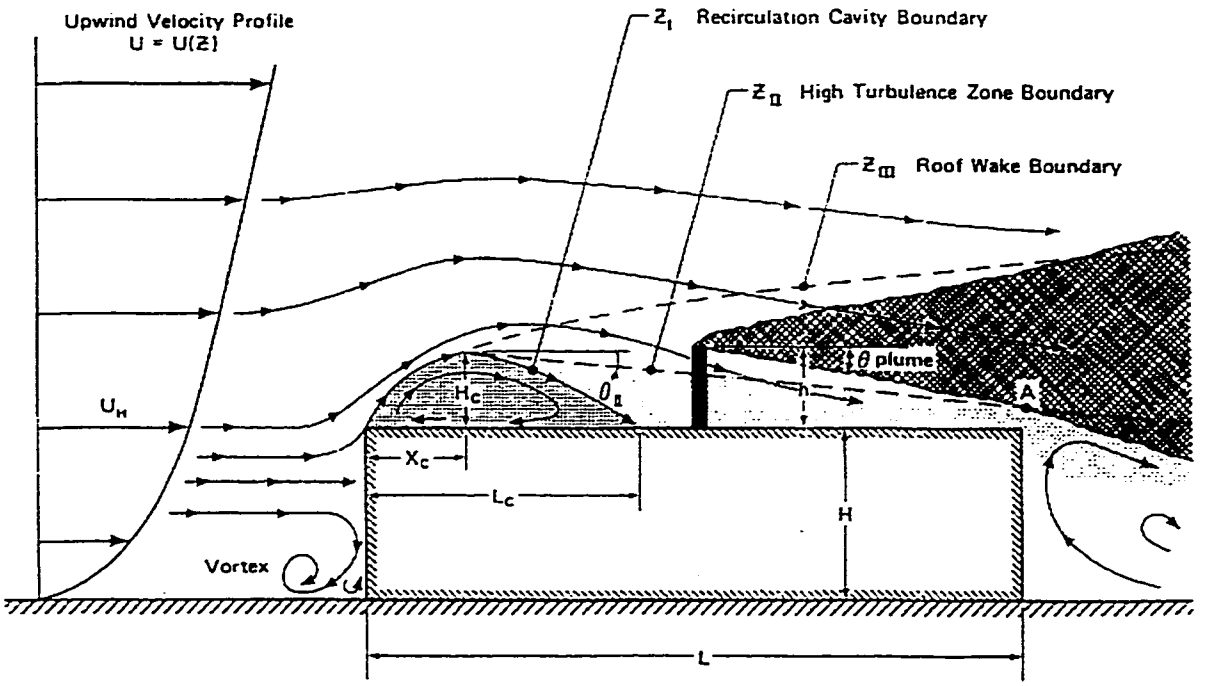

Figure 2-4 Flow regions over a building roof for wind normal to the upwind face [Wilson (1979)]

2.5 Field and wind tunnel studies on pollutant dispersion

A number of field experiments and wind tunnel studies have been performed to evaluate the empirical dispersion models as well as wind tunnel modeling techniques.

2.5.1 Previous field studies

Lam et al. (1985) conducted a tracer gas study at the University of Hong Kong. The sampling period of their test was only 10 seconds. This averaging time is much less than the 10-minute averaging time assumed in the minimum dilution models. Thus, their results may not be suitable for evaluating the dilution models.

Another field test was carried out by Lam and Kot (1993) to evaluate the effect of wind speed on dilution for a single source and receptor pair. Besides the influence of short sample duration, wind direction fluctuation may have affected the validation of experimental data because only one intake location was considered.

Georgakis et al. (1995) carried out 72 full-scale tracer gas tests with stacks of different height and diameter at two buildings at the University of Toronto. The data were used to evaluate eleven minimum dilution models. The Wilson-Chui and Wilson-Lamb models were not included, however. One drawback of the study is that the source and receptor pairs were not always on the same line as the wind direction. Therefore, some of the test data may not be appropriate for model evaluation.

One of the most extensive field studies was performed by Lamb and Cronn (1986), using a chemistry building at Washington State University. A group of stacks with varied

heights and flow rates and an array of rooftop and ground-level receptors were used in the experiment. Results of this study have been analyzed by Wilson and Lamb (1994) as previously discussed. It should be noted that the sampling duration was 1 hour in this study. As a result, an averaging time correction is required in order to evaluate the minimum dilution models. Other possible problems with the data set include the lack of wind stationarity and the influence of stack height.

2.5.2 Previous wind tunnel simulations

2.5.2.1 Wind tunnel and field comparison studies

Although a number of researchers have investigated the accuracy of wind tunnel modeling of atmospheric dispersion, few studies have considered the particular case of near-field dispersion of pollutants from rooftop stacks.

The results of several ground-level source wind tunnel simulations have been found to compare well with field data [Martin (1965), Petersen and Ratcliff (1991), Petersen (1986) and Bächlin et al. (1991)]. Allwine et al. (1980) carried out several wind tunnel simulations of field studies, which were conducted at the Rancho Seco Nuclear Power Station by Start et al. (1977). It was concluded that the wind tunnel results over-estimated ground-level concentrations by a factor of 1.7 on average.

The early wind tunnel simulations of building exhaust diffusion were performed by Halitsky (1963), who introduced the concepts of concentration coefficient and minimum dilution model on the basis of those wind tunnel results. However, the dilution prediction

of Halitsky model were found to be highly conservative [(Munn and Cole (1967), Meroney (1982)]. This was mainly due to the use of non-turbulent flow with uniform mean-velocity profile in the wind tunnel study.

Ogawa et al. (1983) conducted extensive field and wind tunnel studies of the flow and diffusion around a cube. In general, relatively good agreement between full-scale and wind tunnel data were found. Flow visualization experiments showed that the reverse flow region decreased when the upwind turbulence intensity increased.

Higson et al (1994) compared wind tunnel data with the full-scale measurements obtained with a small-scale building. It was found that the highest mean concentrations measured in the field test tend to be overestimated in the wind tunnel experiment. On the other hand, the minimum concentrations were more likely to be underestimated. The possible explanation was proposed as the differences in turbulence scales corresponding to the dimension of the model building.

Saathoff et al. (1996) performed wind tunnel simulations of the field test conducted at Washington State University by Lamb and Cronn (1986). The wind tunnel results were generally within a factor of two of the field data.

2.5.2.2 Fundamental wind tunnel studies

Li and Meroney (1983) conducted a wind tunnel investigation of the dispersion of roof vent exhaust on an isolated cubic-shape building. Three roof stack locations and three building orientations were tested in the study. It was found that wind directions, θ, of 22.5° and 45° produced higher concentrations than a wind direction normal to the front

face (θ=0°). In particular, a secondary peak concentration value was detected at the edge of the near wake at ground level for θ = 45°.

Wilson and Chui (1985) investigated the influences of exhaust momentum ratio and wind direction on minimum dilution in a wind tunnel. The data showed that, for most building shapes, a significant increase in minimum dilution near the exhaust was obtained as the exhaust momentum ratio increased. However, this result did not occur for the cube-shaped buildings. The minimum dilution was found to be insensitive to wind direction, when M is large. This is contrary to Li and Meroney's results obtained with small M.

Thompson (1991) conducted a wind tunnel study to determine concentration distributions on building surfaces and at ground-level for four rectangular buildings with a rooftop exhaust. The largest concentration was found at the downwind edge of the building above the rear recirculation cavity. In general, the concentration measurements were found to be in good agreement with the model predictions of Wilson and Britter (1982).

Wilson and Winkel (1982) investigated the effect of stack height on roof-level pollutant concentrations in the wind tunnel. A simple theoretical model was developed to estimate the reduction of the exhaust concentration due to an increase in stack height. However, it was suggested that when the stack is in or near the flow recirculation region, the formula is not reliable. It was also particularly recommended that the stack should never be located inside the roof recirculation cavity. Unfortunately, for buildings like the Hall Building, unless a very tall chimney is acceptable, placement of the stack in the roof separation region is unavoidable.

Schulman and Scire (1991) carried out a series of wind tunnel tests with four stack heights, four exhaust momentum ratios and two wind directions on a low-rise building (H:W:L = 1:5:5). It was observed that as the exhaust speed and stack height increased, the maximum concentration measurement moved from the rooftop to the far wake of the building model. Regarding the influence of wind direction, even though the largest concentration value occurred with the wind direction of 45°, concentrations with the wind direction of 0° were generally higher.

2.6 Previous flow visualization and digital image processing studies

In wind engineering field, flow visualization has been widely used to study the flow patterns, complement the quantitative estimations and provide guidance for wind tunnel experiments. With the development of computer techniques, digital image analysis is becoming an effective tool in pollutant dispersion studies.

Lee et al (1988) developed a video image analysis system to investigate the vertically integrated concentrations downwind of the building. Smoke was used to visualize the flow and was photographed from above. Image processing provided color-contoured descriptions of the plume, which revealed the vertically integrated concentrations. The image analysis system was calibrated by comparison with concentration measurements. Due to the existence of particular complications, for example the nonlinear relation between smoke intensity and vertically integrated concentration at high smoke intensity levels [Lee et al (1988)], the final image may not be regarded as the true vertically

integrated concentration measurements. However, the application of video image analysis was demonstrated to be very useful in the study of building exhaust diffusion.

Olivari and Babuska (1990) conducted a study of pollutant dispersion in the near wake of a cube using the digital image processing method. The flow was recorded using a high frequency black and white video camera. Similar with Lee's method, the video images were quantified by referencing them with surface concentration measurements. As a result, both qualitative and quantitative results were obtained. Moreover, the digital image analysis method again was proved to be applicable in pollutant dispersion studies.

Wu, Higuchi and Meroney (1991) reviewed the application of digital image analysis in wind engineering studies. Samples were given to illustrate how to use video image processing system (VIPS) to measure the flow velocity and plume dispersion. It was also suggested that an interpretive connection between wind tunnel studies and numerical models may be established using the digital image processing approach.

CHAPTER 3

EXPERIMENTAL METHODOLOGY

3.1 General

As discussed in Chapter 2, both full-scale and wind tunnel experiments have been used in atmospheric dispersion studies. One of the most often used experimental techniques is the measurement of tracer gas concentration. The basic procedure of tracer gas test is composed of three parts: the emission of tracer gas, the collection of air samples at receptors and the analysis of air samples. This method was also employed in the current study.

3.2 Field Tests

Field tests were carried out on Hall Building of Concordia University on four days during the summer of 1997. These tests formed part of a study carried out with the Institut de recherche en santé et en sécurité du travail du Québec (IRSST).

3.2.1 Hall Building Information

The full-scale tracer gas study was performed on the roof of Hall Building, which is one of the major buildings of Concordia University and located in downtown area of Montreal. The Hall Building is approximately a cubical building with a height of 62 m.

A photograph of Hall Building is shown in Figure 3-1. There are several high-rise residential buildings located to the southwest, which was the upwind direction during the field tests. Mount Royal, which is a 233m high hill, is located approximately 500 m west and north of the building.

A few factors were taken into account when choosing the Hall Building for the current study. First of all, many previous studies have been carried out on isolated cubical buildings or models similar in shape to the Hall Building [Li and Meroney (1983) and Ogawa et al. (1983)]. Thus, the present study can complement these previous studies and be used to investigate the effect of upstream buildings on the dilution process. Secondly, the low stack height allows direct comparison with ASHRAE minimum dilution models, which only consider zero stack height. Third, since many laboratories are located in it, the present study may be beneficial for improving the indoor air quality of the Hall Building. The last factor is that the building was easily accessible.

3.2.2 Meteorological Data Acquisition

Meteorological data is crucial in determining the influences of wind direction and exhaust momentum ratio on the dilution of tracer gas. Generally, Dorval Airport, which is located approximately 20 km west of Montreal, is used as the reference location for the wind condition estimation in the Montreal downtown area. As shown in Figure 3-2, the critical wind direction of Montreal is between west and southwest. However, due to the existence of Mount Royal, the frequency and magnitude of westerly winds tend to be reduced in downtown Montreal. The influence of Mont Royal is evident in wind data

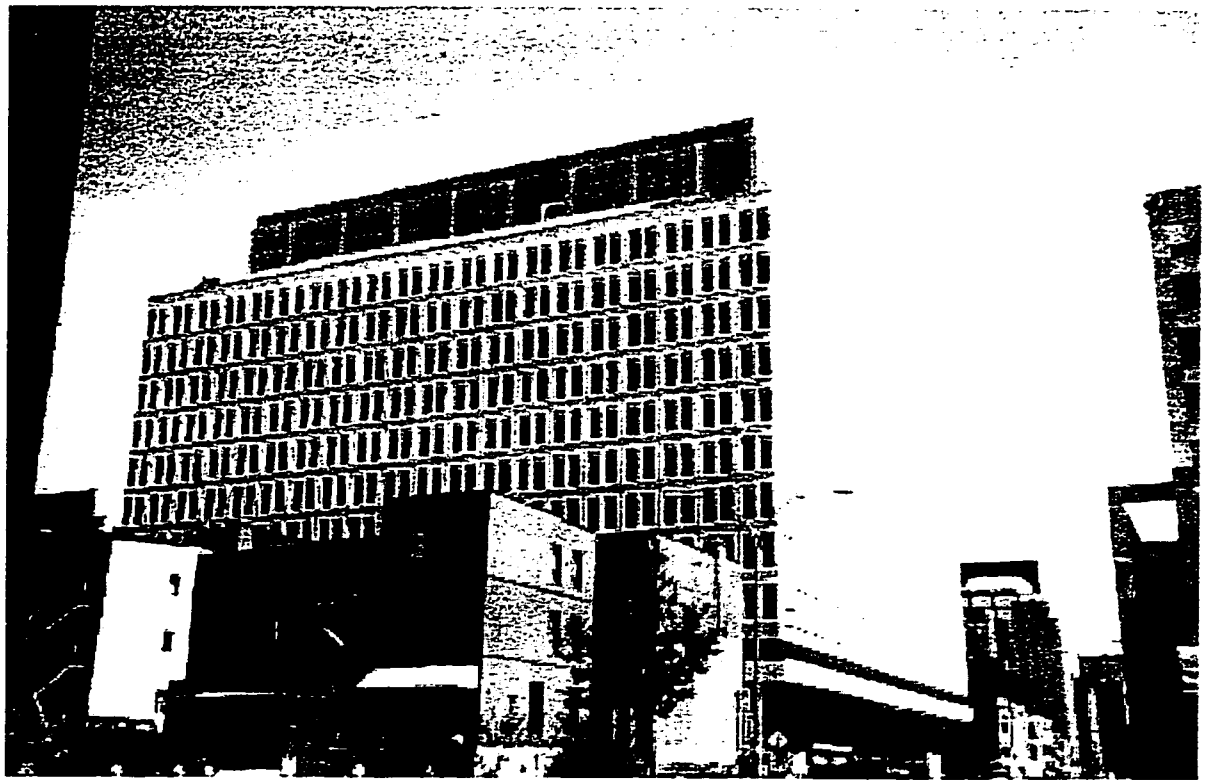

Figure 3-1 The Hall Building viewing from the south west

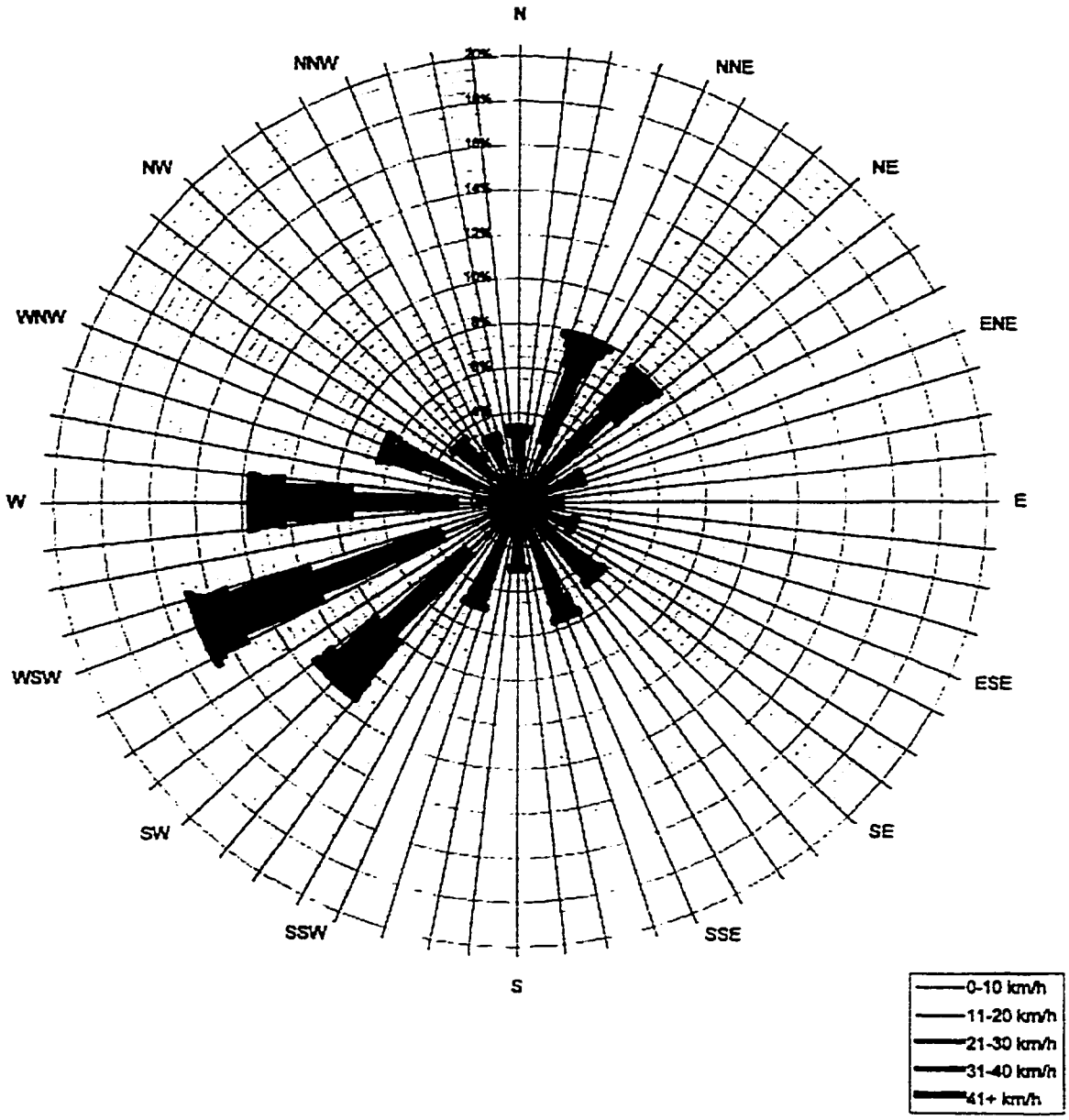

Figure 3-2 Wind rose based on Dorval Airport data

(data adjusted to a height of 300 m)

measured with an anemometer located on a 14-storey building on the campus of McGill University, which is about 1 km northeast of the Hall Building. McGill data shown in Figure 3-3 indicates that the predominant wind direction in the city centre is south-west. Consequently, this wind direction was chosen for field tests.

The Hall Building wind data was obtained using a Gill sonic anemometer, which was mounted at a 7 m height above the roof. The mean and standard deviation of the two horizontal wind components (u, v) and the vertical wind (w) were acquired during the tests. Wind data was also obtained from the Geography Department of Concordia University, which has a Young propeller anemometer placed at a height of 3 m above the roof of Webster Library Building. Figure 3-4 shows the elevation drawing of Hall Building and Webster Library Building from Mackay Street. The relative height of the anemometers can be seen as well in Figure 3-4. Due to the effect of the high-rise buildings located on the south west side of Library Building, the Webster wind speed data needed to be corrected before using it as supplement for the Hall Building data.

Wind conditions for three of the tests were similar: the wind was southwesterly with a mean wind speed higher than 4.5 m/s. This wind speed ensured that atmosphere stability was approximately neutral or slightly unstable [Turner (1994)]. Thus, these tests should correspond to wind tunnel experiments in which the neutral atmosphere is simulated. By restricting the tests to southwesterly wind, the uncertainty of the data was reduced and the plume made contact with a significant portion of the roof.

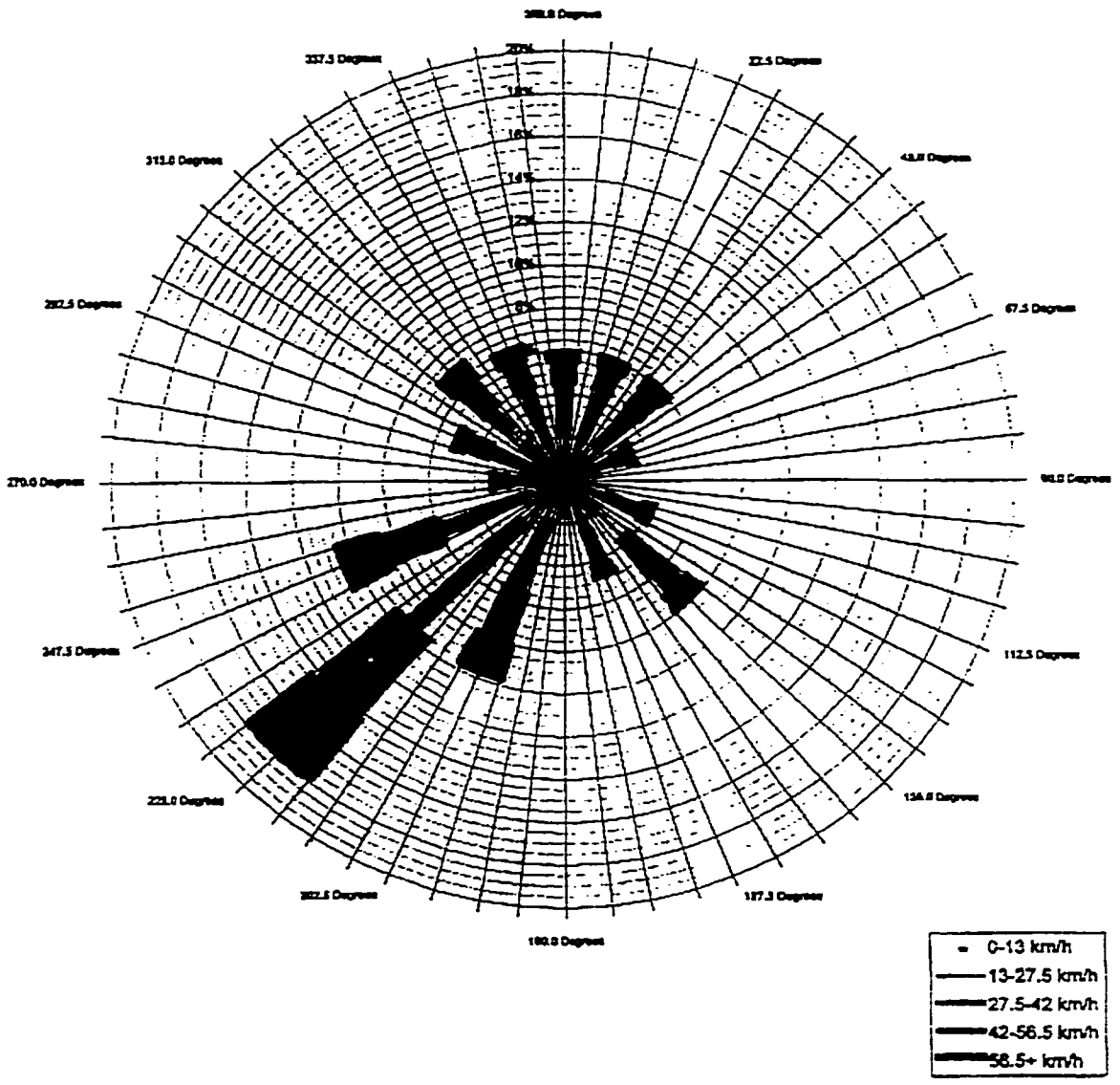

Figure 3-3 Wind rose based on McGill University data (data adjusted to a height of 300 m)

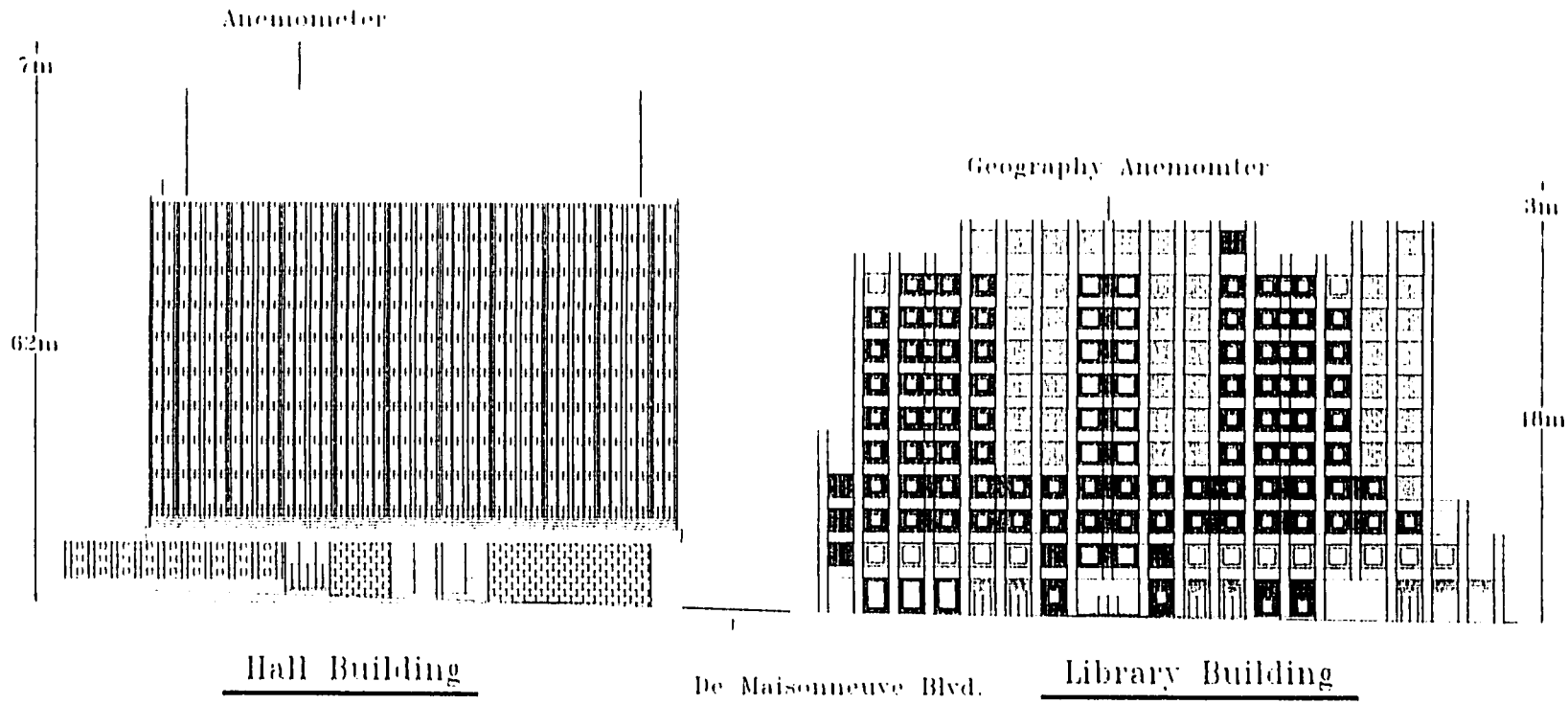

Figure 3-4 Elevation of Hall Building and Webster Library Building from Mackay Street

One of the tests, July 2nd, had quite different wind conditions—low wind speed and variable wind direction. Results of this test are useful for comparison with different cases.

The wind data for the four field tests are listed in Table 3-1. It should be noted that wind data for Test 3 were not obtained from the Hall Building anemometer due to a malfunction of an instrument. Instead, data from the rooftop anemometer on the adjacent Webster Library Building and Dorval Airport were used to estimate the wind conditions of Test 3. Wind data are analysed in detail in section 4.1.1.

Table 3-1 Wind Conditions During the Hall Building Field Tests

Date	*Wind Speed U* (m / s)	*Wind Direction* (degree)	*Turbulence Intensity* σ_u / U	*Temperature* (° C)
June 26, 1997	4.9	217	0.401	24.9
July 2, 1997	2.5	173	0.439	26.6
July 30, 1997	4.5*	215*		25.7
August 7, 1997	5.7	212	0.413	24.8

* Estimated values based on data from Webster anemometer and Dorval Airport

3.2.3 Field Test Procedure

SF_6 was chosen as the tracer gas because it is inert and easily detectable. As mentioned in the beginning of this chapter, the field test procedure can be divided into three stages.

At first, the tracer gas was emitted into a fume hood in a chemistry laboratory on the 11th floor of the Hall Building. The fume hood was connected to stack No.32A; stack parameters are given in Table 2-2. The outlet concentration of the tracer gas, C_e, was controlled approximately at 10 ppm. A Bruel and Kjaer gas analyzer, which was located in the mechanical room of Hall Building, was used to monitor the tracer gas concentration. The stack emission velocity, w_s, was measured with a TSI Velocicalc anemometer.

The chosen stack is located on the south-west side of the roof, as shown in Figure 3-5, and is one of the seven fume hood stacks that are on the same side of the roof. In order to avoid the influence on the stack, during the tests, other adjacent stacks were usually closed. However, effects of nearby stacks on the plume rise of the chosen stack are assumed to be negligible.

Table 3-2 Exhaust Parameters of Stack No.32A

Parameter Name	*Parameter Value*
Height (h_s)	0.5 m
Width (d)	0.59 m
Exhaust Area (A_e)	0.34 m^2
Exhaust Velocity (W_e)	14.7 m/s
Volume Flow Rate	5.0 m^3/s

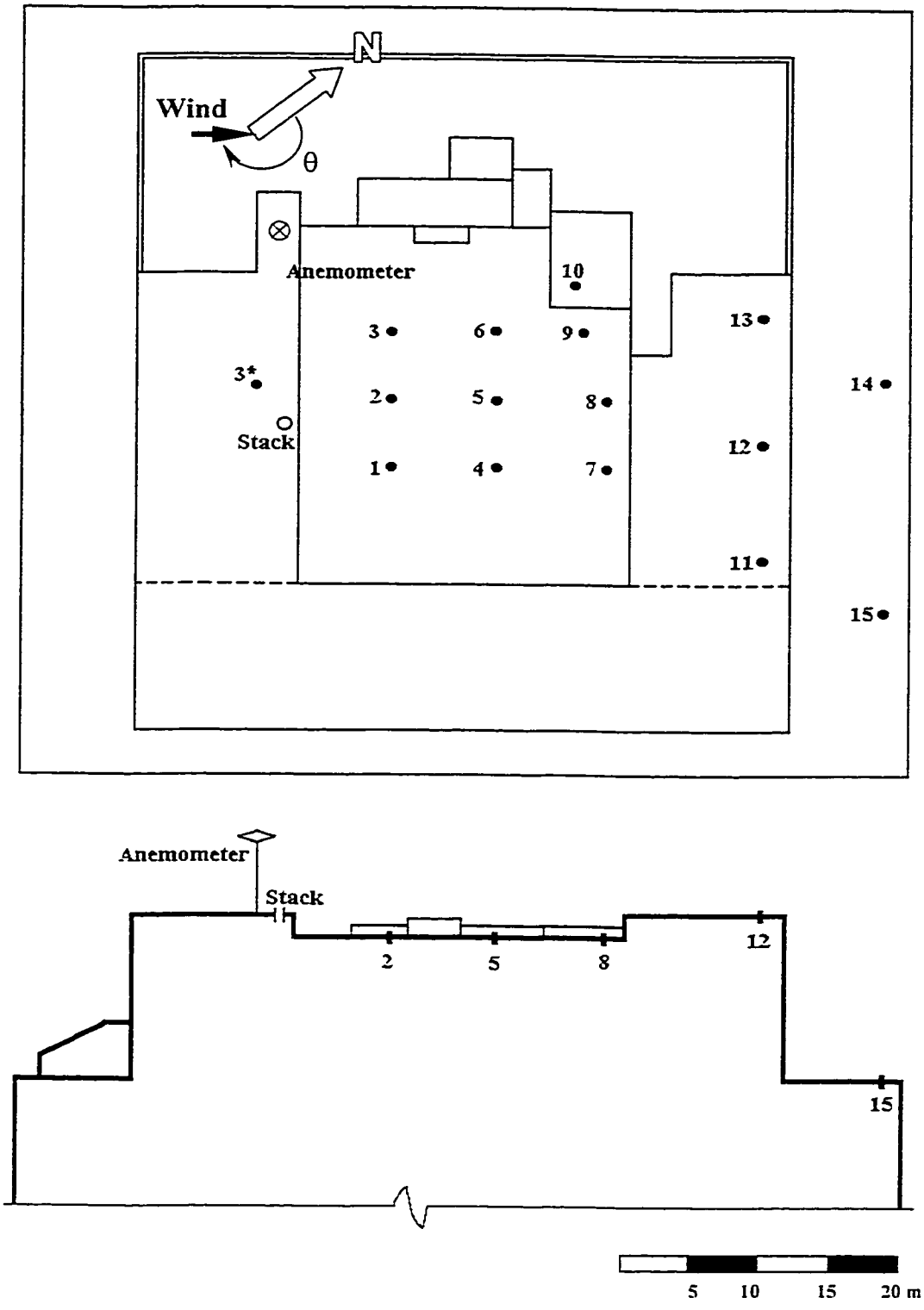

Figure 3-5 Plan and section drawings of Hall Building roof showing locations of the stack, sampler and the anemometer

The samplers that were used to draw the air samples were designed and fabricated by IRSST. Please refer to Appendix A for detailed information about the air samplers. As shown in Figure 3-5, 15 samplers were used in field tests. In general, sampler locations were the same for all four tests. However, sampler No. 3 was moved upwind for the 4th field test (August 7, 1997), after a smoke test showed that the plume travels upwind frequently. The upwind sampler is referred to as location 3* in Figure 3-5. It should be noticed that samplers 1-13 were located on the 14th floor level while samplers 14 and 15 were on the 12th floor level on the leeward side of the building. Note also that the level of the central roof area, where samplers 1-10 were placed, is about 2.5 m lower than the level of stack top, as shown in Figure 3-5.

Normally, 15-min air samples were collected at each sampling location over a total sampling period of 2.5 hours. However, in some cases, because of technical problems, such as improperly installed sampler bags, fewer samples were obtained. According to ASHRAE (1997), the averaging time (i.e. sampling period) is important when evaluating the minimum dilution. Generally, a longer averaging time tends to decrease the time-averaged concentration at a receptor location, due to the exhaust gas plume meandering. However, if the stack and receptor are located in the same recirculation zone, as in the current study, the sensitivity of the concentration at a receptor to the averaging time is expected to be reduced. In this case, ASHRAE recommends that a 3-min average dilution value corresponds to sampling periods of 3 to 60 minutes. Unfortunately, a 3-min averaging time would be too short to be practical for the present study, since more sampling bags would be needed for the same total sampling period.

The tracer gas concentrations of the air samples were measured using two gas chromatographs (GC), made by Varian and Lagus Applied Technology, at the Building Aerodynamics Lab of the Centre for Building Studies. In general, low concentration samples ($C < 25$ ppb) were measured by the Lagus GC. In order to check the measurement accuracy, some samples were analysed by both gas chromatographs and the results revealed good agreement. Calibration curves for the Varian GC are provided in Appendix B.

3.3 Wind Tunnel Simulation

After the completion of the full-scale study, a series of wind tunnel tests were conducted in the boundary layer wind tunnel of the Building Aerodynamics Lab at the Centre for Building Studies. In these tests, the influence of various parameters was investigated. Of particular interest were the effects of wind direction, exhaust momentum ratio, stack height and stack location. In addition, flow visualisation experiments were carried out to check the effect of upstream buildings on flow patterns around the Hall Building model.

3.3.1 Boundary Layer Wind Tunnel of C.B.S.

The boundary layer wind tunnel used in the current study is an open return type with a rectangular cross-section. It is 1.8 m wide and 12.2 m long. The height can be raised from 1.4 m to 1.8 m by adjusting the suspended roof. A turntable with a diameter of 1.21

m is placed at the downstream end of the facility. Figure 3-6 shows the plan view, the elevation and the section view from downstream end of the tunnel.

The wind is generated by a double inlet centrifugal blower, which is driven by a 50HP motor through a constant pitch V-belt drive. A wind speed range from 3 m/s to 14 m/s can be obtained by adjusting the flow controller of the blower outlet. By changing the floor roughness, atmospheric boundary layers for three different terrain exposures can be simulated. Sponge sheets were used in the present study to simulate the suburban exposure.

3.3.2 Wind Tunnel Modelling Criteria

In order to obtain an accurate wind tunnel simulation, various physical modelling criteria need to be satisfied. ASHRAE (1997) recommends the following criteria based on the research work of Cermak (1971, 1976 a,b), Snyder (1981) and Petersen (1987 a,b):

1. Equivalent exhaust velocity to wind speed ratio, W_e/U_H;
2. Equivalent exhaust to ambient air density ratio, ρ_e/ρ_a;
3. Similar emission Froude numbers $Fr^2 = \rho_a W_e^2 / [(\rho_e - \rho_a)\ gd]$, where g is the gravitational acceleration and d is the effective exhaust stack diameter;
4. Similar building Reynolds number $Re_b=U_HD/\nu$ or ensure that it is higher than 11,000, where ν is the kinematic viscosity of outdoor air;
5. Similar stack Reynolds number $Re_s=W_ed/\nu$ or ensure that it is higher than 2000 to ensure turbulent exhaust;

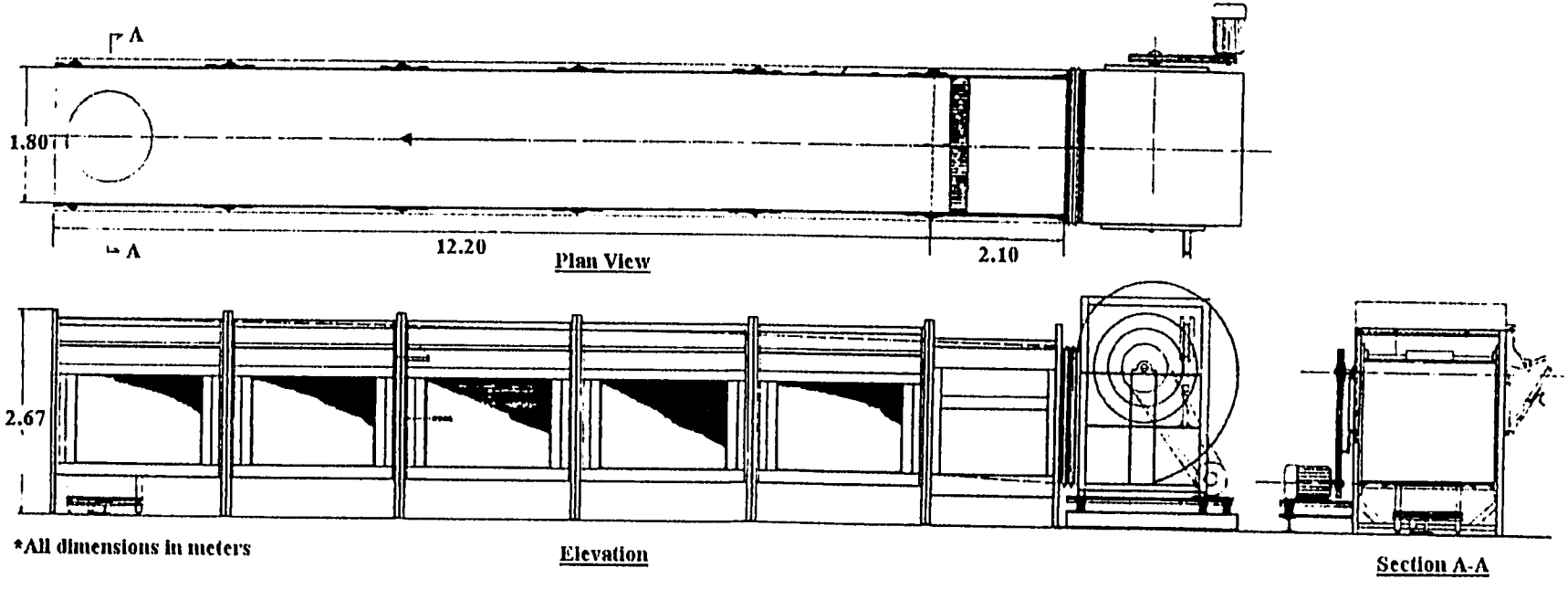

Figure 3-6 Plan view, elevation and section view of the boundary layer wind tunnel at C.B.S.

6. Similar Richardson number $Ri=gz\Delta T/(TU^2)$, where T is the temperature in °K at height z, U is the wind speed at height z and ΔT is the temperature difference between that at height z and at a lower height;
7. Similar vertical profiles of mean wind speed and turbulence intensity;
8. Identical scale applied to all model dimensions;
9. Ensure that the blockage of the wind tunnel cross section is less than 5%.

It is generally not possible to satisfy each of these criteria. Fortunately, some criteria may be relaxed, depending on the type of study. In the present wind tunnel study, the building exhaust is non-buoyant. Therefore, it is not necessary to match the Froude number. Moreover, since the study was limited to neutral atmospheric stability, Richardson number matching became unnecessary.

Because of the small diameter of the stack, the stack Reynolds number matched with above criteria only when the exhaust momentum ratio was higher than 3. For $0.5 \leq M \leq 3$, values of Re_s range between 400 and 2000. However, since the exhaust dispersion is dominated by building generated turbulence [Wilson and Lamb (1994)], it is expected that the relaxation of the stack Reynolds number criteria has little influence on wind tunnel results. Likewise, a laminar exhaust flow was used in the study of Wilson and Chui (1995) since it was difficult to determine the effects of initial exhaust turbulence.

Another very important factor that should be taken into account when comparing wind tunnel data with field data is the averaging time. As discussed previously, an increase in full-scale averaging time causes mean concentrations on the plume centre line to decrease due to the meandering effect. Generally, wind tunnels can only simulate small-scale

plume meander since the lateral flow of air is restricted by the tunnel walls. As a result, mean concentrations acquired in the wind tunnel are normally assumed to be consistent with a full-scale averaging time of 10 minutes. [ASHRAE (1997)] However, Wilson (1995) suggested that this approximation should be applied only to wind tunnels that have a crosswind dimension that is 10 times as large as the boundary layer thickness. Based on this theory, normal wind tunnels can only simulate a full-scale averaging time of 1 to 5 minutes. However, it should also be noticed that for a stack and intake located in the same recirculation zone, as in the current study, the effect of averaging time may not be significant [ASHRAE (1997)].

3.3.3 Wind Tunnel Experimental Procedure

3.3.3.1 Concentration Measurement Procedure

The Hall Building and its surrounding buildings within a radius of 450 m were modelled at a scale of 1:500. Small brass tubes with an outside diameter of 1.2 mm were installed in the model to form the stack and sample tappings. The stack and tappings locations corresponded to field test sample locations. Altogether 16 tappings were constructed on the roof of the Hall Building as shown in Figure 3-5. A photograph of the wind tunnel model is shown in Figure 3-7.

Figure 3-8 shows the wind profile and turbulence intensity obtained with a suburban exposure in the boundary layer wind tunnel at Centre for Building Studies. A power law exponent of 0.17 was measured, which is relatively low comparing with the ASHRAE recommended value 0.22. Note, however, that this profile was obtained without upstream buildings. The wind tunnel simulation included a significant portion of the city

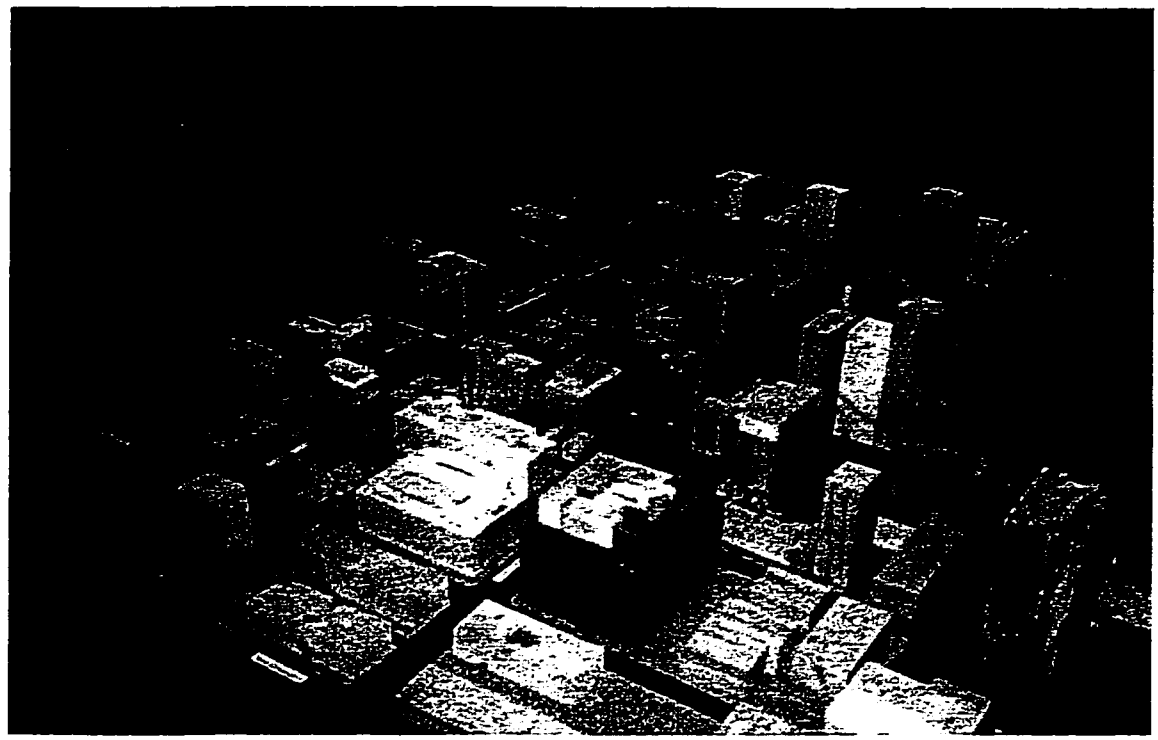

Figure 3-7 Models of the Hall Building and surrounding buildings

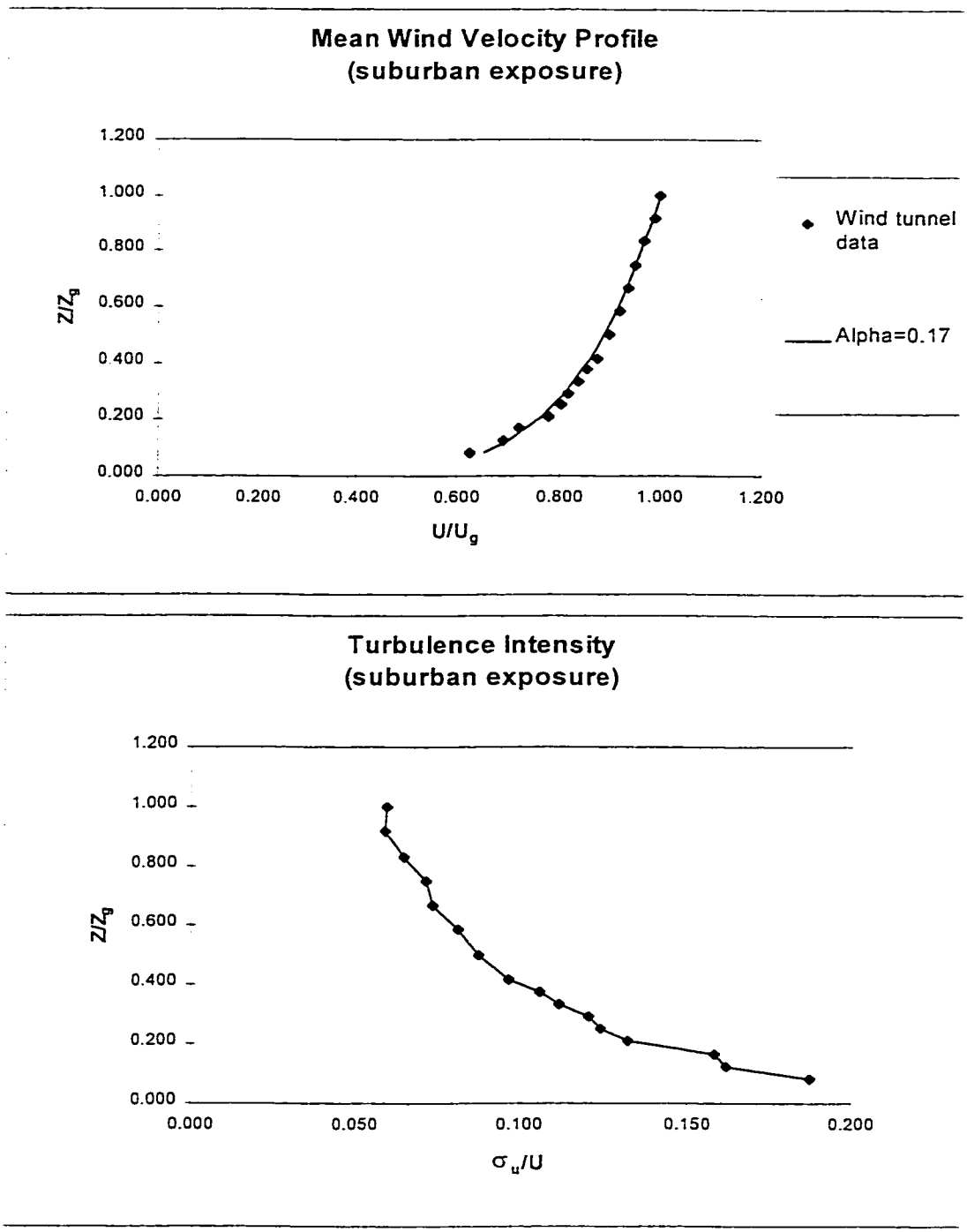

Figure 3-8 **Mean wind velocity and turbulence intensity profile for suburban exposure**

to the south-west of the Hall Building. These upstream buildings increased the power law exponent and created a rough-suburban boundary layer.

Before each test, mean wind speed and turbulence intensity was measured. The reference wind velocity, U_g, was measured with a Pitot tube located 600 mm above the floor of the tunnel. A second reference wind speed, U_H, was measured using a TSI hot film anemometer at a height of 15 mm above the model roof, which corresponds to the anemometer location in the field tests. The position of the anemometer can be found in Figure 3-5. The data were analyzed by a Universal Waveform Analyzer (Model 6100), made by ANALOGIC.

As introduced in Chapter 2, the exhaust momentum ratio is a critical parameter, which is given by $M = (\rho_e / \rho_a)^{0.5} W_e / U_h$. It can be simplified as $M=W_e/U_h$, if it is assumed that the densities of exhaust and ambient air are the same. Once the wind speed at roof height is obtained, the exhaust mass flow rate (referred as MFR) can be varied to provide specific values of the momentum ratio. For example, to obtain M=1, MFR is adjusted so that $W_e=U_h$.

The tracer gas technique used for the wind tunnel study was the same as for the field study. The method is presented schematically in Figure 3-9. The tracer gas source is a gas cylinder, which contains a certified mixture of SF_6 and nitrogen. It should be noticed that the outlet concentration (C_e) was varied depending on dilution measured at the receptors, so that the concentrations remained within the optimum measurement range of the GC. Refer to the calibration curves provided in Appendix B. When the GC reading was over 5.9, a low concentration of SF_6 ($C_e \approx 1090$ ppb) was used instead of the normal

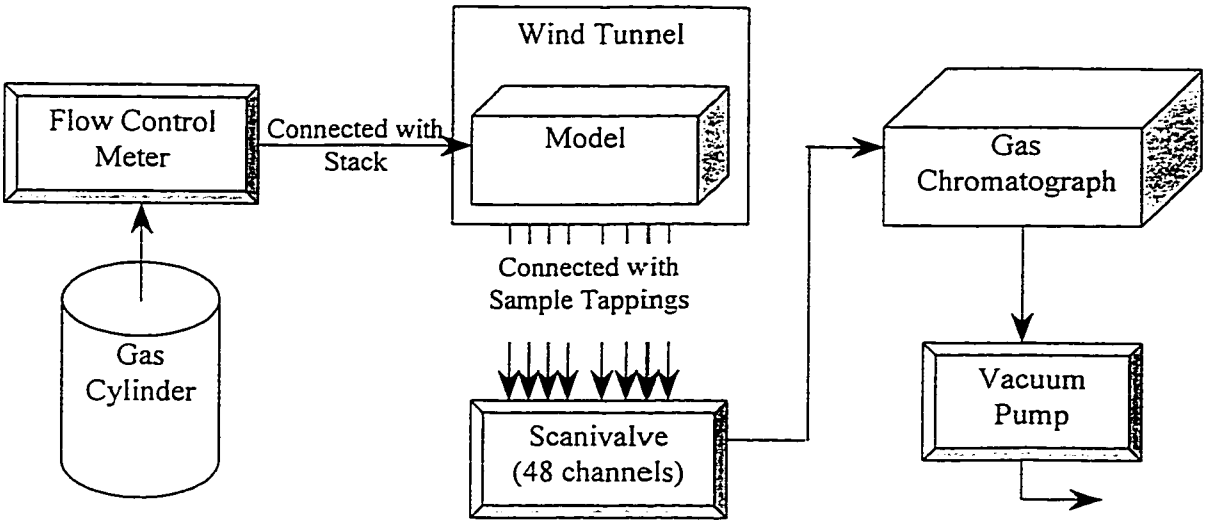

Figure 3-9 Tracer gas measurement system

concentration ($C_e \approx 107$ ppm). After SF_6 was released from the cylinder, a Matheson flow meter was employed to obtain the precise exhaust mass flow rate. The flow control meter was calibrated periodically during the study (please refer to Appendix B for details of the flow meter calibration). The controlled tracer gas was emitted continuously through the stack.

Air samples were collected at each sample location through the tappings. The tappings were connected to a Scanivalve sampling system, which enables the selection of any desired tapping. A constant flow of air through the GC was produced by a vacuum pump. Given that the flow rate of the gas chromatograph is 35 cc/min, a tracer gas intake speed of approximately 0.5 m/s was calculated based on the cross-section area of the tapping. Since this intake velocity is much lower than the wind velocity at roof level, it was assumed that this suction power created no influence on the dispersion process.

As in the field test, the concentrations of air samples were measured using the Varian gas chromatograph. However, instead of using syringe samples, the air sample was drawn continuously and automatically through GC. Generally five samples were collected over a total period about two minutes and the average GC value was used to determine the mean concentration. Using the pre-determined GC calibration equations (GC calibration method is described in Appendix B), GC readings were converted into concentrations.

The repeatability of the experimental technique was validated by repeating the same test on several different days. Typical test results are shown in Figure 3-10. The variances between dilution values measured on two different days were generally lower than 15%, although variances of up to 20% were obtained in some cases.

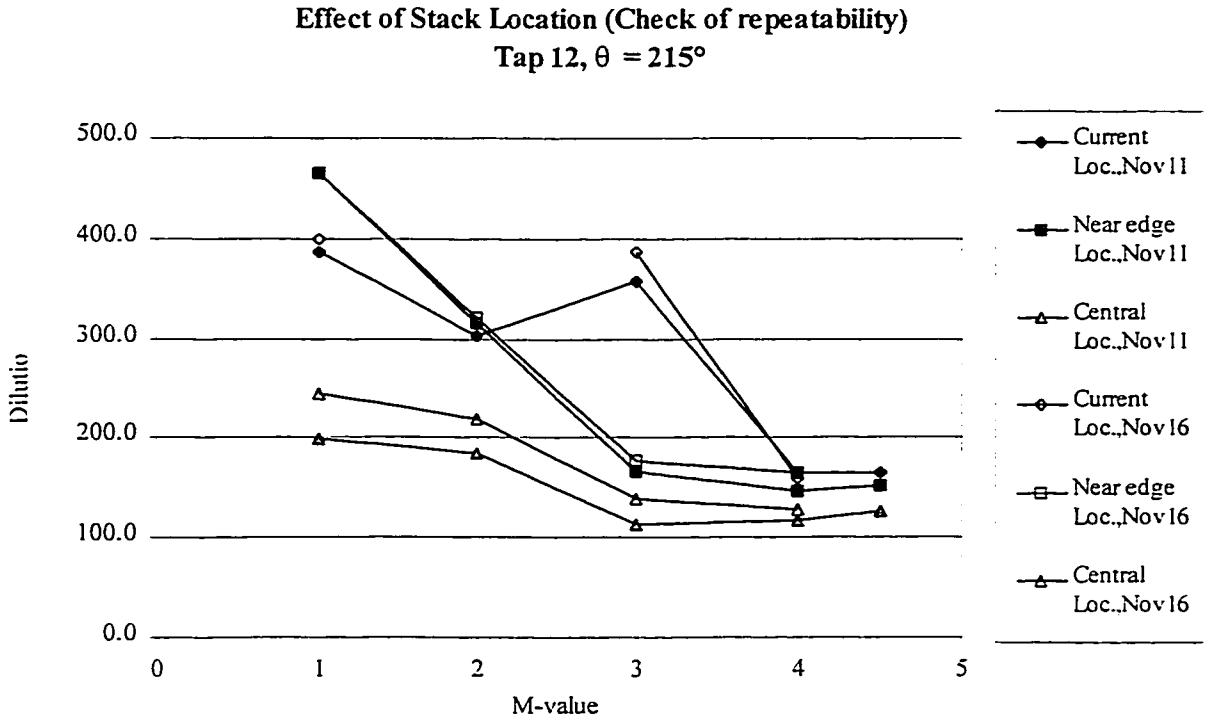

Figure 3-10 Repeatability of concentration measurements

3.3.3.2 Flow Visualisation Procedure

Basically, the procedures of flow visualisation are similar to those used for concentration measurement, except that the tracer gas is replaced with a visible plume. Results of these experiments have been only qualitative.

An RCA video camera was used to record the plume behaviour. The camera was fixed at the right side (viewing from the open end) of the wind tunnel and perpendicular to the plexiglass window. The centre of the lens was set up at the same level as the stack surface so that the magnitude of the plume rise could be captured. Several light positions were tested in order to produce the best plume visualization. The optimum light position was at a distance of 30 cm downwind of the Hall Building model, with an angle of 45° to the left side of central line of the test section and at the similar height with the stack, as shown in Figure 3-11. Opposite the camera location, a board covered with a black cloth was situated to provide a dark background.

Before performing the visualization test, wind velocity measurements were obtained to ensure that the wind conditions were similar to those used in the tracer gas study. The flow visualization system is illustrated schematically in Figure 3-12. The plume was generated using a Rosco 1500 fog machine. A sealed plexiglass tank was used as a smoke reservoir, which had a fill pipe at the bottom and two holes on the cap. Once the tank was filled up by the fog machine, the fill pipe was disconnected and sealed. Then two plastic tubes, one connected with a N_2 cylinder and another with the stack, were plugged into the two top holes. N_2 was used to force the smoke out of the reservoir at a

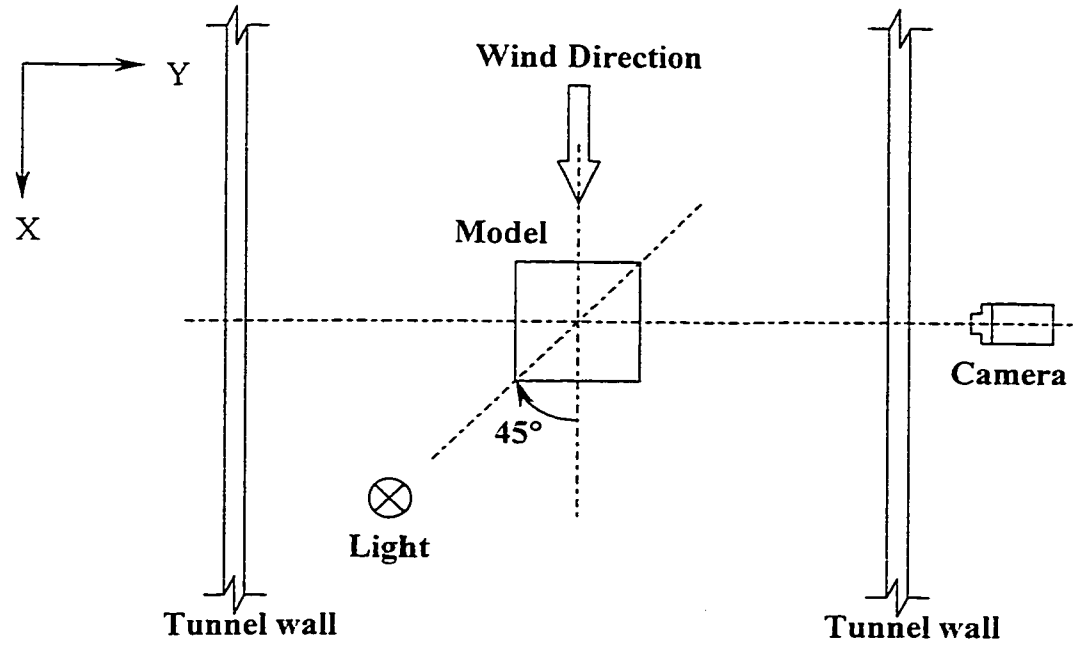

Figure 3-11 Plan view showing positions of camera and light with respect to model

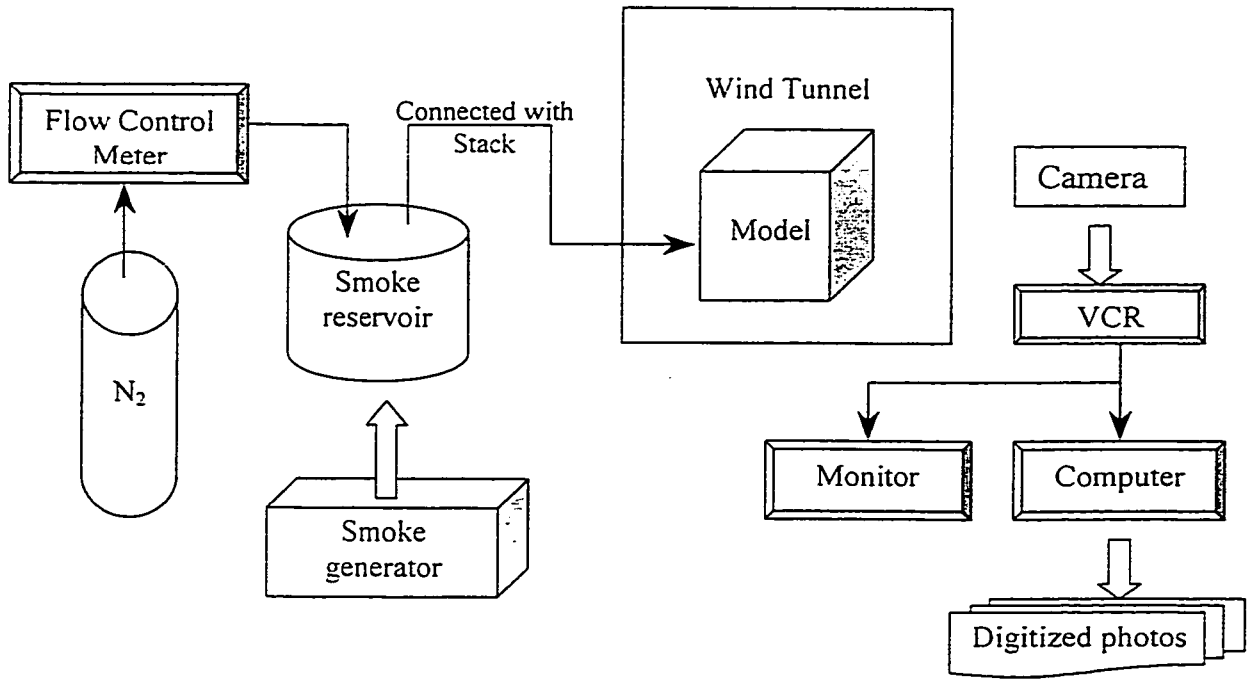

Figure 3-12 Flow visualization system

specified rate. Different exhaust momentum ratios could be obtained by adjusting the mass flow rate of N_2.

Flow visualisations for both model assemblies, with and without upstream buildings, were recorded on a VHS tape at the standard speed (30 frames per second). The video picture was digitized using a video image analysis system, which is also shown in Figure 3-12, composed of a SONY SLV-R5UC VCR, an IBM PC-AT and a Jandel Scientific Frame Grabber. As a supplement to the current tracer gas experiments, the results of the flow visualization are quite valuable. Detailed discussion of the digitized video images is presented in section 4.3.

CHAPTER 4

RESULTS AND DISCUSSION

4.1 Field study

As already mentioned, field studies reveal the real situation best, even though they are costly and time consuming. In the present study, four field tests were performed on June 26, July 2, July 30 and August 7, 1997. The results were used to evaluate the ASHRAE dilution models and the accuracy of the wind tunnel simulation.

4.1.1 Meteorological data analysis

Wind speed and wind direction data for the four test days can be found in Figure 4-1 to Figure 4-4. The data were gathered from three sources—the Hall Building, Dorval Airport and Webster Library. It should be noted that data were not obtained from the Hall anemometer during Test 3 (July 30). As a result, the wind speed and wind direction had to be estimated from other data for this particular test.

Wind speed at the top of the Hall Building, U_{hall}, can be estimated by applying terrain and height corrections to the Dorval Airport wind speed measurement, U_{dorval}, obtained at a height of 10 m in open country terrain. Wind speed decreases with the increase of upstream roughness; whereas wind speed increases with the increase of measurement height. Using the power law approximation, the correction factor is given by:

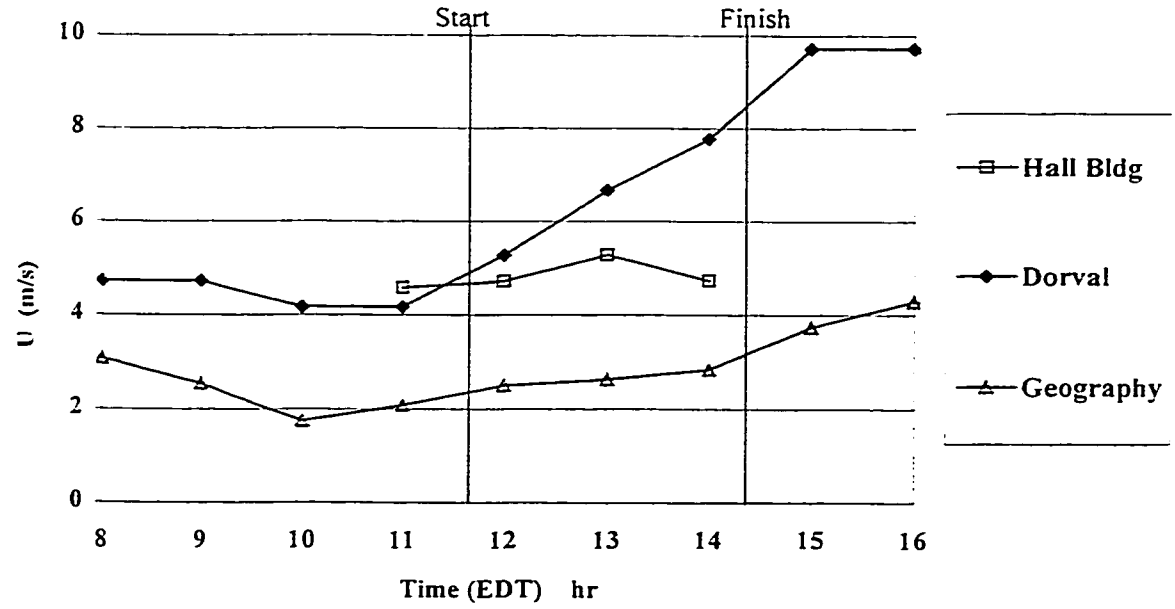

a) Wind speed

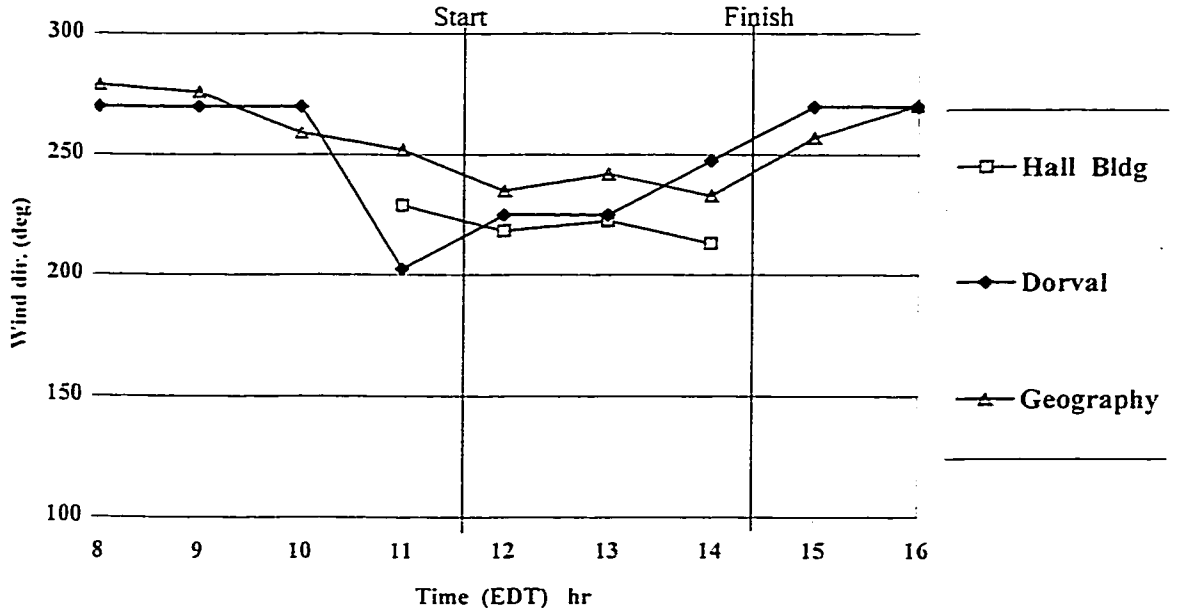

b) Wind direction

Figure 4-1 Wind conditions during Hall Building field test No.1 (June 26, 97)

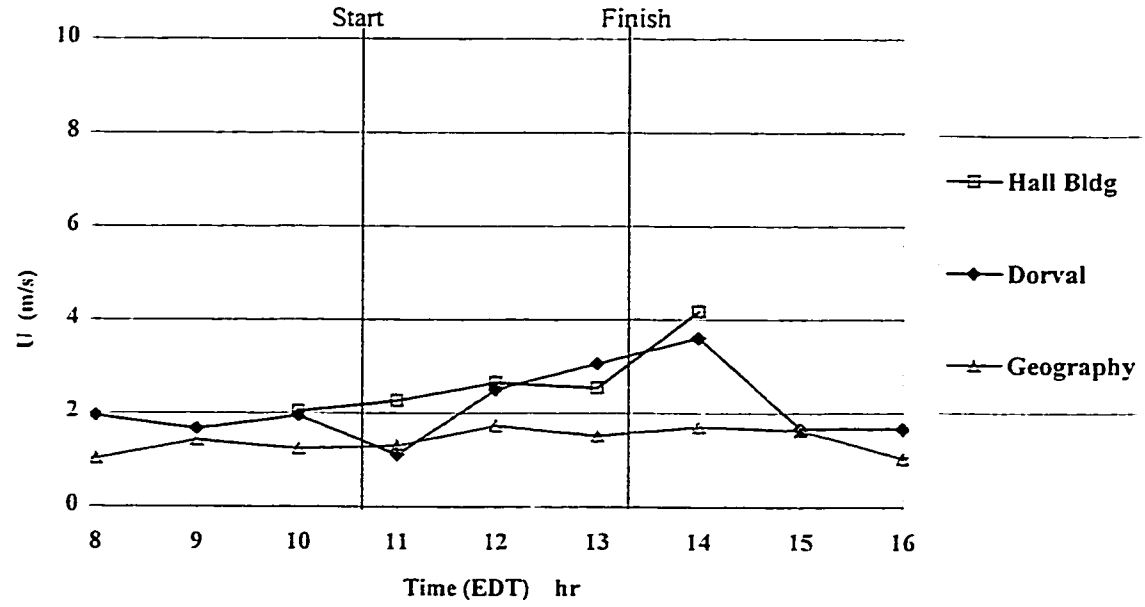

a) Wind speed

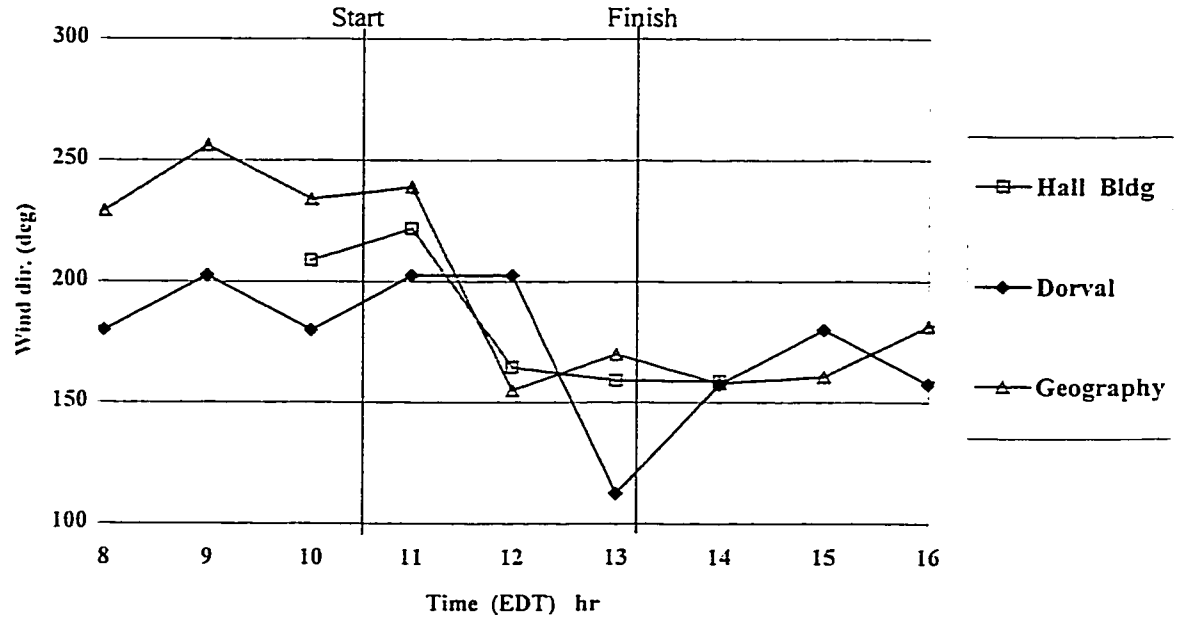

b) Wind direction

Figure 4-2 Wind conditions during Hall Building field test No.2 (July 2, 97)

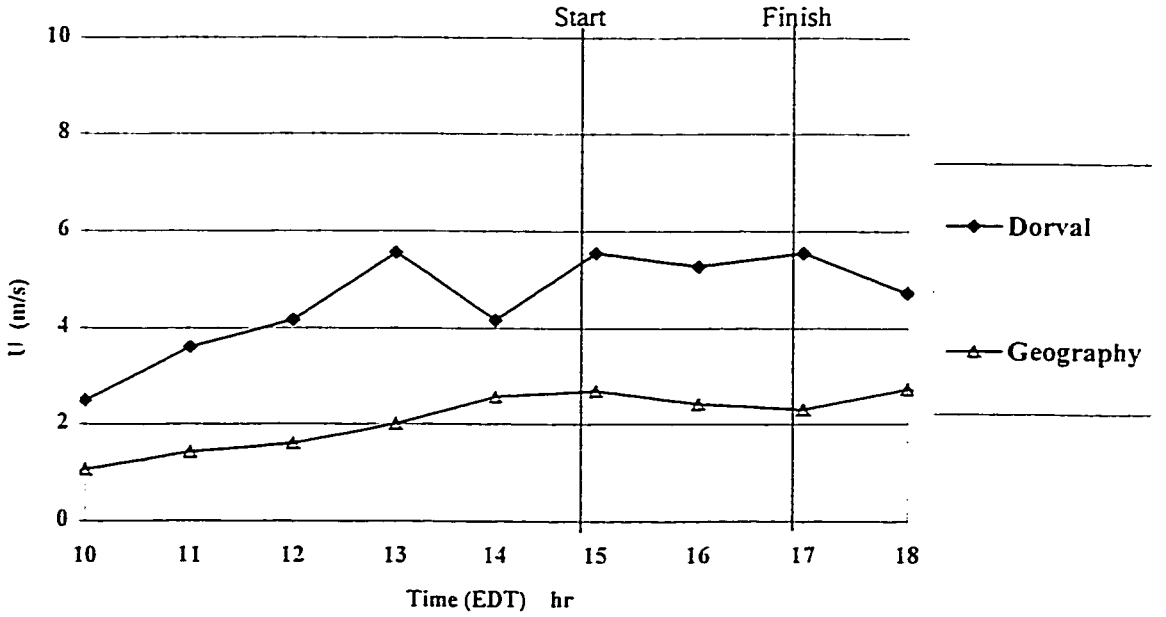

a) Wind speed

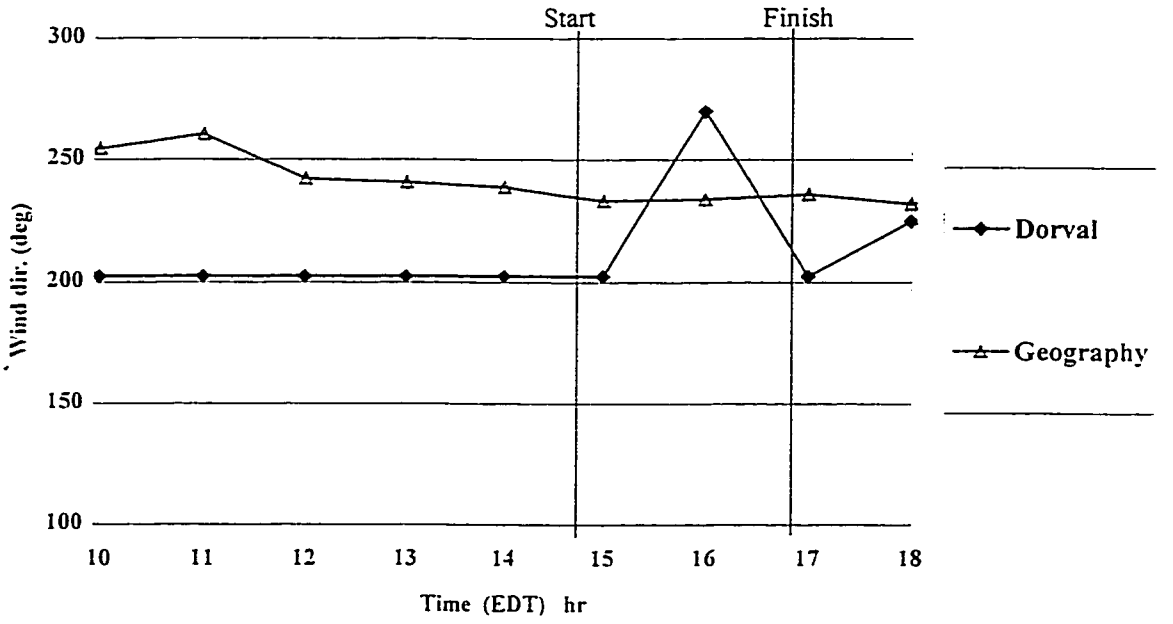

b) Wind direction

Figure 4-3 Wind conditions during Hall Building field test No.3 (July 30, 97)

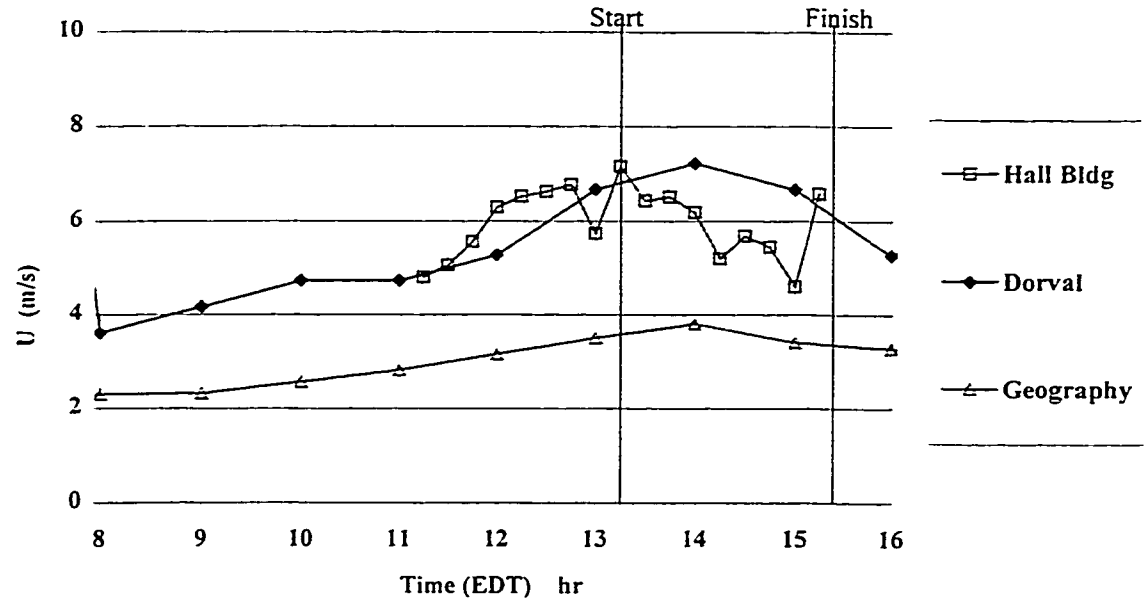

a) Wind speed

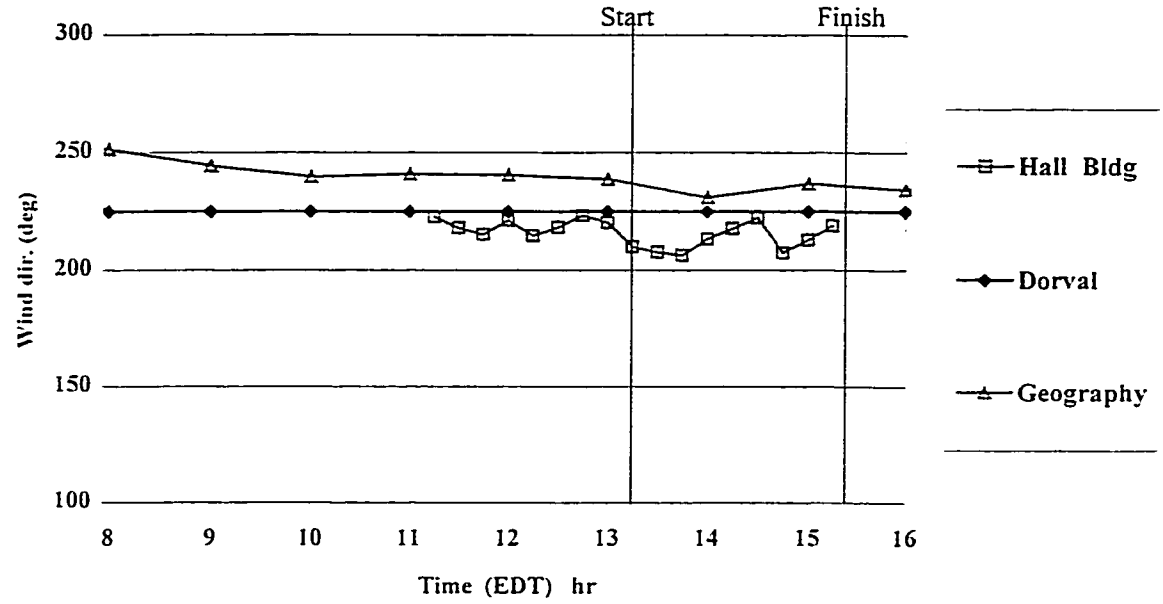

b) Wind direction

Figure 4-4 Wind conditions during Hall Building field test No.4 (August 7, 97)

$$U_{Hall} / U_{Dorval} = (Zg_{oc} / Z_{Dorval})^{0.15} (Z_{Hall} / Zg_{urb})^{0.28} \qquad (4.1)$$

$$= (300 / 10)^{0.15} (70 / 500)^{0.28} = 0.96$$

where Zg_{oc} is the height of the atmospheric boundary layer for open country terrain and Zg_{urb} is the atmospheric boundary layer height for urban terrain; Z_{Dorval} and Z_{Hall} are the measurement heights at Dorval Airport and Hall Building respectively. The correction factor of 0.96 indicates that the wind speeds at the Hall Building should be approximately equal to the Dorval wind speed. Thus, the increase in wind speed due to the increase in measurement height at the Hall Building is balanced by the effect of an increase in roughness. In general, wind speed data obtained at Dorval shows good agreement with wind speeds at the Hall anemometer, as expected.

However, it should be noted that the existence of large upwind obstructions might have significant effects on wind conditions, for particular wind directions. It may explain the discrepancy of Hall Building and Dorval data in Figure 4-1, where Dorval data shows an increase of wind speed and a change of wind direction from SW to W, while the Hall Building anemometer did not show significant change in wind speed or wind direction. This discrepancy is most likely due to the presence of the Mont Royal.

Using equation (4.1), the wind speed at the top of the Webster Library is estimated as 0.88 U_{dorval}. However, as shown in the figures, the actual measurements are only about 0.5 U_{dorval}. The low wind speed may be due to the low height of the anemometer. It was located only 3 meters above the roof and thus was certainly in the separated flow region.

The presence of tall upstream buildings located only 15 m to the southwest of the library was also probably a significant factor.

4.1.2 Flow pattern analysis

According to Wilson (1979), the flow separation zone for a cube-shape building covers the entire roof. In the Hall Building case, it was estimated using equation 2.15 that the dimensions of the recirculation region are: L_c=57 m and H_c=32 m. However, this estimation may not be accurate due to the effect of upstream buildings. It was confirmed by the wind tunnel flow visualization afterwards that the rooftop flow pattern is significantly influenced by upwind buildings. Moreover, smoke tests conducted during Test No.4 revealed that the plume rise varied from 1 m to more than 10 m in a 15-minute period. Two digitized video images recorded in Test No.4 were shown in Figure 4-5 indicating the plume variation. Frequent upwind excursions were observed also.

Concentration measurements fluctuated considerably between various sample periods. Figure 4-6 shows the concentration distributions for two typical sample periods, No.1 and No.2 in Test No.1. Generally, concentration values obtained in sample period No.2 were higher than those obtained in period No.1 by as much as a factor of 3 at all sample locations. This phenomenon may be partially due to an increase in exhaust momentum ratio, M, during sample period No.2. As will be discussed, wind tunnel tests indicated that concentration values increase significantly for this building/stack configuration when M exceeds a critical value of approximately 3.5.

a) Straight-up plume

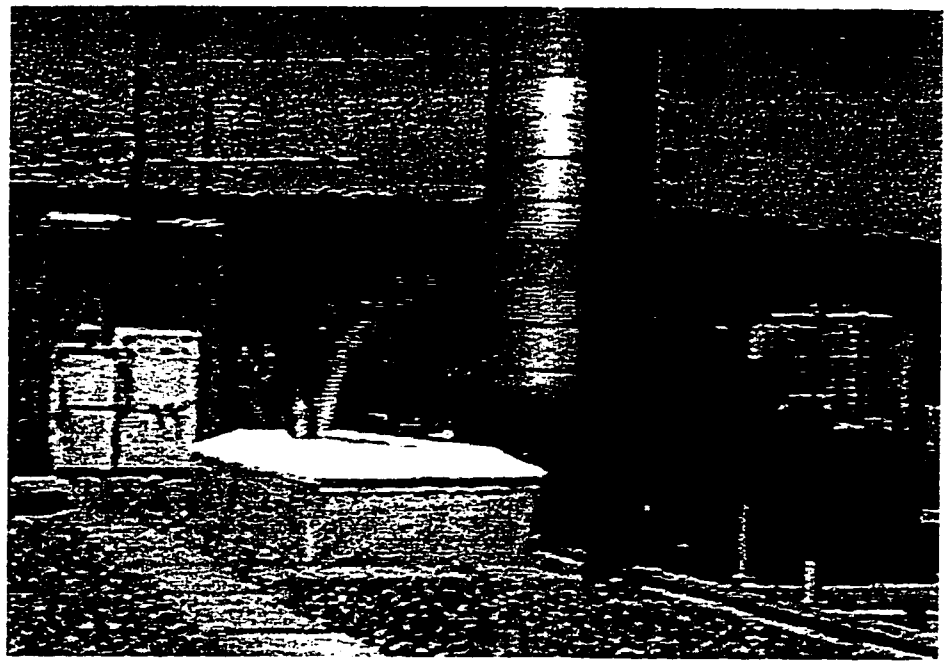

b) Bent-over plume

Figure 4-5 Digitized video images of plume rise recorded in field Test No.4

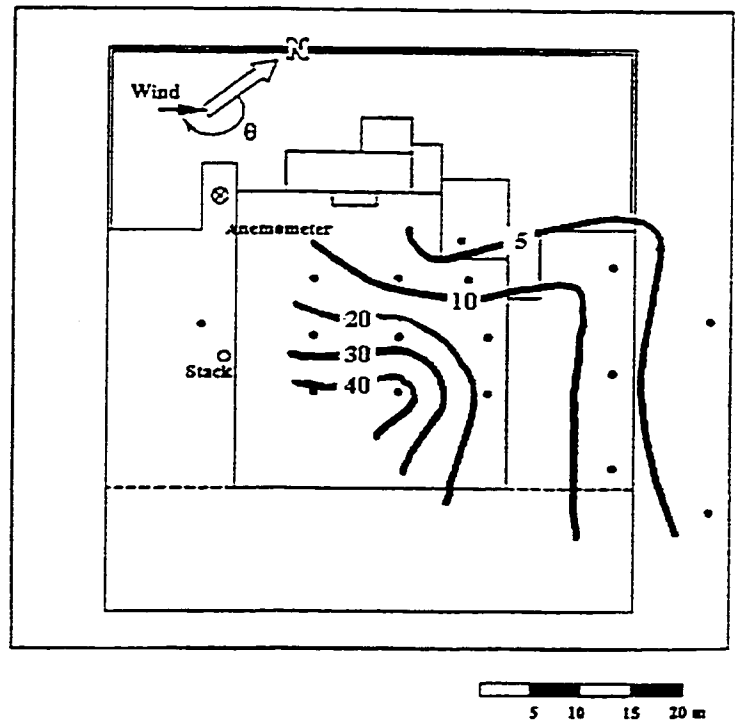

a) Sample Period No.1

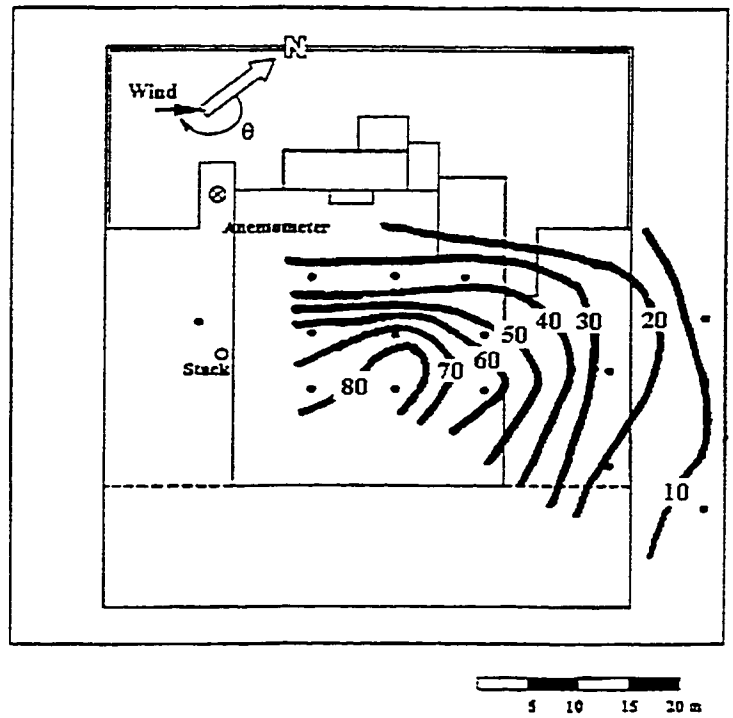

b) Sample period No.2

Figure 4-6 Concentration values (ppb) obtained in sample periods No.1 and No.2 of field Test No.1.

A significant characteristic of the full-scale dilution data is the high correlation between samplers. This is evident in the time variation of field data shown in Figure 4-7 to 4-10. Dilution data measured at different sample locations tend to show similar variation with time. For instance, in Figure 4-7, dilution measurements during sample period 2 were found to be the minimum at most sample locations.

Another example is that in sample period 6 of Test No.4, as shown in Figure 4-10. The minimum dilution occurred at all sample locations except location no. 3, which was relocated upwind of the stack. This indicates that the frequency of upwind gusts was lower than downwind gusts during this 15-minute period.

4.1.3 Comparison of field data with ASHRAE model results

Field concentration measurements were compared with ASHRAE model estimations in terms of dilution, $D=C_e/C$, because of two reasons. The first reason is that it is convenient to compare the field results with ASHRAE predictions since ASHRAE model estimates are in terms of minimum dilutions. Secondly, the exhaust concentration of the tracer gas varied during the test period. For example, at the beginning of Test No.1 (June 26), the emission concentration of SF_6 was 10.29 ppm, while it decreased to 8.39 ppm at the end of the test. As a result, concentration data for different sample periods generally cannot be compared directly; the data must be expressed in terms of dilution.

Dilution data from the four field tests are plotted in Figure 4-11 to Figure 4-14 with the minimum dilution curves obtained with the Halitsky, Wilson-Chui and Wilson-Lamb models.

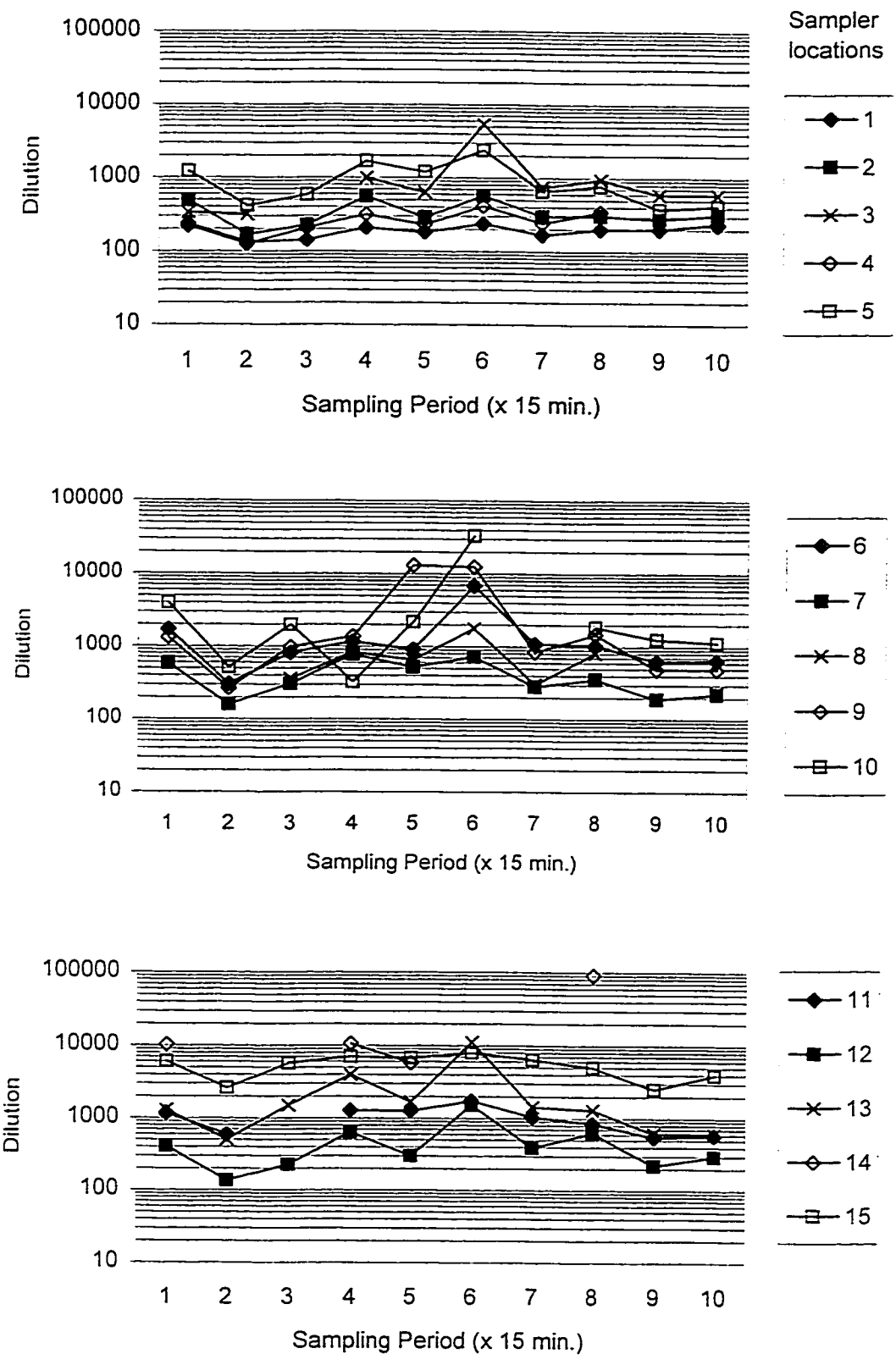

Figure 4-7 Dilution variation with time during Hall Building Test No.1

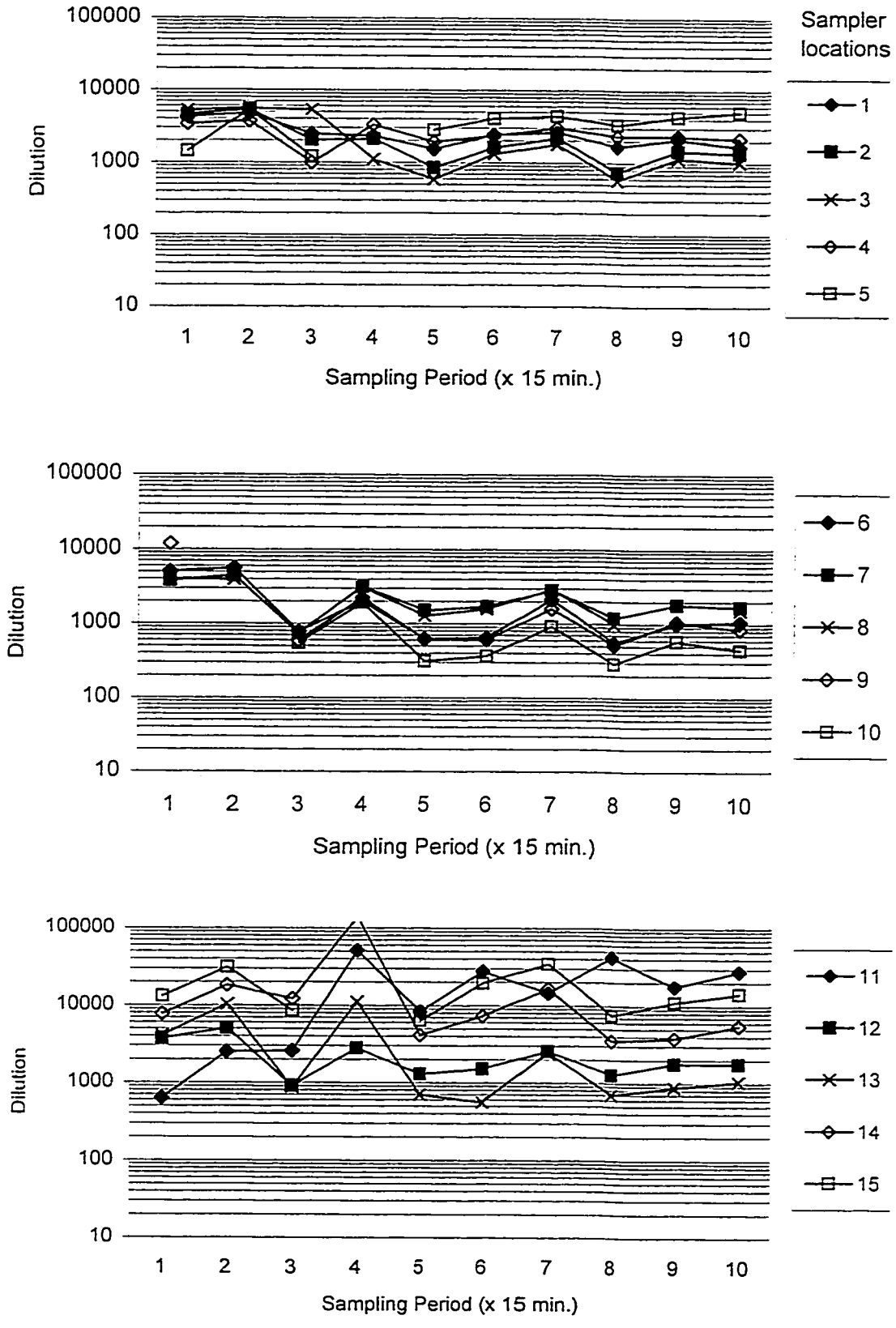

Figure 4-8 Dilution variation with time during Hall Building Test No.2

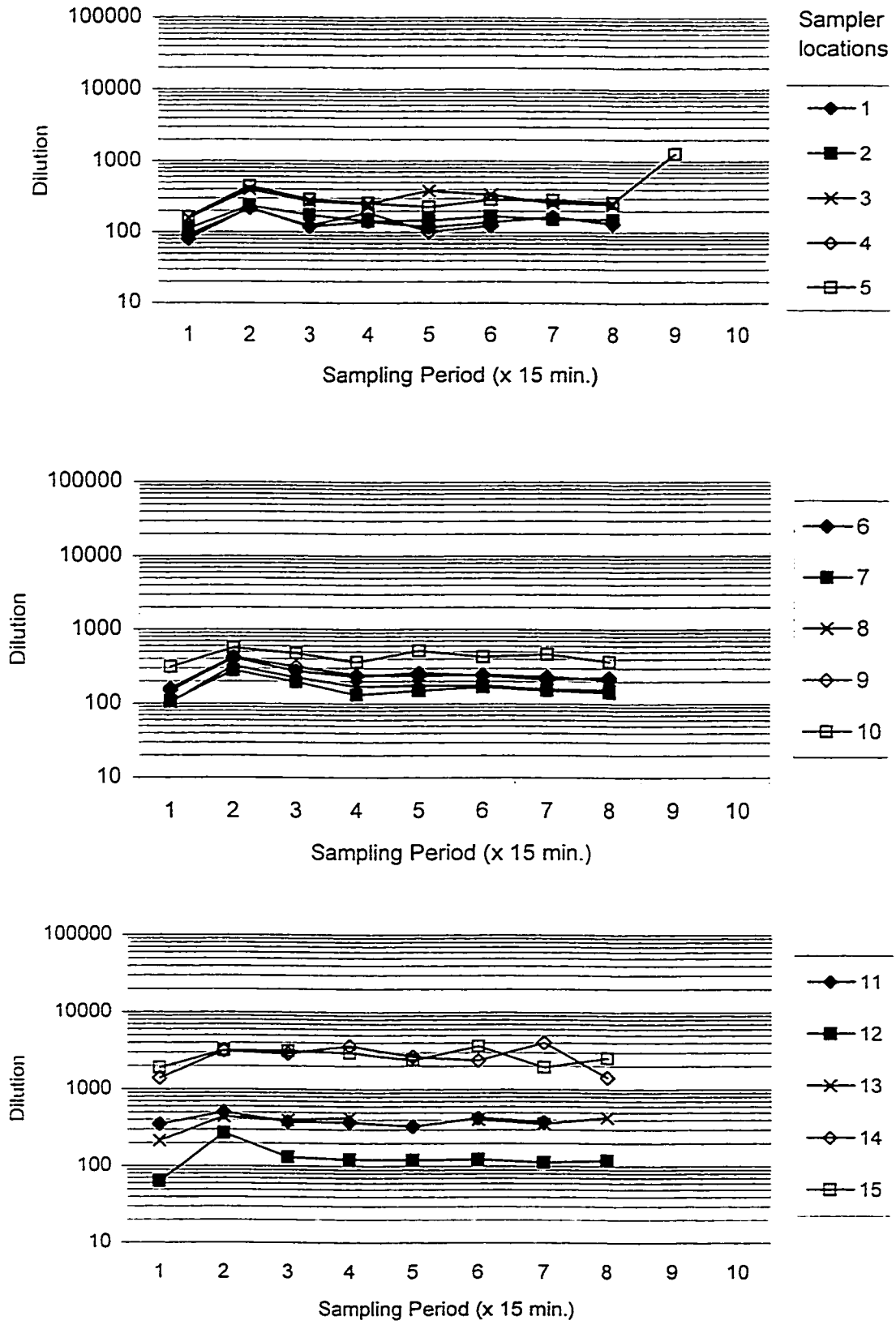

Figure 4-9 Dilution variation with time during Hall Building Test No.3

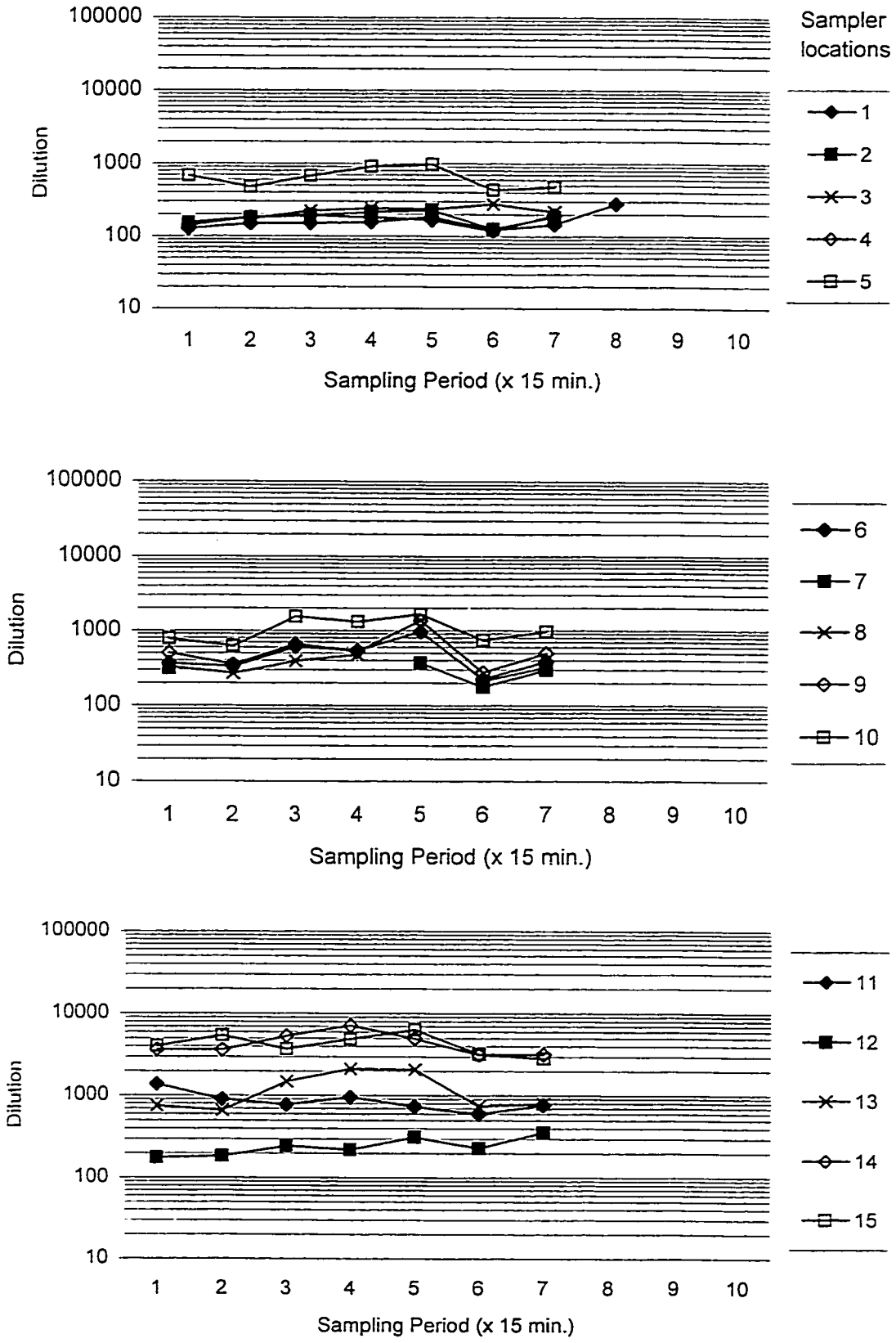

Figure 4-10 Dilution variation with time during Hall Building Test No.4

For the Halitsky model, (equation 2.3), minimum dilution curves were obtained for α=2 and α=5. The former value is used to predict plume dilution on the plume centre-line and is recommended by Halitsky (1990). The latter value may be more appropriate for the present case where samplers were usually not on the plume centre-line. For the Wilson-Chui model, equation (2.4-2.6), the distance dilution parameter, B_1, was set at 0.0625 as recommended for rooftop receptors. For the Wilson-Lamb model, the value of B_1 is calculated using equation (2.13), as suggested by ASHRAE (1997). Based on the turbulence measurements obtained during field tests 1,2 and 4, σ_θ is estimated to be 20°. Equation 2.14 yields a B_1 value of 0.069, which is similar to that used in the Wilson-Chui model. The exhaust momentum ratio, M, used in both Wilson-Chui and Wilson-Lamb models is the average value for the entire test period. Note, however, that M for individual 15-min samples may have varied significantly during a test.

Dilution data for Test No.1 (June 26) is shown in Figure 4-11. Wind speeds and directions during this test were relatively consistent, as can be seen in Figure 4-1. However, as shown in Figure 4-7, dilution values obtained in the test varied by a factor of 2 or higher. The large variation of D at each location may possibly be because of the high turbulence intensity (over 40%) during the sample period. As a consequence, M-values for the 15-minute samples may vary from 2 to 4. As will be discussed, dilutions are affected as the M-value changes. It should also be noted that relatively high dilution values were found at sample locations 14 and 15, which are located on 12th floor, approximately 10 m lower than the roof level.

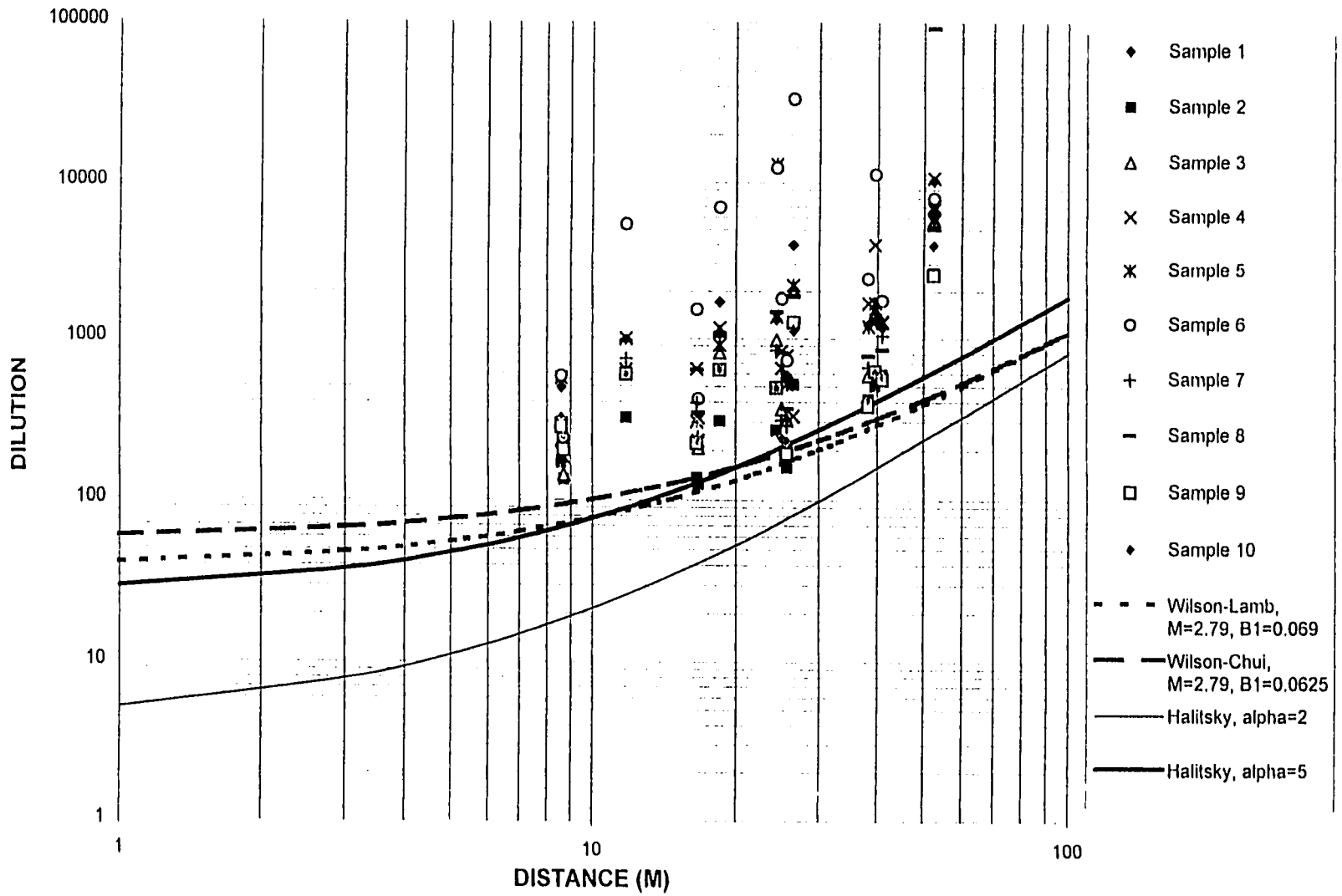

Figure 4-11 Dilution data of Hall Building Test No.1 (June 26th, 97) with ASHRAE minimum dilution curves

The minimum dilution estimations given by the Wilson-Chui and Wilson-Lamb models are appropriate, since most of the field measurements are above the curves, as shown in Figure 4-11. In contrast, the Halitsky model with α=2, which is recommended by ASHRAE [Halitsky (1990)], is relatively conservative as it underpredicts minimum dilution values by factors of 2.5 to 8. However, when the α value is increased to 5, the Halitsky model provides better predictions, which are similar with those obtained from the Wilson-Chui and Wilson-Lamb models.

Figure 4-12 shows the field dilution data obtained in Test No.4 (August 7). Dilution data for Test No.4 are very similar to Test No.1 values. One of the possible reasons that could explain the similarity is that the momentum ratios during both tests were approximately identical, (M=2.79 for Test No.1 and M=2.72 for Test No.4).

It should be noticed that, during Test No.4, sampler no. 3 was moved to an upwind location, which is about 4.5 m from the stack. As shown in Figure 4-12, relatively low dilution values ($170<D<280$) were obtained, which shows that even when intakes are located upwind of a stack, significant contamination can occur. Therefore, this fact should be taken into account when determining the intake locations.

Dilution values acquired in Test No.2 and shown in Figure 4-13 were significantly higher than dilution values obtained in the other tests. This is due to two factors – large plume rise and large variations in θ. The average wind speed was only 2.5 m/s during Test No.2, giving an average momentum ratio M=6.46. Thus the plume centreline was well above roof level. Note also that low wind speeds are associated with large changes in θ.

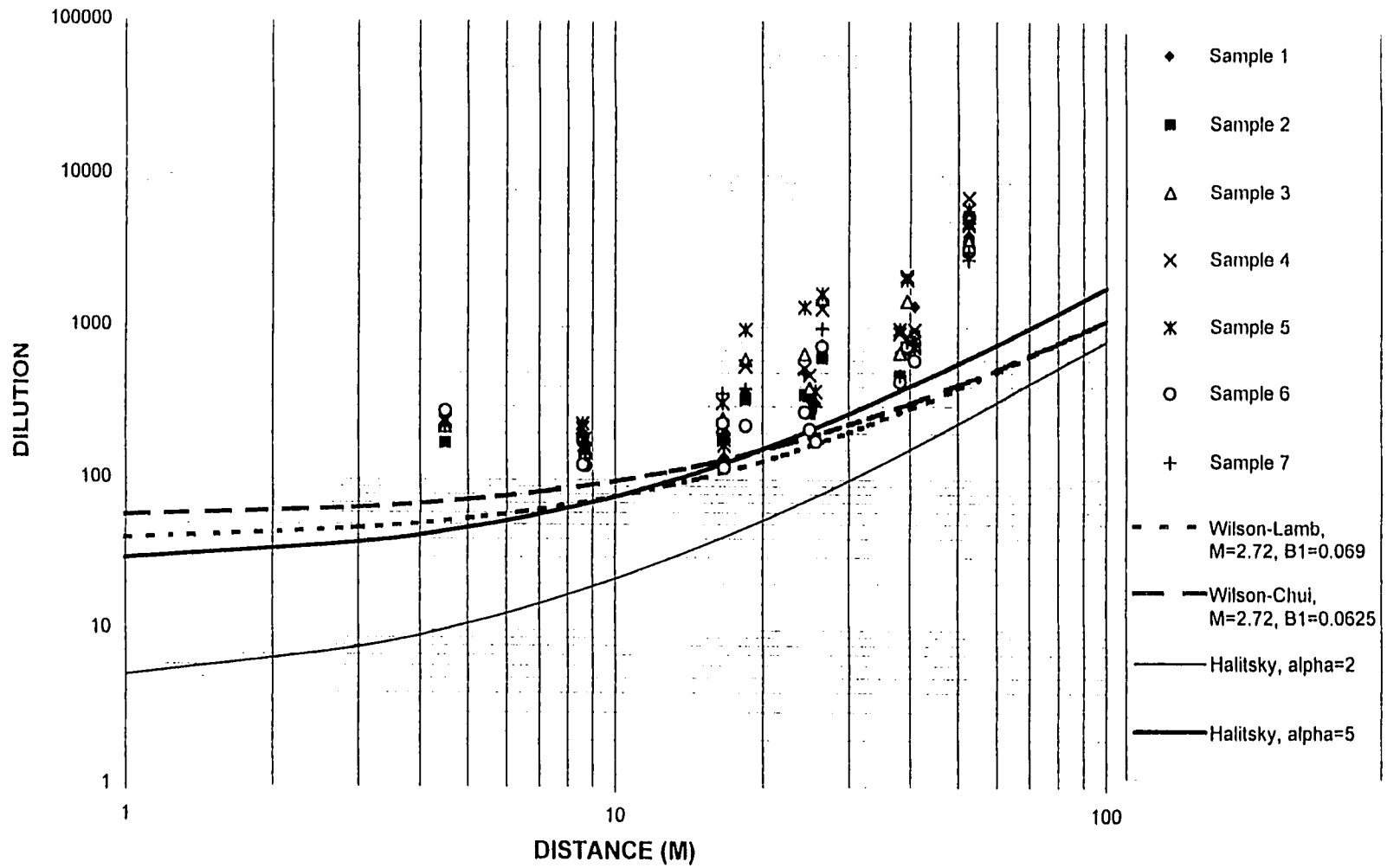

Figure 4-12 Dilution data of Hall Building Test No.4 (August 7th, 97) with ASHRAE minimum dilution curves

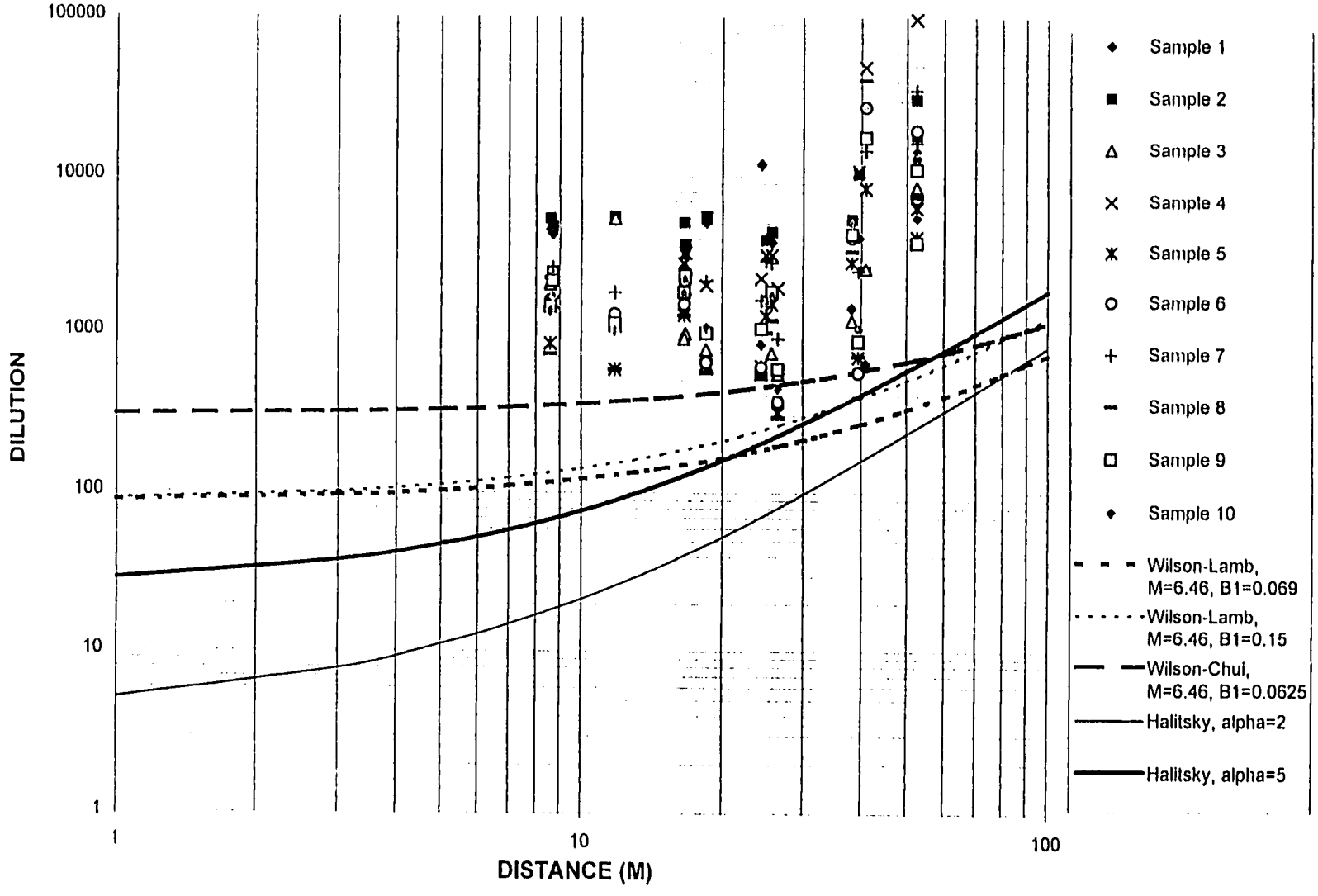

Figure 4-13 Dilution data of Hall Building Test No.2 (July 2nd, 97) with ASHRAE minimum dilution curves

During the two and half hours of sampling, θ varied from 152° to 232°. Consequently, both the Wilson-Lamb curve and the Halitsky curves are well below the dilution data. On the other hand, the Wilson-Chui model overestimates D_{min} due to the high value of M, which produces an unrealistically large initial dilution (D_e=293). Note that the Wilson-Lamb model predicts an initial dilution of only 85.5.

As previously discussed for Test No.1 and No.4, the Halitsky model with α=2 provides conservative estimations of D_{min}; however, with α=5, it gives better predictions than the other two models especially for distances greater than 20m. As for the Wilson-Lamb model, the reason why it underpredicts the dilution data of Test No.2 may be partly due to the inaccurate B1 value. Since wind direction varied significantly during Test No.2, perhaps a higher B1 value should be applied in this case. An additional Wilson-Lamb curve with B1=0.15 (σ_θ=60°) was included in Figure 4-13 and seems to provide a more appropriate bottom line for the full-scale dilution data.

Figure 4-14 shows the dilution data of Test No.3 (July 30). Minimum values of dilution for this test were lower than those obtained in Test Nos. 1 and 4 by a factor about 2, even though the wind conditions were similar. Wind data from the Hall Building anemometer were not available, but could be estimated. Wind direction for each sampling period can be determined approximately by examining the concentration distribution on the roof. For example, Figure 4-15 shows concentration data for sampling periods No.1 and No.6. Note that the shaded region, which contains the lowest dilution values, indicates the mean wind direction. Based on this analysis, the wind direction for Test No.3 was assumed to be approximately 215°.

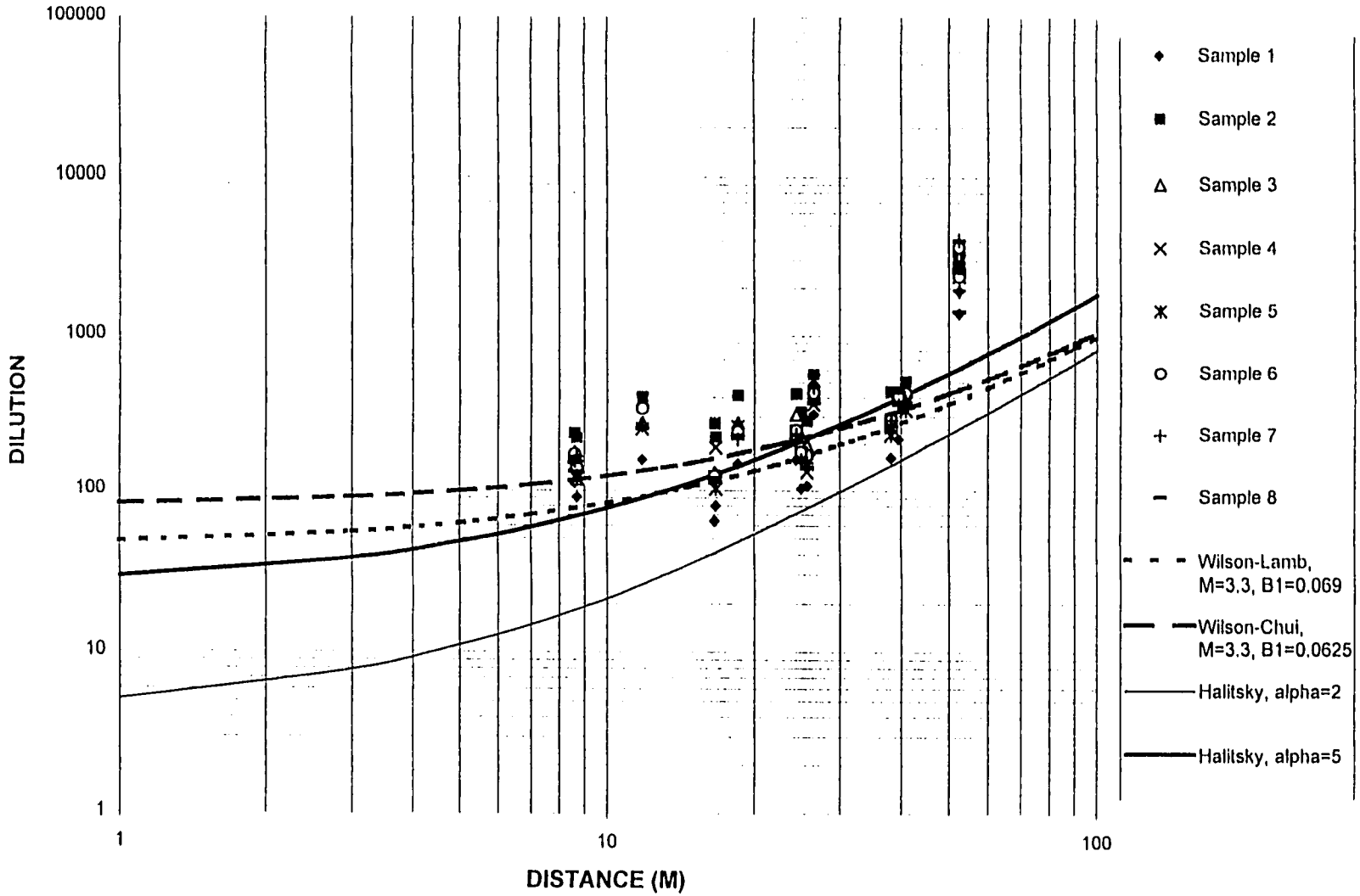

Figure 4-14 Dilution data of Hall Building Test No.3 (July 30th, 97) with ASHRAE minimum dilution curves

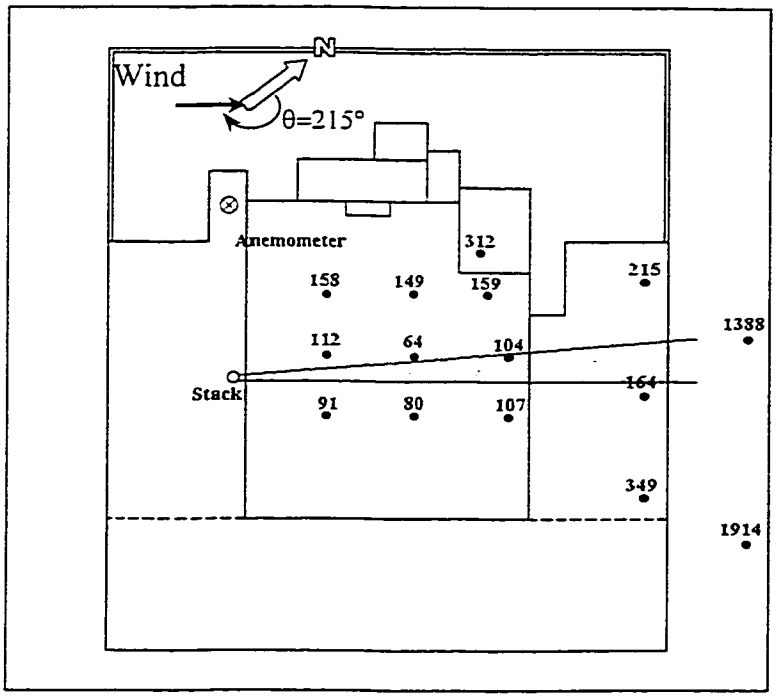

a) Dilution data of sample period No.1 in Test No.3

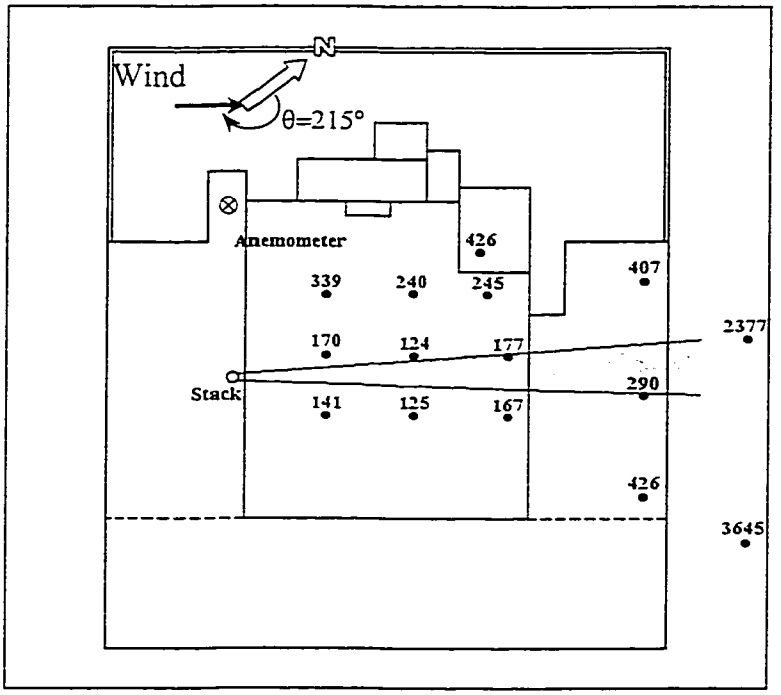

b) Dilution data of sample period No.6 in Test No.3

Figure 4-15 Wind direction estimation for field Test No.3 using dilution data

Wind speed must be determined from the hourly wind data obtained on the Webster Building. Based on data from the other tests, $U_{Hall} \approx 1.8\ U_{Web.}$ Therefore, it was assumed that, for Test No.3, the mean wind speed was approximately 4.5 m/s (M=3.3).

As plotted in Figure 4-14, both Wilson-Lamb and Wilson-Chui model overestimate the minimum dilution by a factor of 2, whereas the Halitsky model with $\alpha=2$ provides slightly conservative predictions. As will be discussed later in section 4.2, the low D values obtained in Test No.3 may be due to a relatively high M value, compared to those measured in Tests No.1 and No4.

Critical dilution values were calculated using the ASHRAE model for zero stack height [equation (2.14) and (2.15)] and plotted with field data in Figure 4-16. It appears that the critical dilution curve provides a satisfactory lower bound for field data obtained during Test No.1 (see Figure 4-16 a). However, some of the data from Test No.3 are found to be under the critical dilution curve, as shown in Figure 4-16 b. Therefore, based on the limited data set of the current study, the ASHRAE model for estimating the critical dilution with zero stack height may provide unconservative dilution estimations under particular wind conditions.

4.2 Wind Tunnel Study

After the completion of the field study, a series of wind tunnel experiments were performed with a 1:500 scale model of the Hall Building and surroundings in the

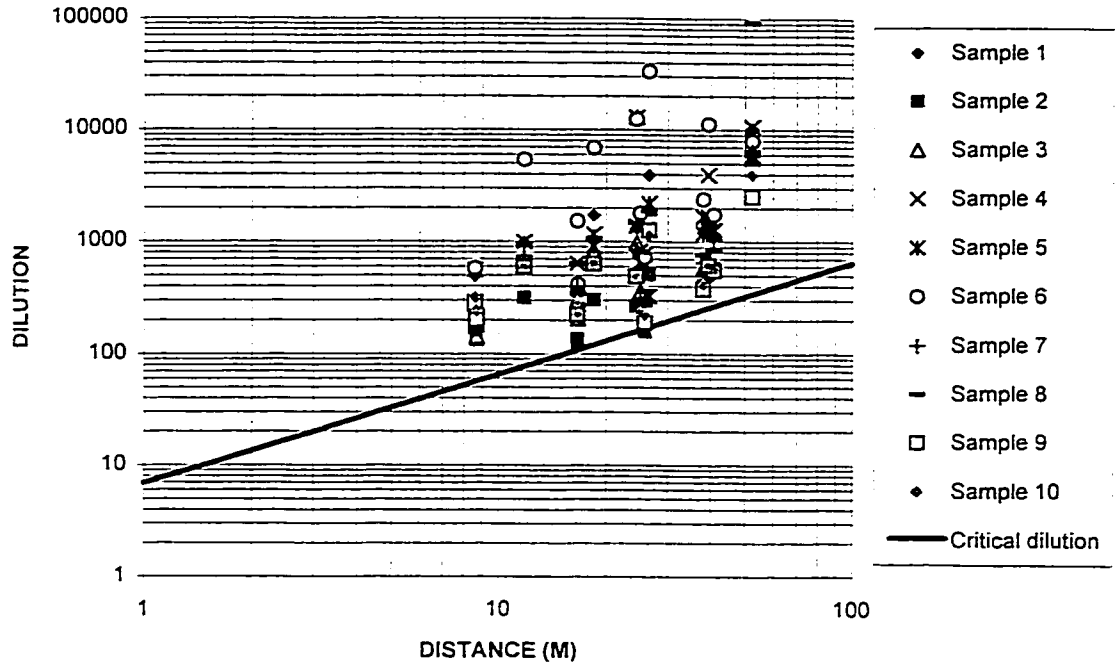

a) Field Test No.1 (June 26th, 1997)

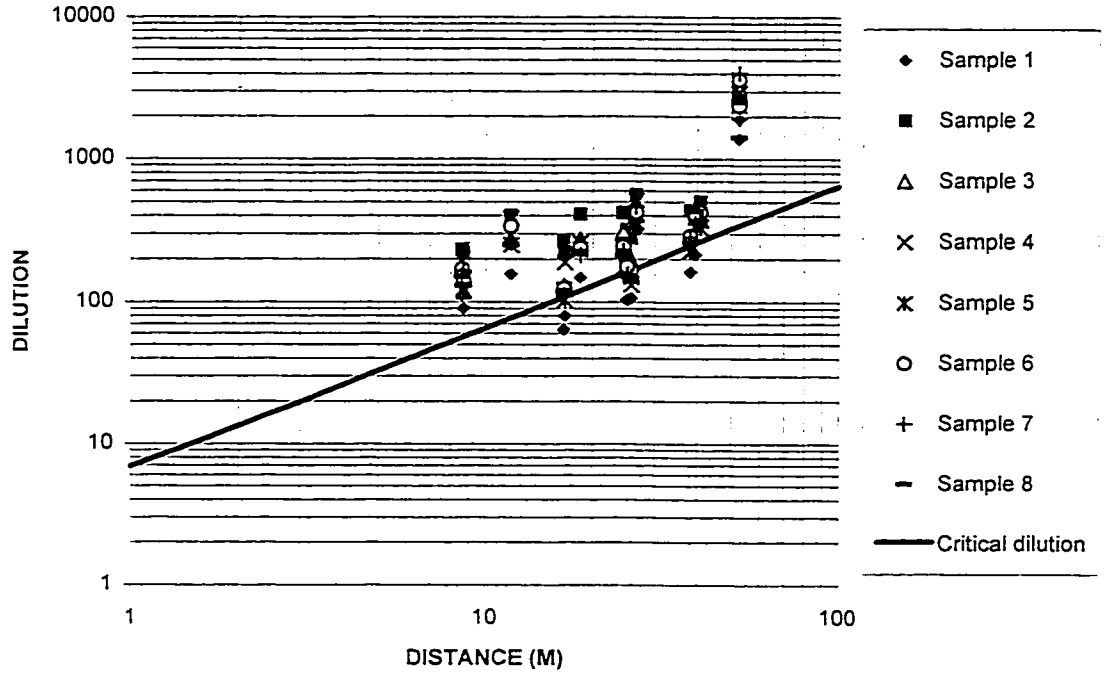

b) Field Test No.3 (July 39th, 1997)

Figure 4-16 Comparison of field data with critical dilution curve

boundary layer wind tunnel. This part of the study had several goals. Firstly, it was important to evaluate the validity of wind tunnel tracer gas measurements by comparing with field data. Secondly, the influence of surrounding buildings was evaluated by repeating the experiments with an isolated Hall Building. The third topic concerned the influence of stack height and stack location. Finally, the influence of the building shape on exhaust dilution was investigated.

4.2.1 Effect of momentum ratio on dilution

Preliminary wind tunnel experiments indicated that dilution values at some locations dropped by a factor of eight as the M-value was increased from 3 to 4. The effect of momentum ratio was investigated in detail at selected tappings by evaluating the variation in D produced by an incremental change in M. Figure 4-17 shows the dilution variation versus M-value at tappings 2, 5, 8, and 12 for θ=215°, at which direction that wind is approximately normal to the windward face of the building. Results show that dilution measured at each tapping keeps increasing with M until the M-value reaches about 3.5. A sharp reduction in dilution by factors of 2.5 to 4 occurs when M increases from 3.5 to 4. Similar variation in dilution was found for other wind directions. Data for θ=210° are also shown in Figure 4-17.

Although the limited amount of field data does not allow firm conclusions to be drawn, it is very interesting to find that the field dilution data appear to show similar variation with M. As previously mentioned, the wind velocity was constantly changing during the field tests, which resulted in high uncertainty of full-scale momentum ratio. In order to reduce

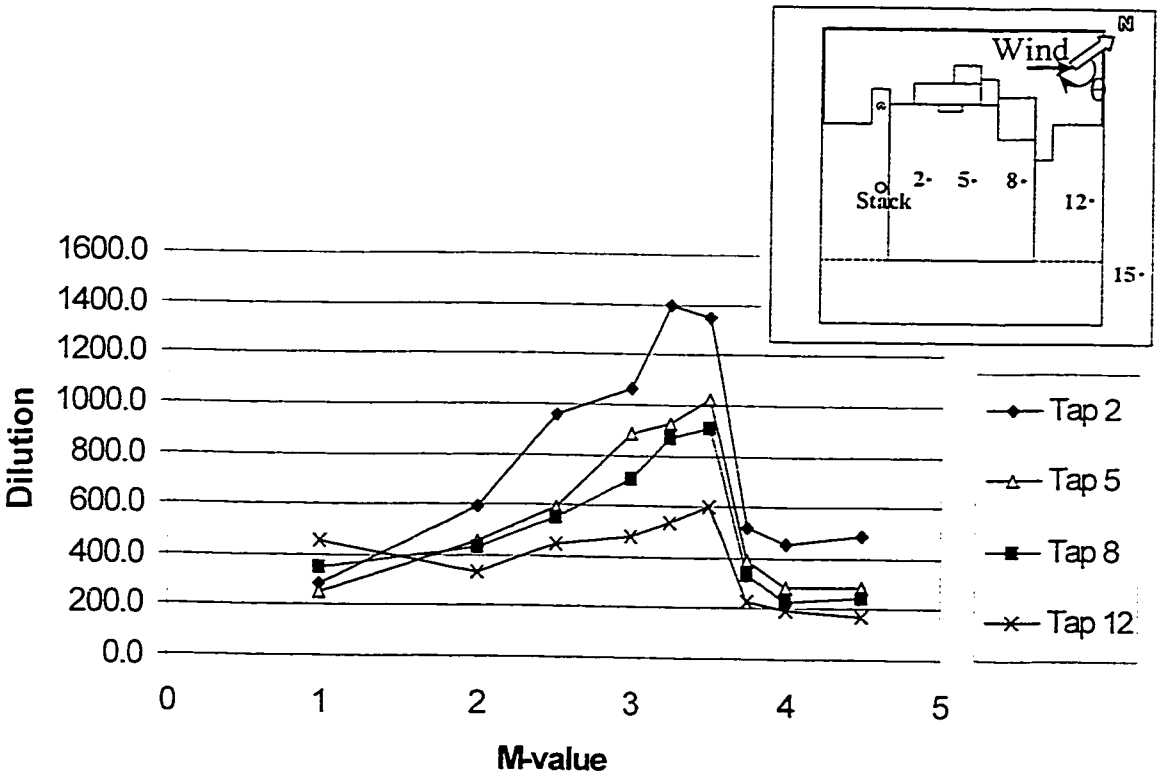

a) $\theta = 215°$

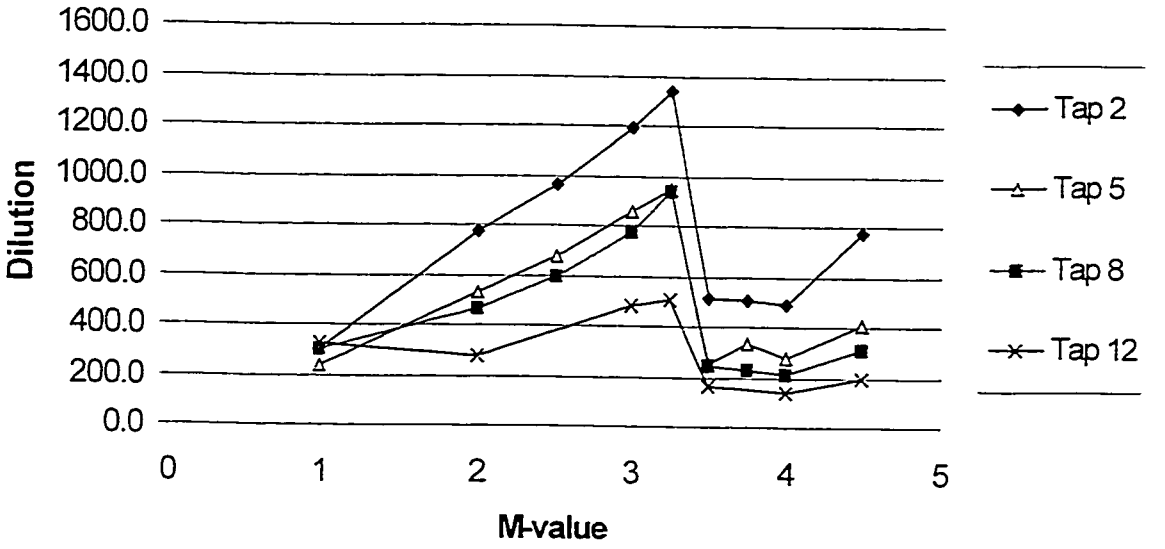

b) $\theta = 210°$

Figure 4-17 Dilution variation with M-value, at $\theta = 215°$ and $\theta = 210°$

the inaccuracy caused by the uncertainty of M-value, averaged dilution values of two adjacent sample locations (i.e. locations 2 and 5, 8 and 12) were plotted in Figure 4-18, with the similarly-averaged wind tunnel data. Both the magnitude of the full-scale dilution variation and the critical M-value, at which dilution values start to decrease, are lower compared to the wind tunnel results, especially at near stack locations. Nevertheless, the field data for locations relatively far from the stack (Nos. 8 and 12) show a similar drop in dilution as M is increased above a value of 3.

The large discrepancy between full-scale and wind tunnel dilution data may be partly due to the significant changing of wind speed and direction during the full-scale tests. As will be discussed, for the near stack locations, dilution values at θ=205° and θ=230° were found significantly lower than that at θ=215°. Besides, as previously discussed, real M-values may have been actually higher than those recorded. However, further experiments still have to be done to investigate the real cause of the discrepancy.

Wind tunnel experiments were also carried out without the surrounding buildings to determine whether the upstream buildings cause the peculiar variation of dilution with M. In this case, the dramatic change of dilution data did not occur. Figure 4-19 shows that dilution values measured at all 4 tappings decrease smoothly with increasing M up to M=4 and increase very slightly with M for 4<M<6. For the isolated Hall Building, the reduction of dilution with increasing M becomes larger as S increases. For example, increasing M from 1 to 4 causes dilution to decrease by a factor of 4.3 at the farthest tapping 12; whereas, at the near stack location (tapping 2), dilution is reduced only by a factor of 2.5. Note that results obtained with upstream buildings show the opposite trend:

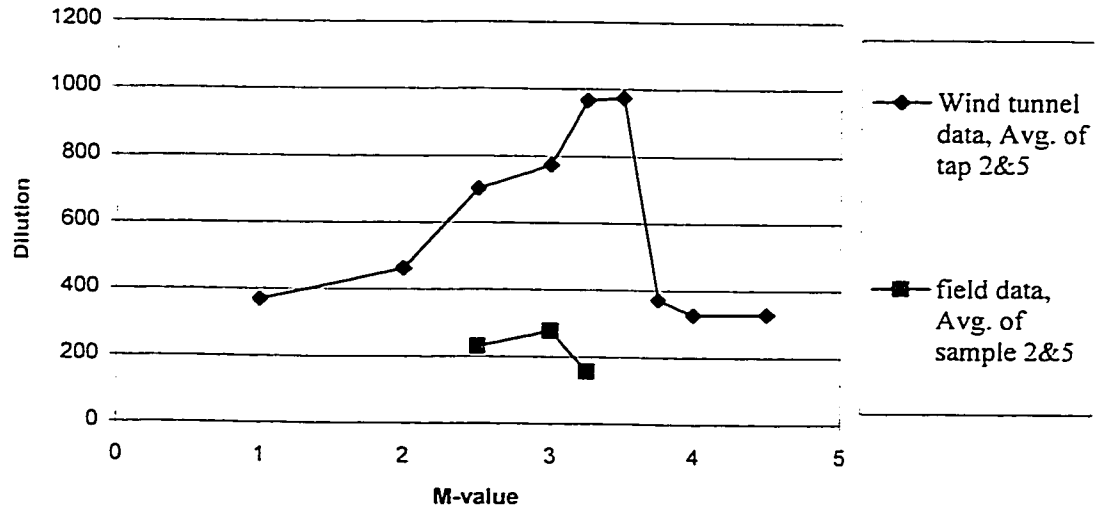

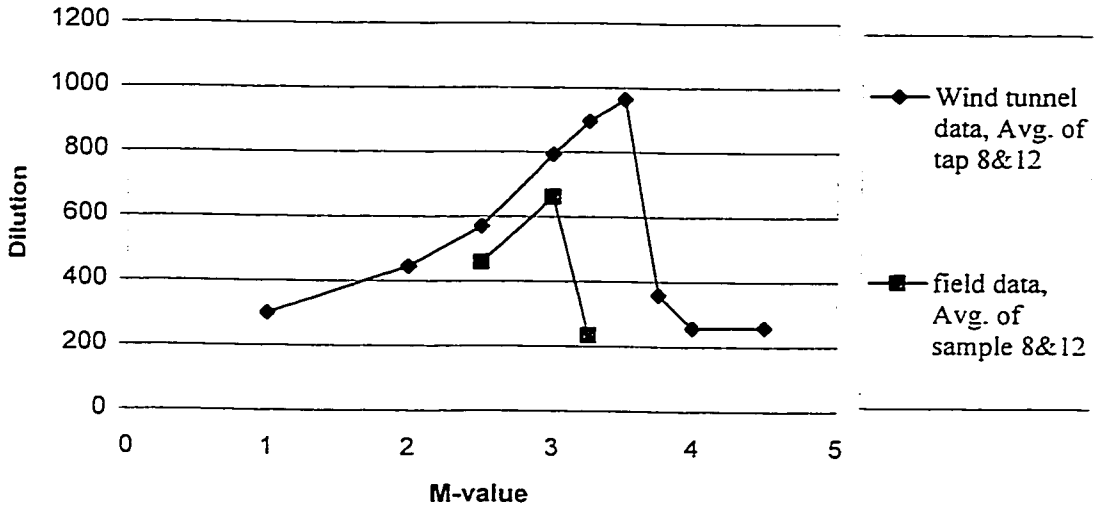

Figure 4-18 M-value effect on averaged dilutions of field and wind tunnel tests, at θ=215°

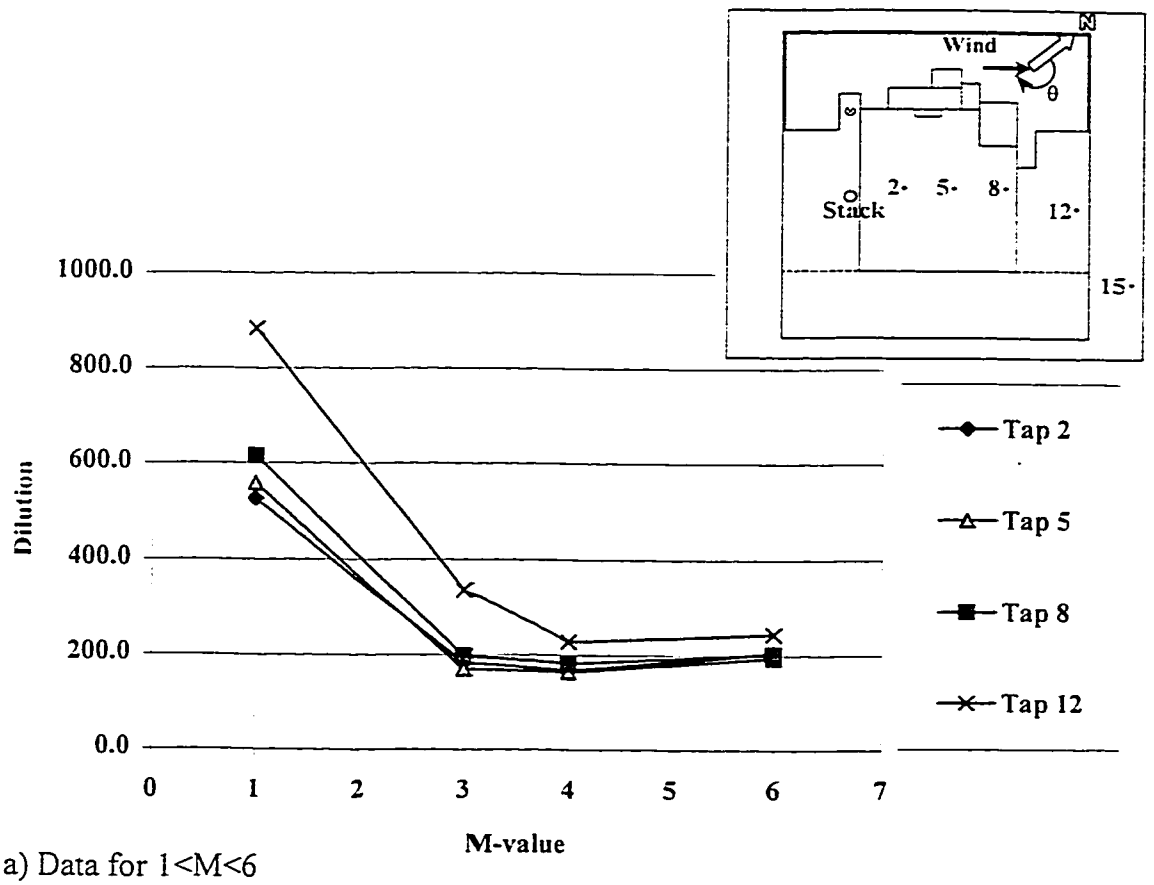

a) Data for 1<M<6

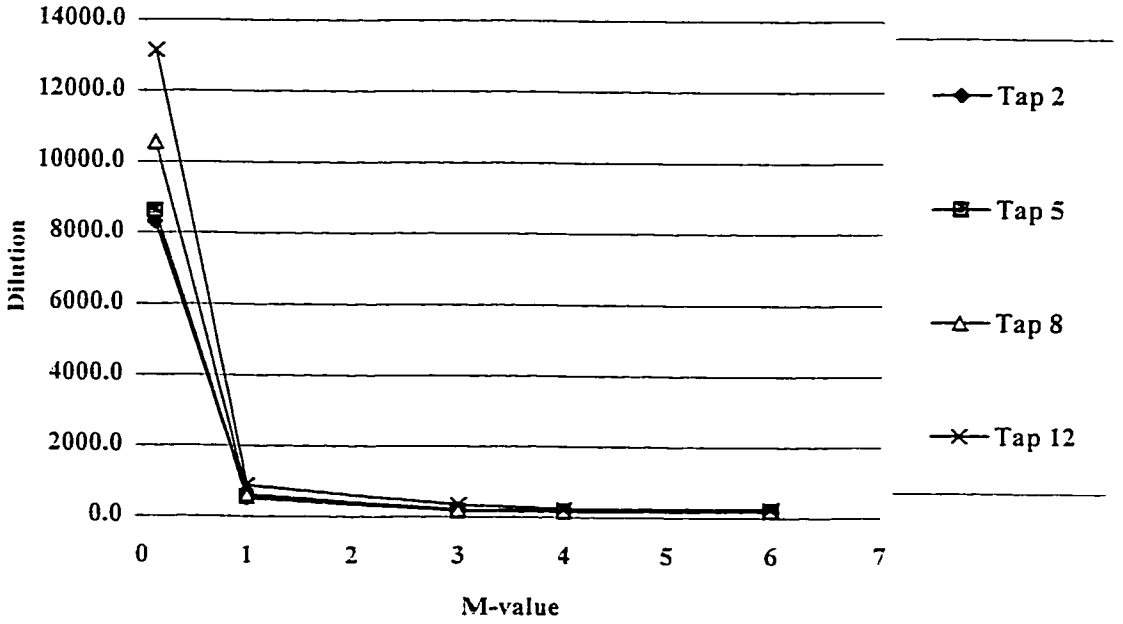

b) Data for 0.1<M<6

Figure 4-19 Dilution variation with M-value for isolated building, at θ=215°

increasing M from 1 to 3.5 causes D to increase and the effect is more significant as S decreases.

The variation of dilution with M for the isolated Hall Building shown in Figure 4-19 is expected to be typical of buildings with small aspect ratio, (i.e. L/H<1.5, where L is the building dimension in the flow direction). For this particular building geometry, the roof is almost entirely covered by the flow separation zone. A flush vent with a typical flow rate will inevitably produce low dilution when M is between 2 and 6, since the exhaust is trapped in the separation region and brought back to the roof by the recirculation flow. This special phenomenon is also shown by flow visualisation tests, which will be discussed later in section 4.3. Note that a low flow vent (M<<1) is associated with high dilution values (see Figure 4-19 b), since the amount of contaminant in the recirculation zone is small.

4.2.2 Comparison of wind tunnel data with field data

Figure 4-20 and 4-21 show dilution contours of field and wind tunnel data obtained with M=3 for θ=205° and θ=215°, respectively. All of the full-scale data were acquired in Test 1 (June 26). Generally, the wind tunnel data show good agreement with the field data. Discrepancies are usually within a factor of two. However, Figure 4-21 shows that for θ=215°, wind tunnel dilution measurements obtained at location No.1, 2 and 3 exceeded the full-scale results by as much as a factor of four. These discrepancies may be due to the variations in M-value during the sampling period of the field test.

Wind tunnel and field data were compared in more detail for a few specific locations. Locations 2, 5, 8 and 12 were chosen because they are roughly along the centre-line of

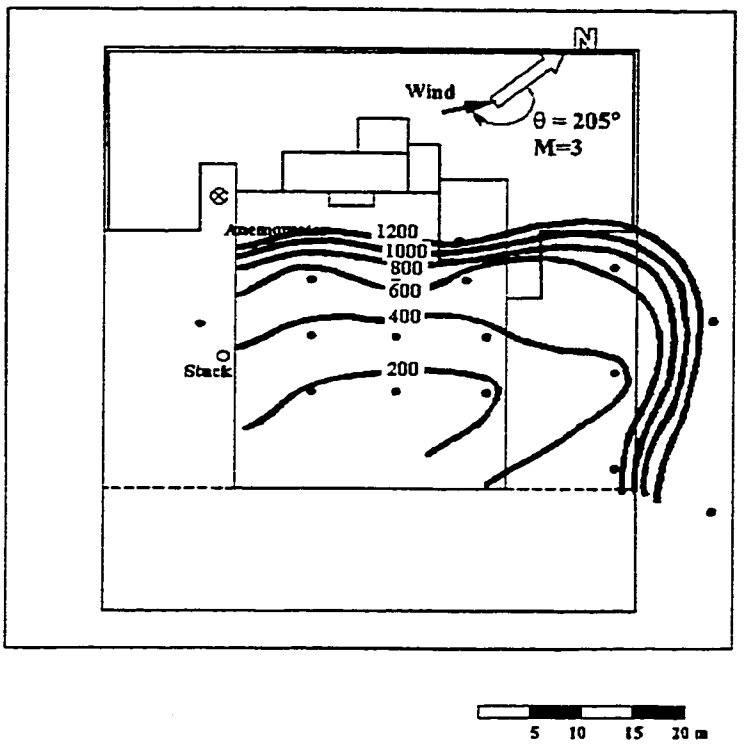

a) field data

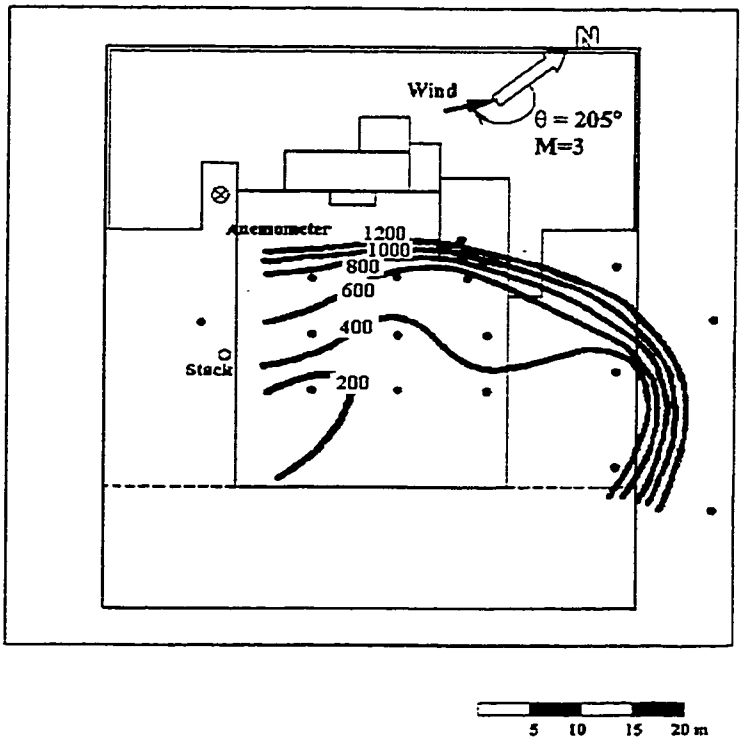

b) wind tunnel data

Figure 4-20 Dilution contours of field and wind tunnel data, θ=205° and M=3

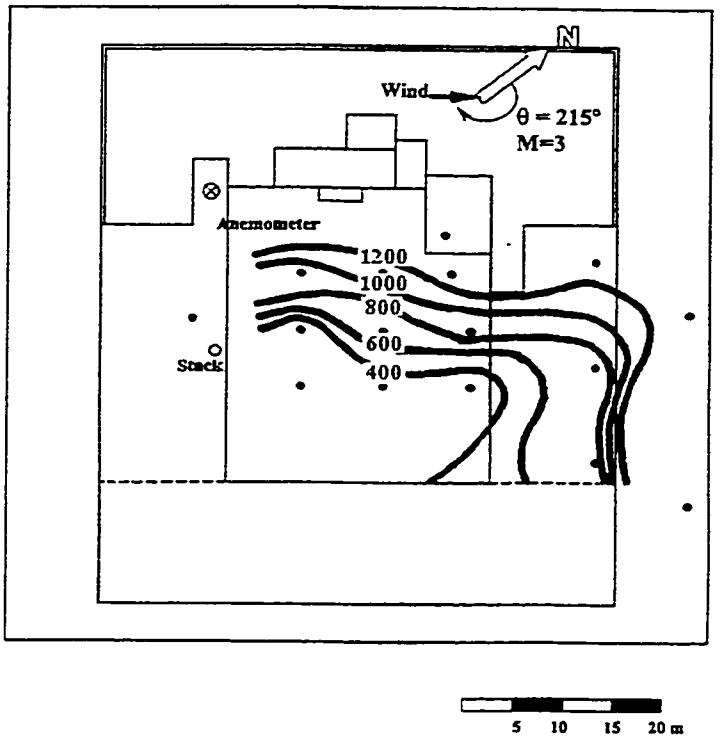

a) field data

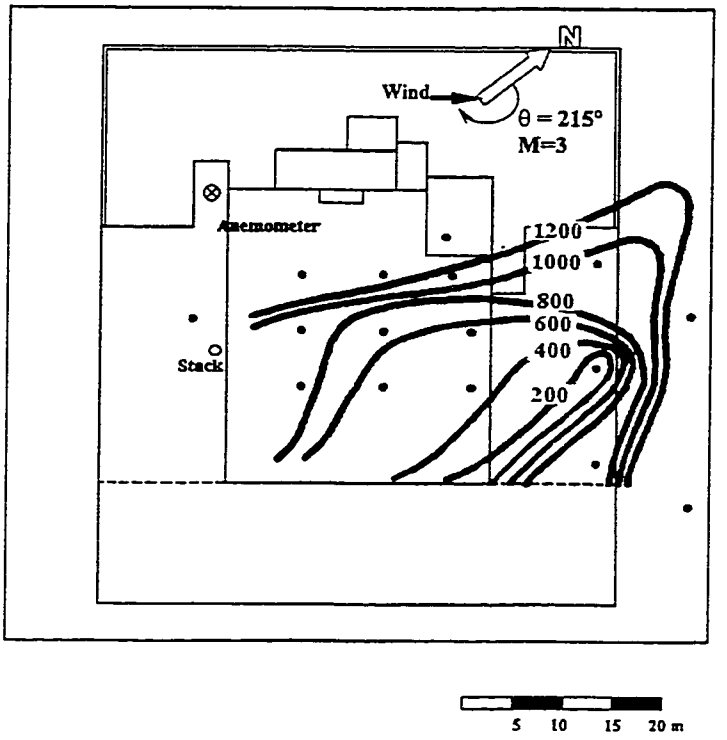

b) wind tunnel data

Figure 4-21 Dilution contours of field and wind tunnel data, θ=215° and M=3

the predominant wind (θ=215°), starting from near the stack to rear edge of the building roof. Sampler No.15, located on 12th floor ledge has also been considered.

Data from Test 2, which had a high M-value and low wind speed, have not been included, since low wind speed conditions cannot be accurately simulated in the wind tunnel. Figure 4-22 and 4-23 compare field and wind tunnel data for the selected locations for a range of wind directions (200°<θ<235°). Considering the importance of the momentum ratio, data have been obtained for 2<M<4. It should be noted that due to the lack of wind data for Test 3, a single value of θ=215° has been used for all samplers and a constant M-value of 3.3 was assumed.

The accuracy of wind tunnel data appears to depend on distance from the stack. At location 2, most of the full-scale dilution values fall below the wind tunnel data curves. On the other hand, full-scale dilution data at other tappings, Nos. 5, 8 and 12, are generally bounded by wind tunnel data curves. Data obtained at location 15 show a larger scattering; when θ<215°, field data are generally below the wind tunnel data, whereas when θ>215°, field data are well above the wind tunnel data curves. As previously discussed, the wind tunnel data show M has a significant impact on D-values. Generally, minimum dilution at each θ was obtained for M=3.5 and M=4, while maximum dilution occurred for M=3.

Because field M values are averaged over a 15-min sample period and wind speed fluctuated significantly during the tests, the uncertainty of the field M-values is significant. Figure 4-24 shows the turbulence intensity and standard deviation of wind direction measured on 29th of July, 1997, one day before the field test No.3. During the

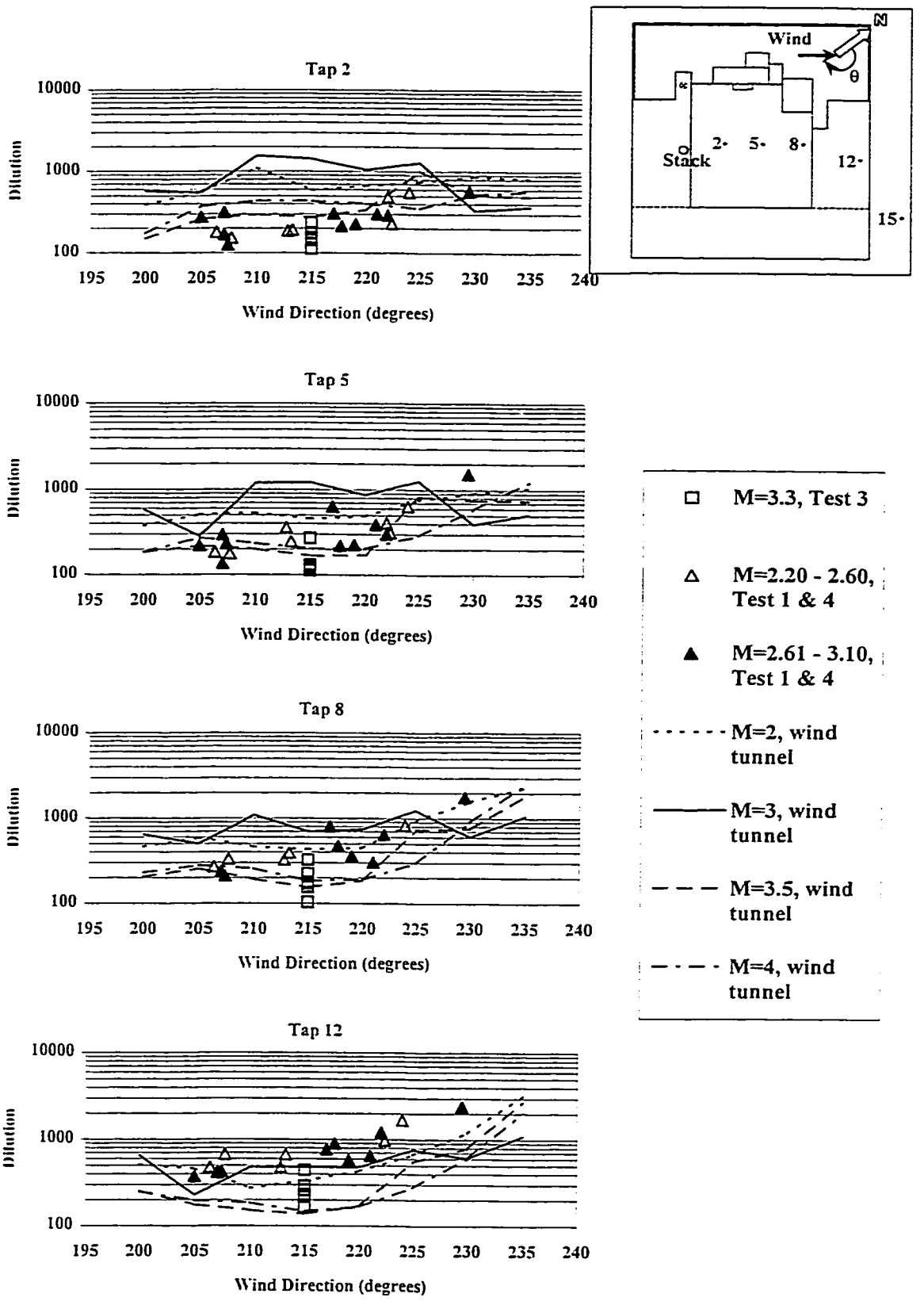

Figure 4-22 Comparison of field and wind tunnel dilution data, tappings 2, 5, 8 and 12

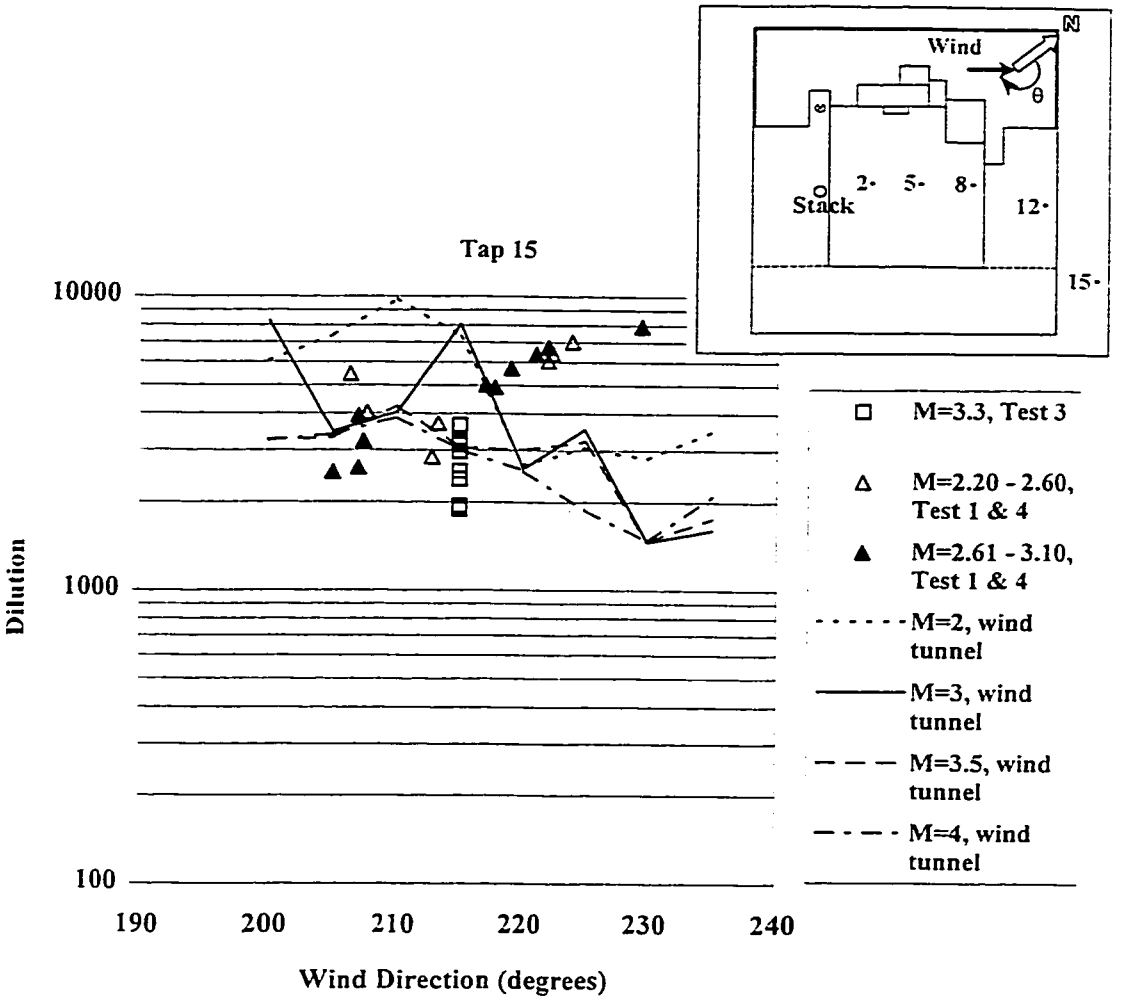

Figure 4-23 Comparison of field and wind tunnel dilution data, tapping 15

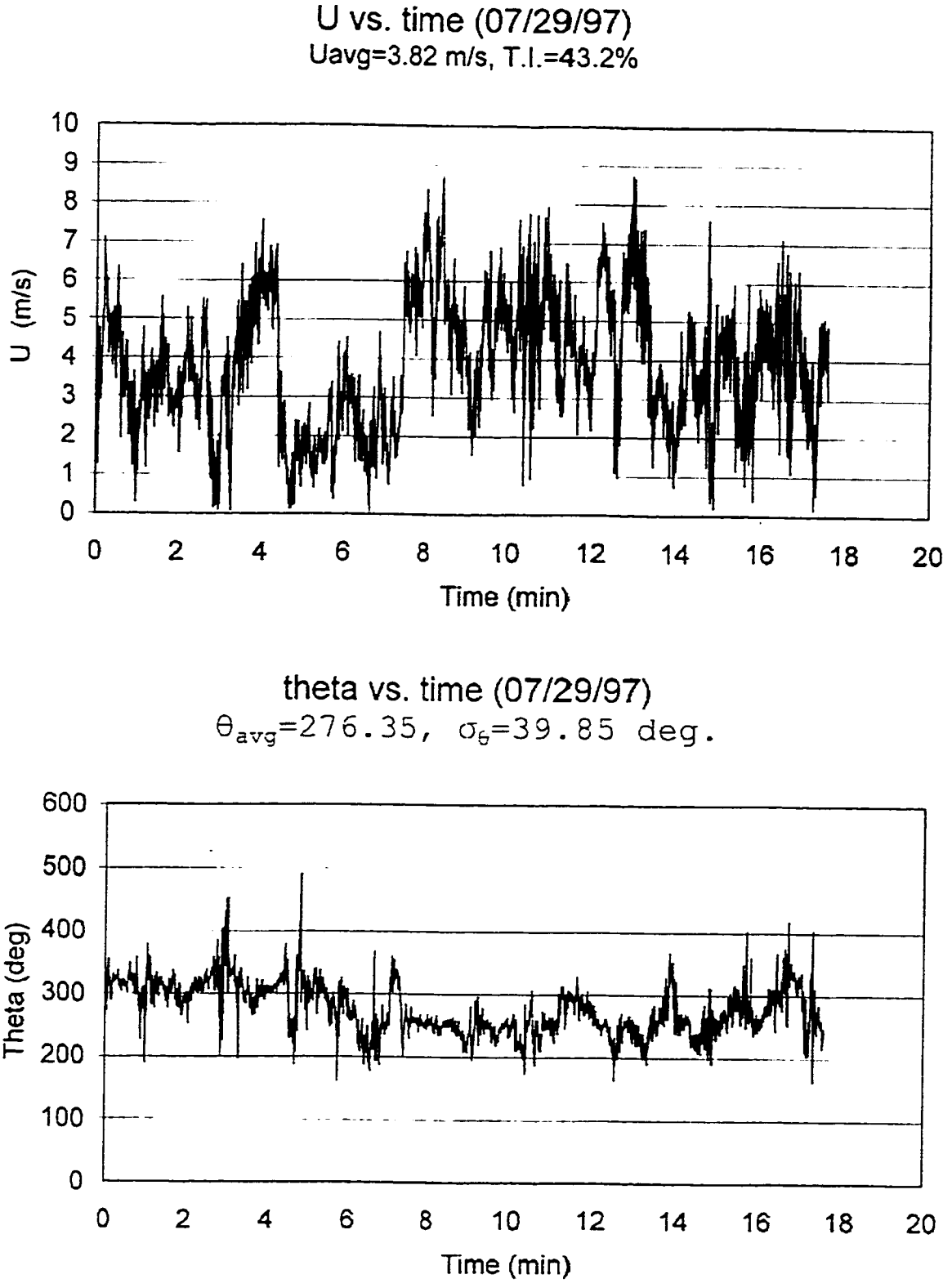

Figure 4-24 Short period wind record obtained at Hall anemometer

18 minutes, wind speed fluctuated from nearly 0 m/s to a peak value of 8.7 m/s, which results in a very high turbulence intensity of 43.2%. Similar values of turbulence intensity were recorded during Test 1 and Test 4. In contrast, the highest turbulence intensity detected in wind tunnel experiments was only 25% to 30%. The high turbulence intensity in the field tests is due to low frequency fluctuation in wind speeds. The discrepancy in turbulence intensity and the high variability of the full-scale M-value during the 15-minute sampling period are important factors when comparing the field and wind tunnel data.

The high variability of full-scale momentum ratio is evident in Test 1 data, which were obtained using 5-minute samples of wind speeds and directions. For example, three 5-minute average M-values of 2.0, 2.27 and 3.4 were recorded during sample period 3 of Test No.1. In this case the M-value exceeded the critical M-value (see Figure 4-18) during much of the sampling period even though the average M-value of 2.56 is well below the critical M.

Similarly, the uncertainty of wind tunnel M-values must also be considered when comparing wind tunnel and field data. The reference wind speed measured above the roof may vary by ±10% depending on the location of the hot wire probe. Likewise, the effective exhaust speed is not known precisely since the flow is laminar at the stack outlet. Near the centre of the stack, the velocity is significantly higher than that for a turbulent flow. Thus, it may not be appropriate to directly compare the field M-value with those of the wind tunnel study. Considering the uncertainties in the M-values, the wind tunnel data have been plotted in Figure 4-25 showing the range of dilution values

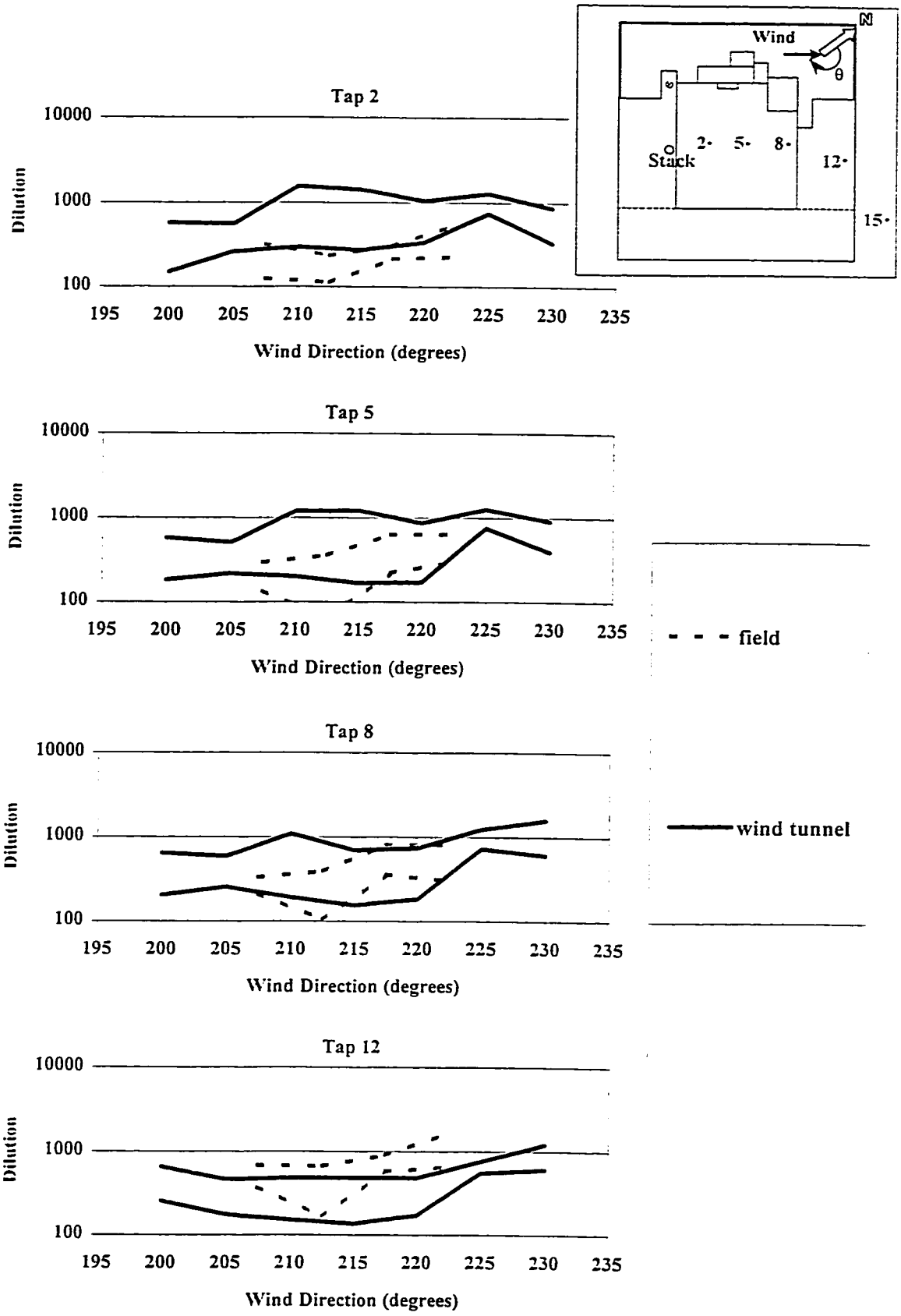

Figure 4-25 Field and wind tunnel dilution range for 2<M<4

obtained with M-values between 2 and 4. As shown in Figure 4-25, the overlap area of field and wind tunnel data ranges increases, or in other words, the agreement between field and wind tunnel data improves as the distance between stack and sample location increases.

4.2.3 Comparison of wind tunnel data with ASHRAE curves

Wind tunnel data obtained for the wind approximately normal to the front face ($210° \leq \theta \leq 220°$) are plotted in Figure 4-26 a) for a range of M-values from 2 to 4. Note that data for tappings 14 and 15 are not included in the figure, since those tappings are located in the wake region of the building. The Halitsky curve with $\alpha=2$ and the Wilson-Lamb model with parameter $B_1=0.069$ (the same as has been used in field data analysis) have been included in Figure 4-26. Generally, the Wilson-Lamb model provides an appropriate lower boundary for the wind tunnel data, although it gives unconservative predictions in some cases. In contrast, the Halitsky model provides relatively conservative estimations except at the location farthest from the source.

For comparison, field data from Tests 1, 3 and 4 are shown in Figure 4-26 b) with the same minimum dilution curves. The field results are similar to the wind tunnel data, which is not surprising since they have a similar range of wind directions and M-values. An interesting finding is that field dilution data tend to increase as the distance from the source increases, which matches with the estimations of minimum dilution models. However, wind tunnel data show an insignificant variation as the distance from the stack increases. The reason why this particular phenomenon occurred is not clear.

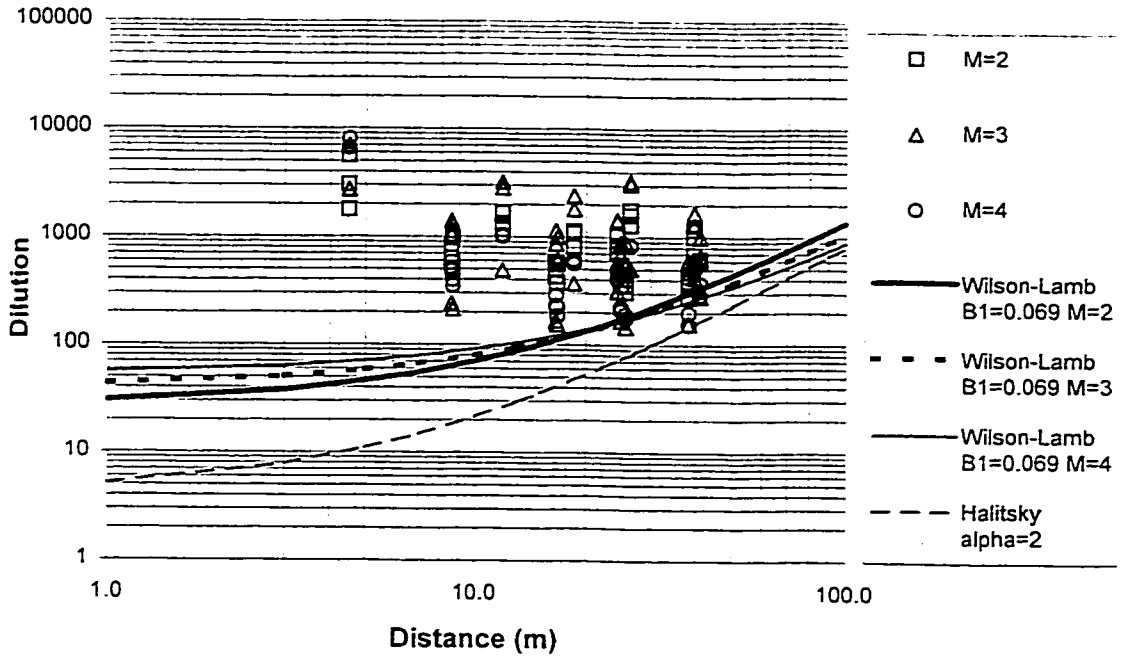

a) Wind tunnel data, $\theta = 210° \sim 220°$

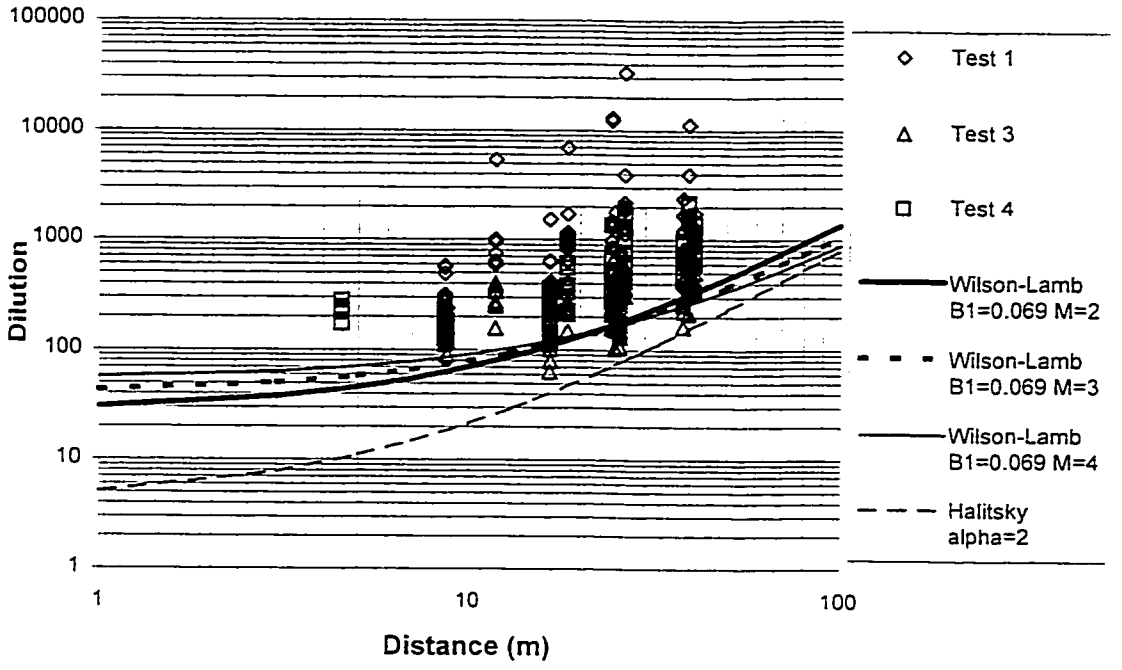

b) Field data

Figure 4-26 Comparison of wind tunnel data and ASHRAE model estimations

4.2.4 Effect of stack height on dilution

A common method for increasing dilution at critical roof receptors (e.g. fresh air intake) is to increase the stack height. ASHRAE (1997) provides design formulas for predicting the critical dilution at a particular location for various stack heights. These formulas are based on wind tunnel experiments with isolated building models and have not been evaluated extensively for buildings in an urban environment.

Dilution variations with three different stack heights were measured and the results are plotted in Figure 4-27 and 4-28. Generally, as a consequence of raising the stack height, higher dilution will be obtained at all locations. However, the magnitude of the increase in dilution varies significantly depending on the tapping location, with near stack locations being most strongly affected. For example, dilution data obtained at tapping 2, which is nearest to the stack, increases by a factor of nearly 25 when the full-scale stack height is raised from 0.5 m to 5 m (i.e. 1 mm to 10 mm in wind tunnel). In comparison, at the farthest tapping 12, the dilution value increases by only a factor of 3. Therefore, it can be concluded that as the distance from stack increases, the influence of stack height on roof level dilution becomes less significant.

Similar results have been obtained by Wilson & Winkel (1982) and Schulman & Scire (1991). However, these results are mainly based on experiments carried out on low-rise building models, for which the roof recirculation zone is small. Wilson (1982) concluded that 'if the stack is buried in a flow recirculation cavity, an increase in stack height has virtually no effect on contamination concentrations at air intakes'. However, it should be noted that Wilson's experiments involved relatively low M values. The high M values

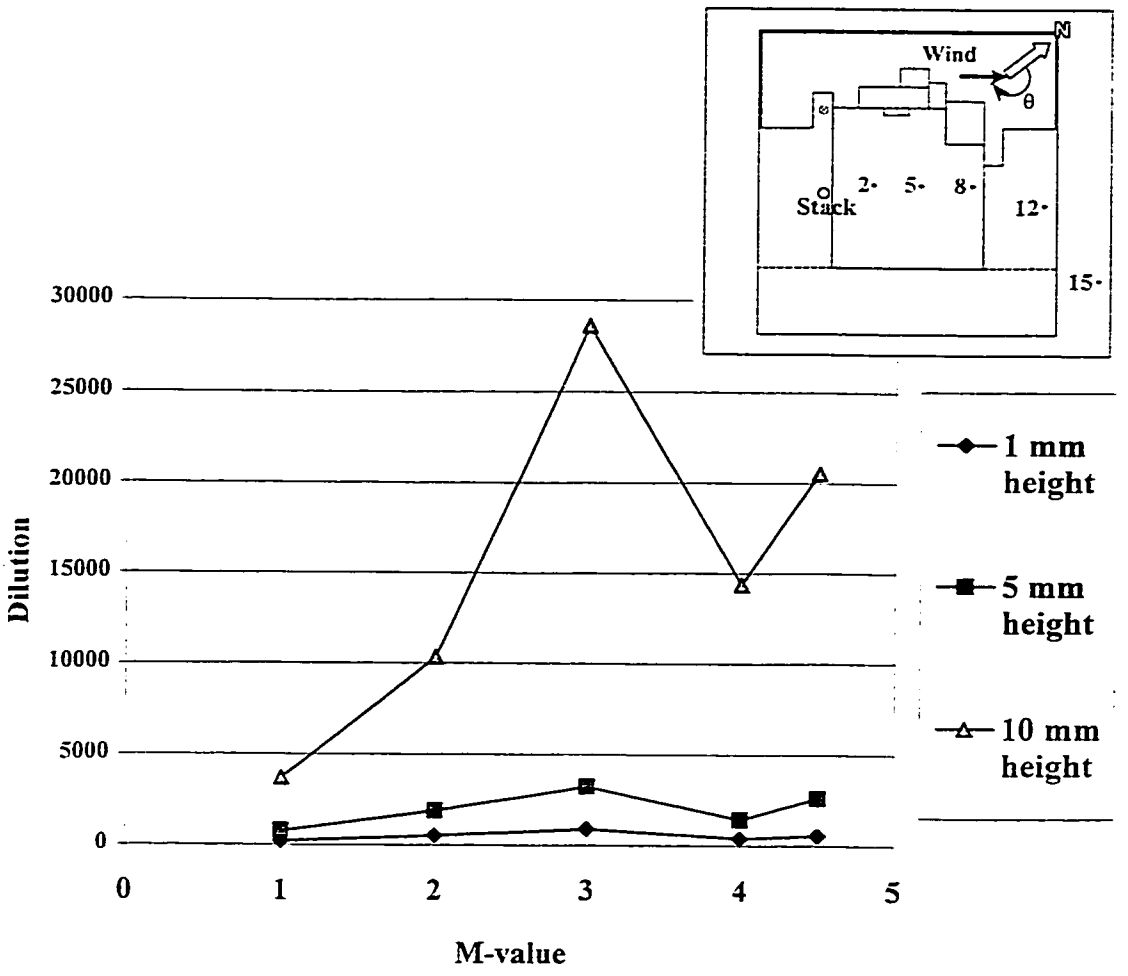

Figure 4-27 Stack height effect on dilution value, Tap 2

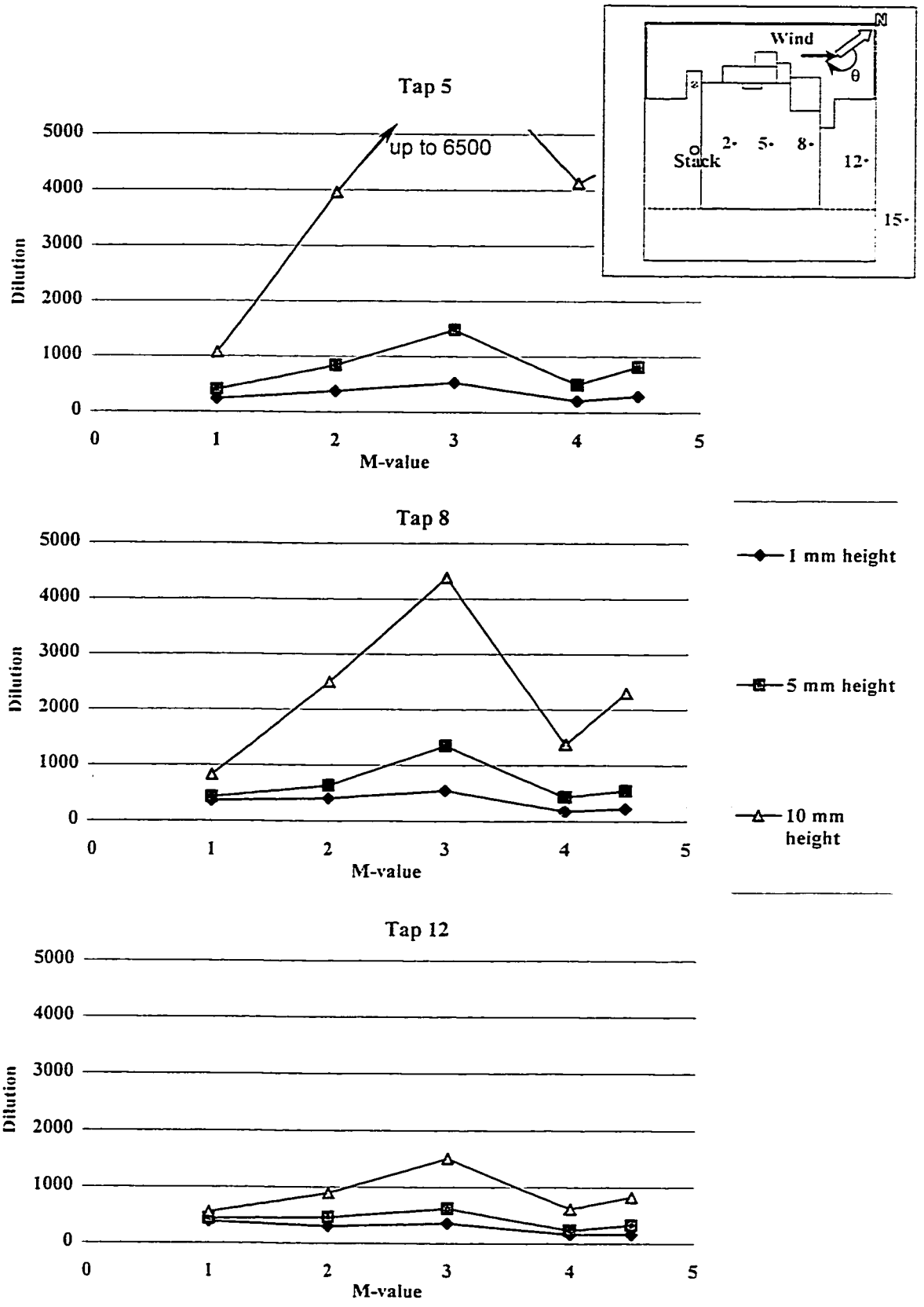

Figure 4-28 Stack height effect on dilution value, Tap 5, 8 and 12

used in the present study appear to contradict this statement. It should also be noted that the previous studies have been carried out with isolated models.

As disussed in Chapter 2, ASHRAE provides formulas for estimating the effect of stack height on the critical dilution, D_{crit}, at a particular distance from the stack. Using these formulas (equations 2.16-2.18), D_{crit} curves for h_s=2.5 m and h_s=5.0 m have been plotted in Figure 4-29, along with the wind tunnel values. For both stack heights, D_{crit} curves overestimate the minimum dilution values obtained in the wind tunnel. As the stack height is increased from 2.5 m to 5 m (i.e. from 5 mm to 10 mm in the wind tunnel), a more unconservative result is obtained using the ASHRAE model. Thus, these results indicate that the ASHRAE stack height design formula may not be appropriate, at least for cubical buildings in an urban environment.

Another interesting finding is that the peculiar dilution variation with M, which has been found for the short stack (h_s>0.5 m), appears to exist for all stack heights up to h_s=5m, at least. As shown in Figure 4-28, dilution values increase with M up to 3 and drop at an M-value between 3 and 4 and increase again for M>4. Note that the sharp drop in dilution for M>3 is not evident in Figure 4-28, since data were not obtained for the small increments of M used in the flush vent analysis. The reason for the large variation in dilution with M is still unclear.

4.2.5 Effect of stack location on dilution

Three different stack locations were investigated in the present study. In addition to the original stack location, data were obtained for a stack near the leading edge and a

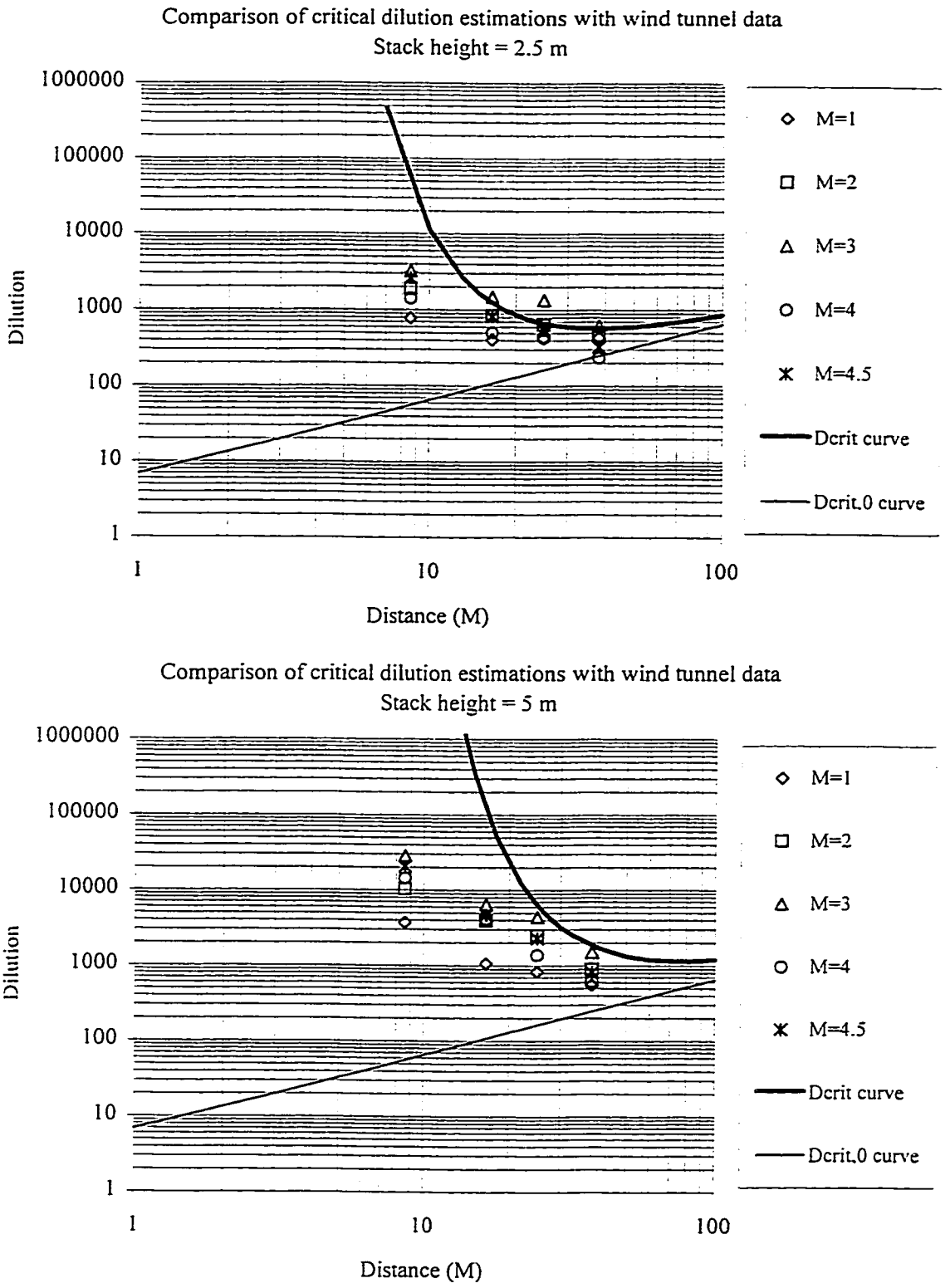

Figure 4-29 Comparison of wind tunnel data with D_{crit} curve considering the stack height effect

centrally located stack. Data were obtained only for θ=215°. Concentration values were measured at tappings 2 and 12, which are expected to be representative tappings.

As shown in Figure 4-30, moving the stack to the leading edge does not improve the exhaust dispersion. On the contrary, a lower dilution value was measured near the stack at tapping 2. For the farthest tapping 12, the results are similar to the previous data obtained with the current stack location, except at M=3, where dilution is reduced by a factor of 2. When the stack was changed to the central location, dilution decreased significantly at tapping 12. Since very high dilution values were measured at tapping 2 for the central location due to the far upwind distance from the stack, these data are not included in Figure 4-30. It is interesting to note that changing the stack location diminished the peculiar rise of dilution with M found with the original stack location.

4.2.6 Effect of building shape on dilution

The effect of building shape on exhaust dispersion has been extensively investigated by Wilson (1979) and Wilson and Chui (1985). These studies have found that building shape has a significant influence on plume dilution. In order to demonstrate the importance of building shape, a series of wind tunnel experiments were carried out using an isolated model of the building used in field test of Lamb and Cronn (1986) and Wilson and Lamb (1994). This building is located on the campus of Washington State University (WSU) and is shown in Figure 4-31. It is approximately 90 m long and only 18 m high, and thus the aspect ratio of 5 is much larger than that for the Hall Building.

Two tests were carried out with the isolated WSU model for four exhaust speeds, as

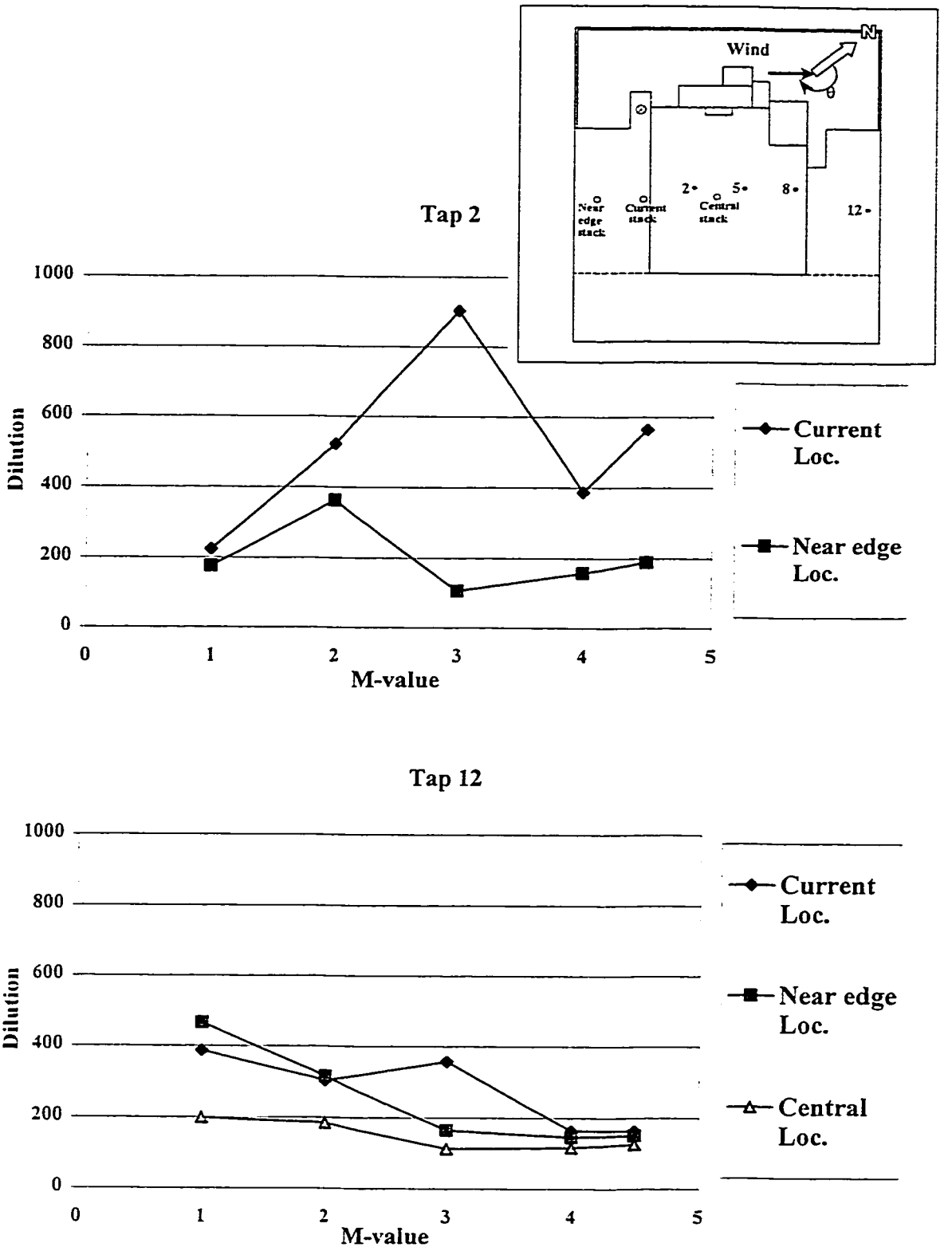

Figure 4-30 Stack location effect on dilution value, Tap 2 and 12, θ=215°

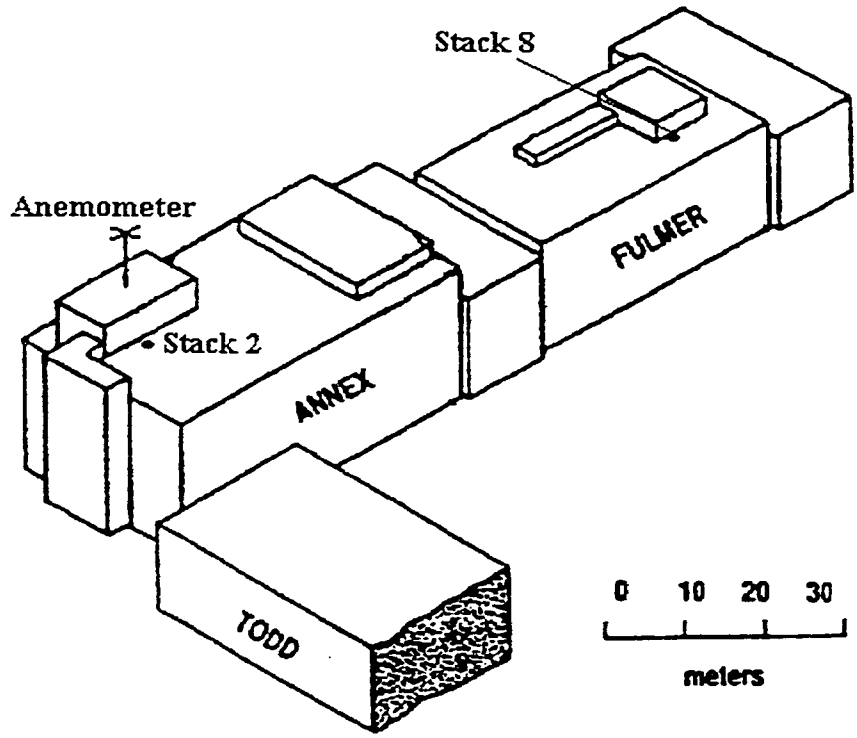

a) The Fulmer Hall/Annex

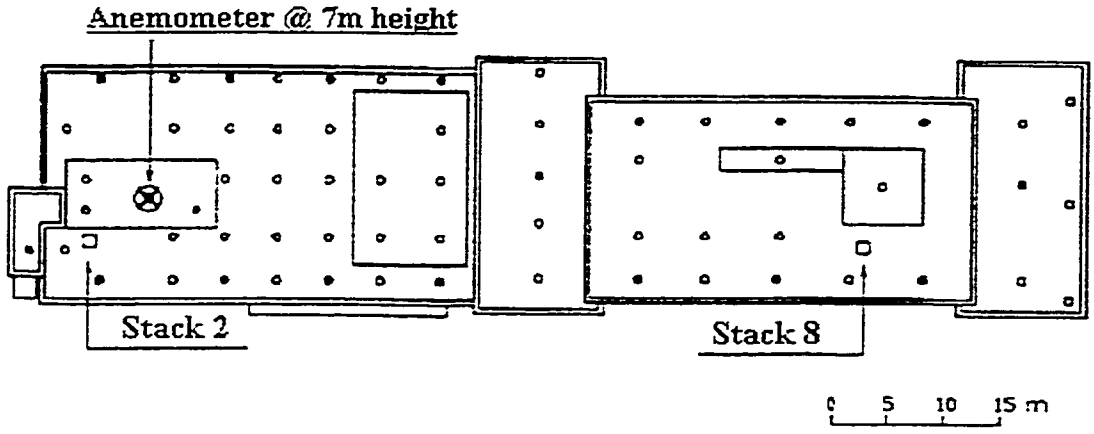

b) Roof plan of Fulmer Hall/Annex

Figure 4-31 Fulmer Hall/Annex building of Washington State University

shown in Figure 4-32. In the Hall Building case, results obtained with the isolated building and with upstream buildings, were examined for the same M-values. Note that the stack height was zero to allow comparison with the Hall Building results.

The dilution data obtained with the two models are plotted on logarithmic charts with the Wilson-Lamb model curves in Figure 4-32 and Figure 4-33 respectively. In general, dilution data acquired with the WSU model increases with increasing distance between stack and receptor. This compares well with results obtained for this building shape by Wilson and Chui (1985). In this case, the aspect ratio, L/H, is relatively large, so that only a small part of the roof is covered by the recirculation region. Since the exhaust vent is located outside this region, the plume is not affected by the strong vortices in this region. Consequently, for the lowest M value (M=0.1), dilution measured near the stack is only 50 – much lower than the value of 8000 obtained with the isolated Hall Building.

Dilution data obtained with the WSU model tend to increase with distance from the stack (neglecting the effect of plume rise near the stack at high M). However, for the Hall Building case, since both stack and receptors are located within the roof recirculation zone, the increase of dilution data with distance from stack is not as recognisable as that obtained with the WSU model. As shown in Figure 4-33, for the isolated Hall Building, dilution does not vary significantly with distance. On the other hand, dilution increases by as much as a factor of 10 for the WSU model.

In order to compare results for the WSU and Hall Building, it is useful to fit the ASHRAE (1997) D_{min} curve with the data by adjusting the distance dilution parameter, B_1. Note that as the M-value increased from 0.1 to 4, B_1 of the isolated Hall Building

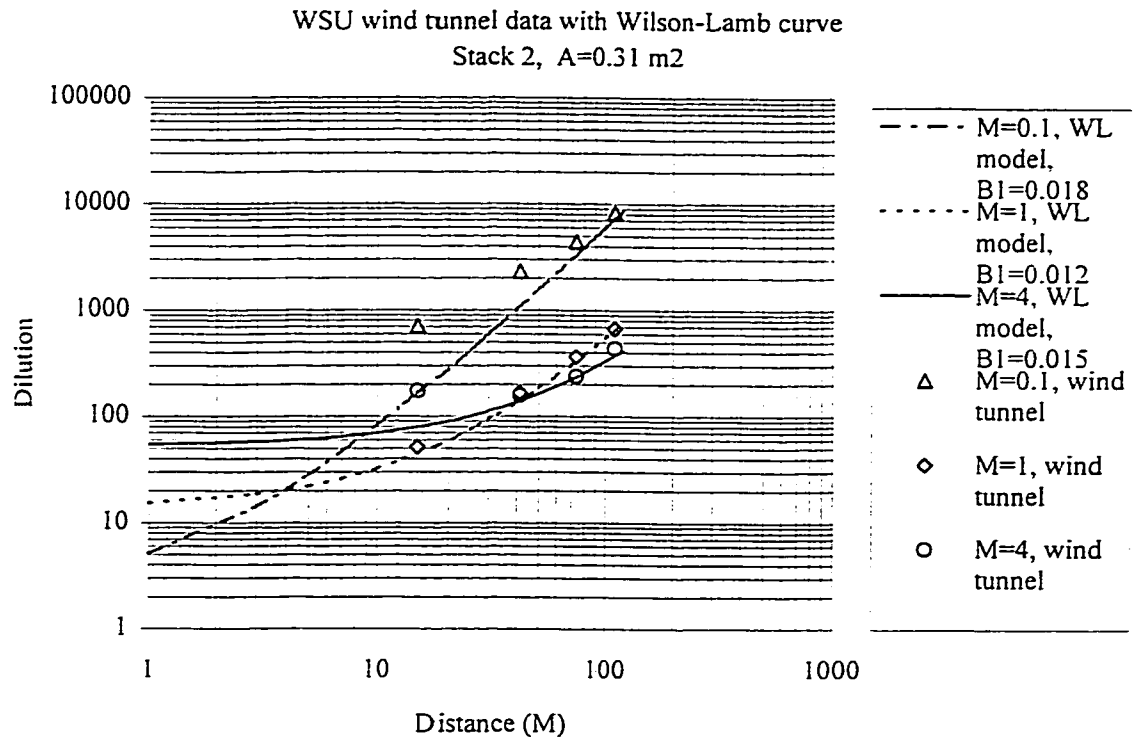

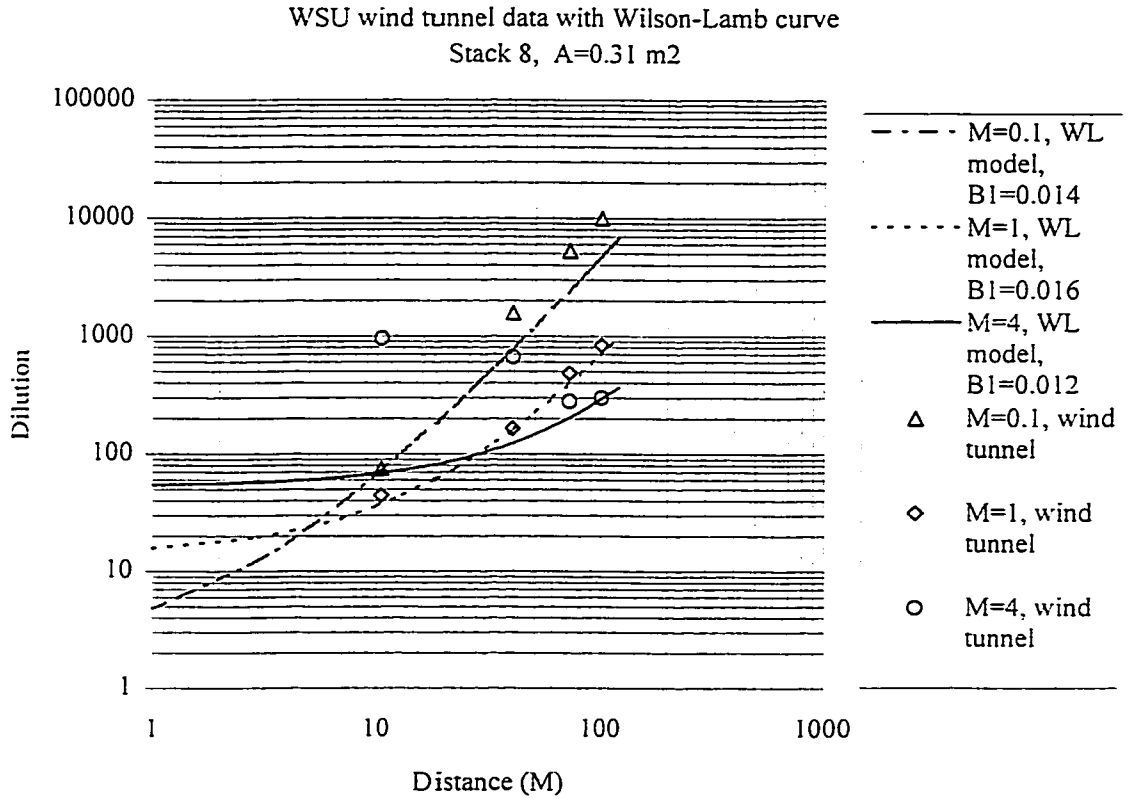

Figure 4-32 Wind tunnel data of WSU model with Wilson-Lamb curves

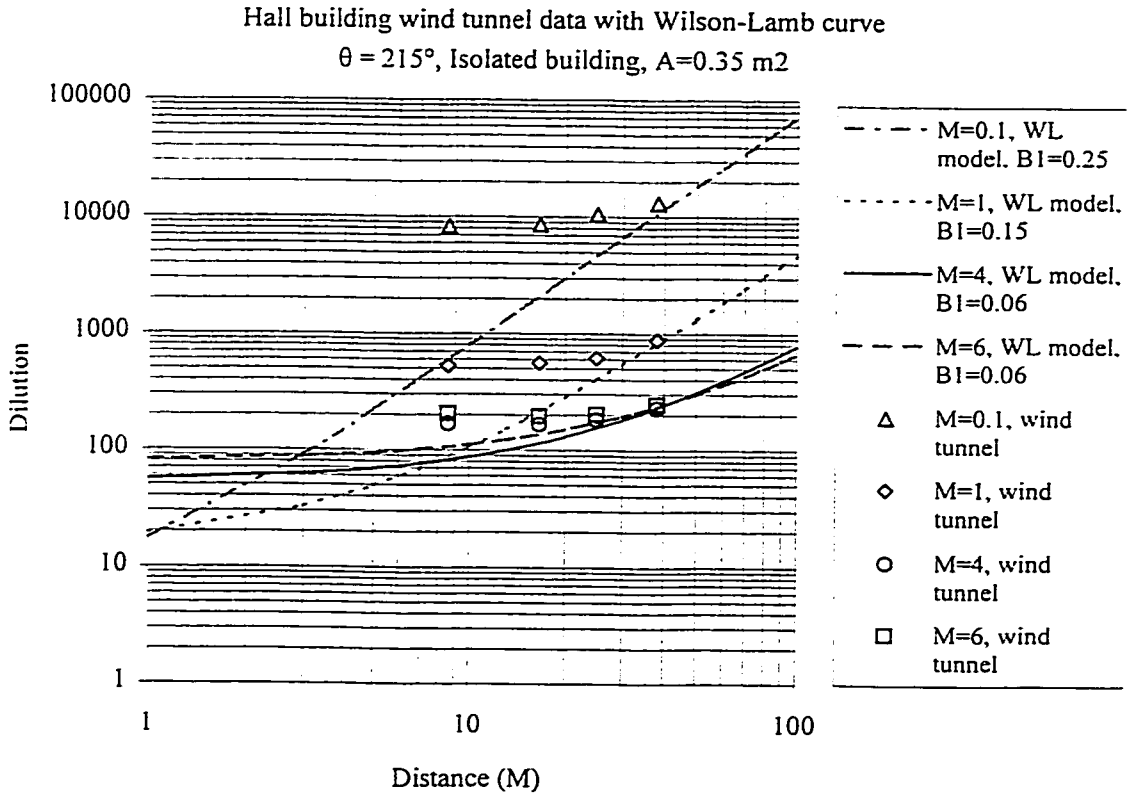

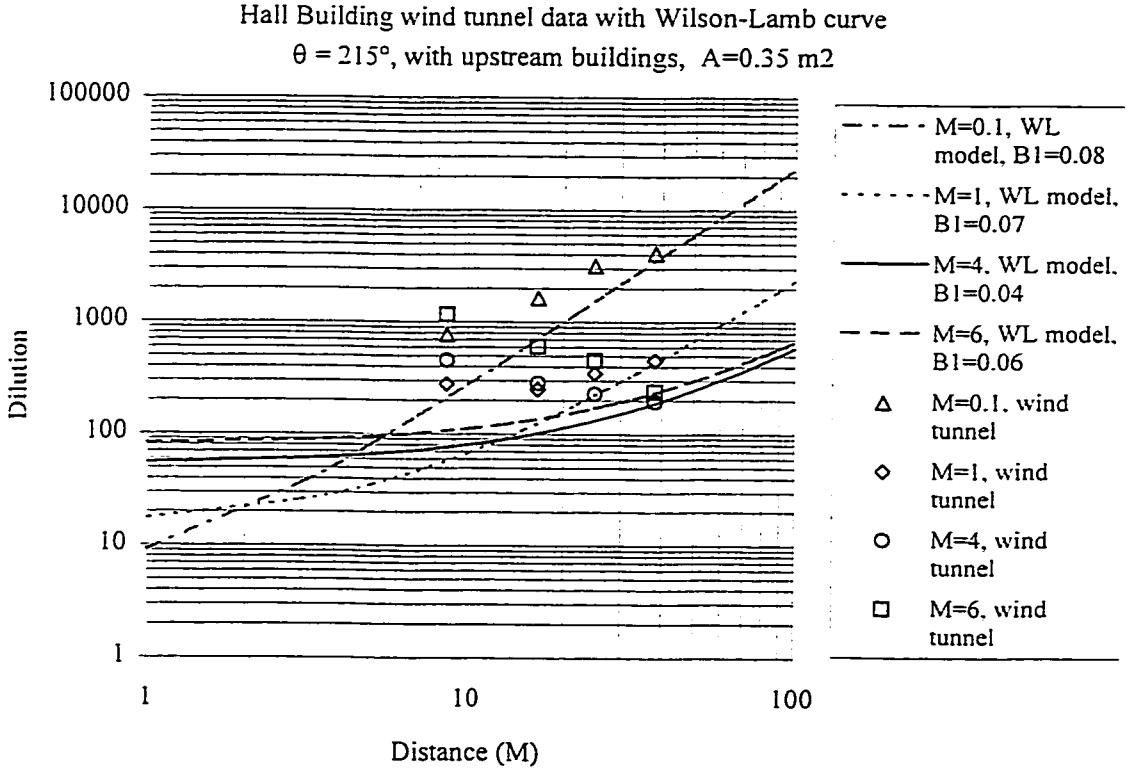

Figure 4-33 Wind tunnel data of Hall Building with Wilson-Lamb curves

decreased from 0.25 to 0.06. On the other hand, only slight differences of B_1 (i.e. 0.018 and 0.015) were found for the WSU model when the M-value changed from 0.1 to 4. Thus, B_1 appears independent of M for the WSU building but it is not independent of M for the isolated Hall Building.

4.3 Flow Visualisation

Although the tracer gas experiments have provided a considerable amount of information regarding the dispersion of building exhaust, the data do not provide insight into the instantaneous behavior of the plume. Furthermore, the data only describe the plume at roof level – characteristics in the vertical plane are not provided.

In order to investigate plume behavior more thoroughly, flow visualization experiments were conducted. The primary concern of the flow visualization study was to determine how M affects the plume behaviour both with and without upstream building models.

Wind speed and turbulence intensity profile measurements were also carried out before the flow visualization test to provide the preliminary estimation of the effect of upstream buildings on flow patterns above the Hall Building roof. Figure 4-34 shows the wind speed and turbulence intensity profiles. It is assumed that significant variations of the wind speed only occur within the separation zone. Thus, it is estimated that the heights of the recirculation region above the anemometer location are 15 mm and 10 mm for the isolated building and with upstream buildings respectively.

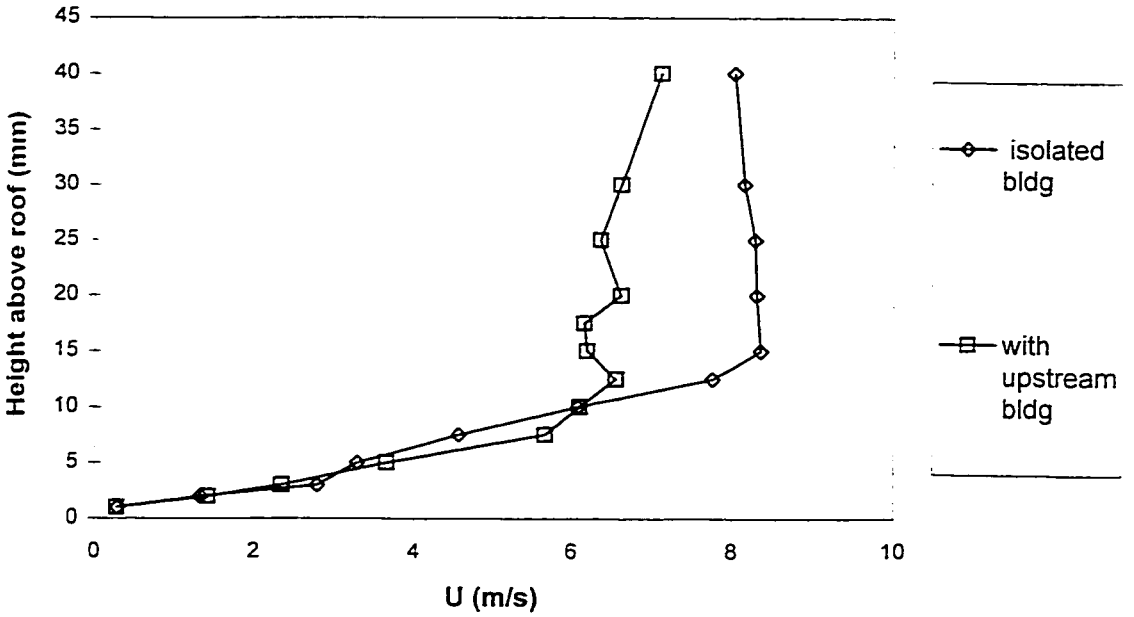

a) Wind speed profile

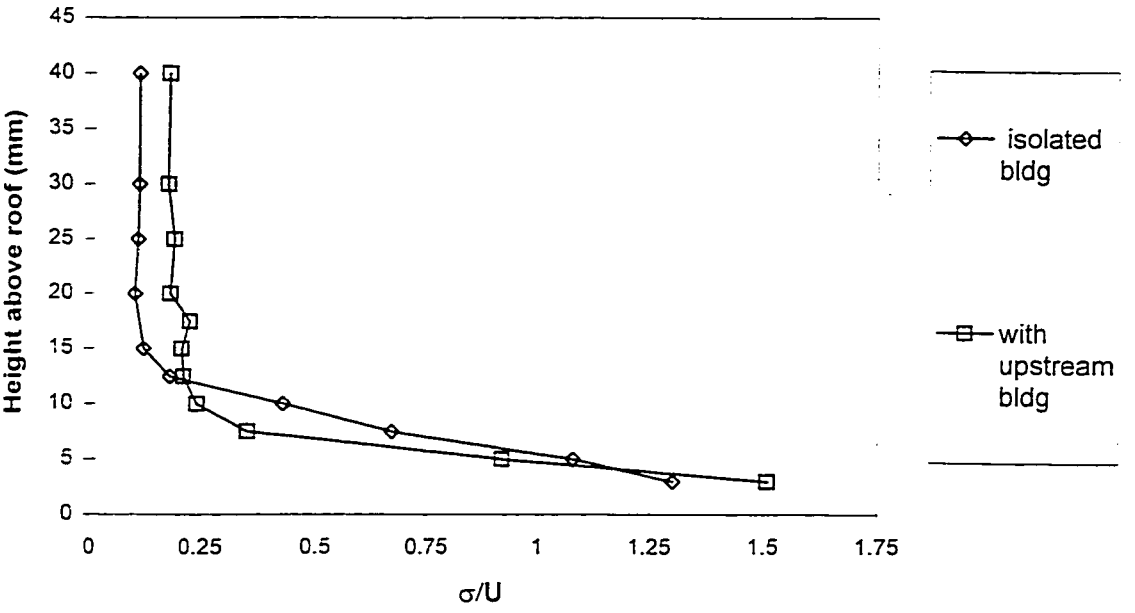

b) Turbulence intensity profile

Figure 4-34 Wind speed and turbulence intensity profiles above the Hall Building model measured at leading edge

The high turbulence intensity associated with the upstream buildings caused the instantaneous plume rise to vary significantly, as shown in Figure 4-35. For example, frame No.2 shows the plume making contact with a large portion of the roof while frame No.3 shows the plume well above the roof.

Figure 4-36 shows the digitized video images of smoke flux above the roof of the Hall Building model without and with the upstream buildings. The images clearly show that the recirculation region covers the entire roof for the isolated building. Since the smoke is trapped in the recirculation region, increasing the exhaust mass flow rate causes higher contaminate concentrations on the rooftop. This explains the significant reduction in dilution as M increases for the isolated building (see Figure 4-19).

It is interesting that with the isolated building, the smoke density is relatively high upwind of the stack, especially at low M. However, the inclusion of surrounding buildings significantly reduces the smoke density upwind of the stack. The lack of upwind excursions of the plume in the latter case may be due to the high levels of turbulence produced by the buildings. The wind profile measurements above the roof level, as shown in Figure 4-34, indicate that, with upstream buildings, the free-stream turbulence at h>15 mm (7.5 m full-scale) becomes notably higher than for the isolated building case. However, note that the turbulence levels in both cases are similar and relatively high for heights less than 15 mm. Previous research has shown that increasing the level of free-stream turbulence promotes intermittent reattachment of the separated shear layers near the leading edge of rectangular prisms [Saathoff and Melbourne (1997)]. This shear layer behavior may limit the upwind movement of the plume when the upstream buildings are present.

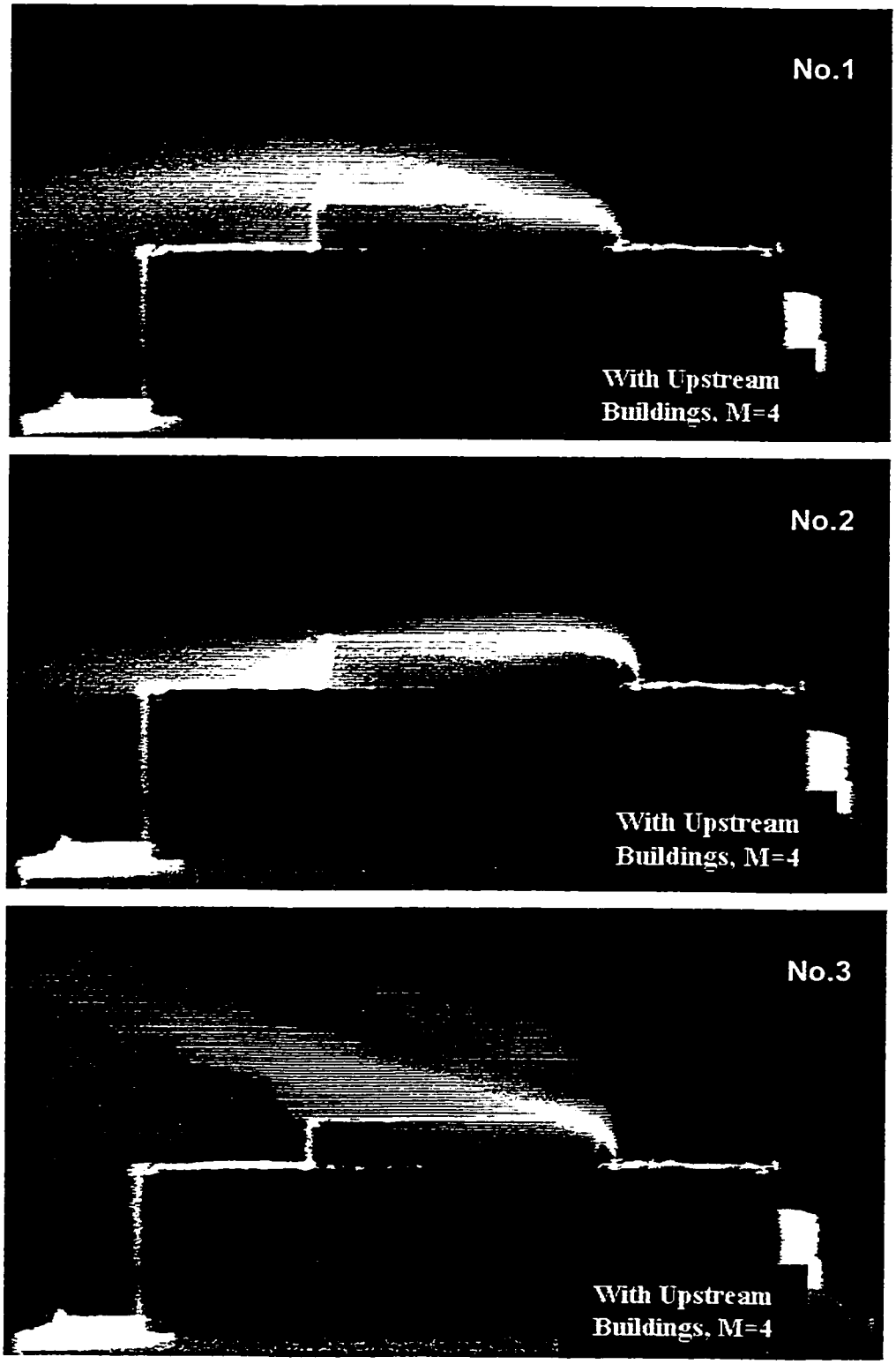

Figure 4-35 Video images showing the effect of upstream buildings with M=4

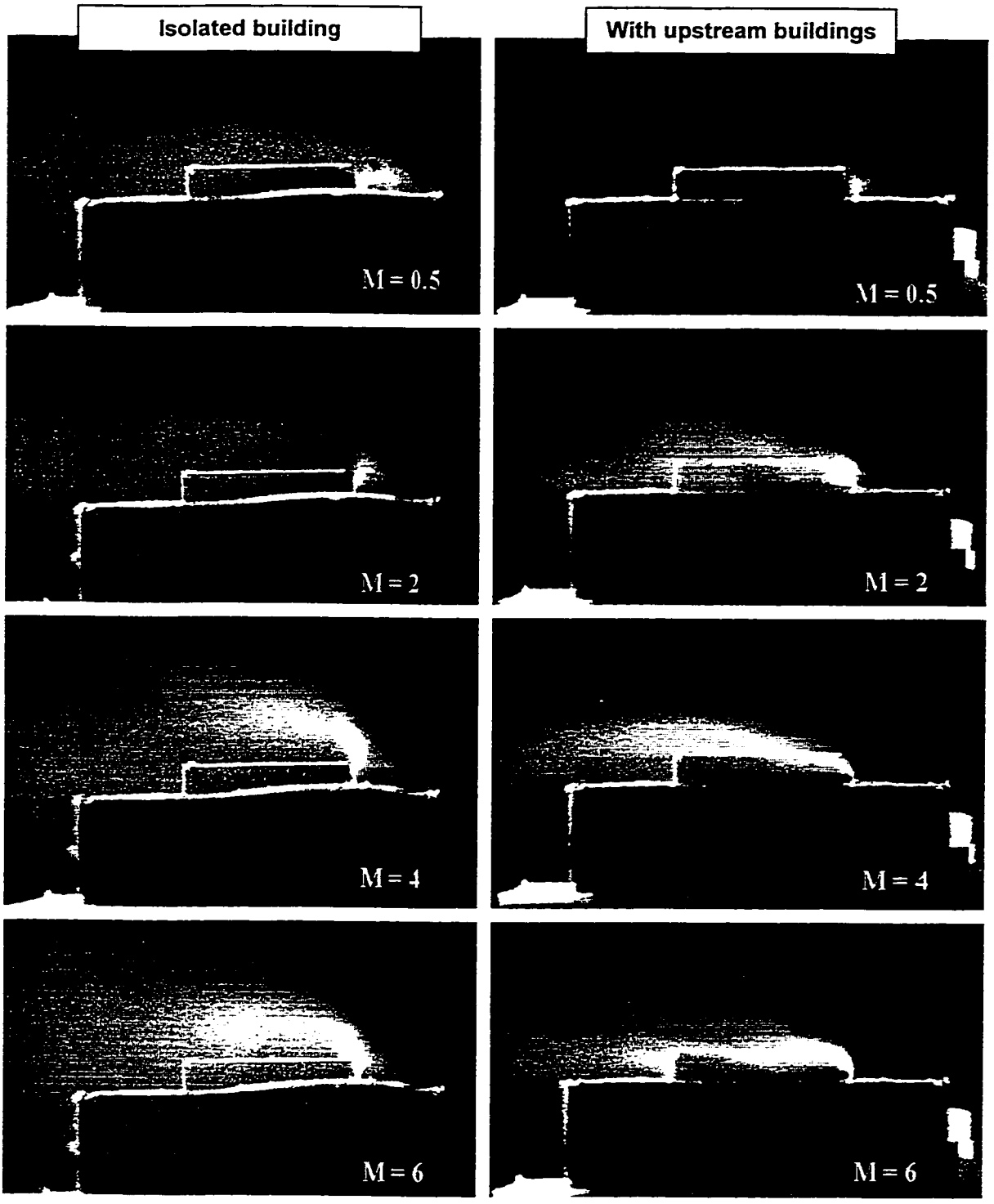

Figure 4-36 **Comparison of flow patterns for isolated building and with upstream buildings for different M-values**

The height of the recirculation zone, H_c, fluctuates. As Figure 4-36 indicates, regardless of the value of M, the mean height is approximately 30 mm for the isolated building and 25 mm when surrounding buildings are included. The estimated height from the images compares well with the velocity profile. Note that the previously estimated heights from the wind speed profile (Figure 4-34) are at the anemometer location, which is slightly upwind of the stack (see Figure 3-5).

CHAPTER 5

CONCLUSIONS AND SUGGESTIONS FOR FUTURE WORK

In the present study, results of four full-scale tracer gas tests performed on the roof of the Hall Building of Concordia University have been analyzed. Dilution data were used to evaluate the accuracy of ASHRAE dispersion models and the accuracy of a wind tunnel simulation. Numerous wind tunnel experiments have also been carried out to investigate the effects of exhaust momentum ratio, stack height, stack location and building configuration. As a consequence, a significant amount of experimental data regarding the diffusion of building exhaust around a cubical building in an urban environment has been acquired. In addition, flow visualization tests have been conducted to examine the effect of upwind building models on the flow pattern around the Hall Building model. The study has six major findings, which can be summarized as follows, along with some relevant suggestions for future works, where appropriate:

1. ASHRAE diffusion equations have been evaluated with field data. In general, the Halitsky model tends to provide conservative dilution estimates with the recommended model parameter α set at a value of 2. However, when the α-value was adjusted to 5, the model provided better estimates of D_{min}. Therefore, determining the appropriate α-value is very important when applying Halitsky model in dilution estimations. The Wilson-Chui and Wilson-Lamb models generally give reasonable minimum dilution predictions, except that the Wilson-Chui model overestimates the initial dilution component when the exhaust momentum ratio is

high (M>4). In comparison, the Wilson-Chui model with the revised initial dilution formula used in the Wilson-Lamb model is preferred because of its simpler format and moderately conservative prediction for an urban environment.

2. Wind tunnel data generally compared well with the field data. In most of the cases, the wind tunnel dilution values were within a factor of 2 of full-scale data, which is acceptable in this type of measurements. The agreement of wind tunnel and full-scale data improves as the distance from the stack increases. Considering the variation of the field M-values over the 15-min sampling period, it was not possible to compare field and wind tunnel data for specific M-values. Future field tests should use a shorter sampling period of the order of 5 minutes to allow the direct comparison with wind tunnel data.

3. Wind tunnel tests carried out with upstream buildings showed that the plume behavior is dramatically affected by the exhaust momentum ratio. Dilution values decreased significantly when the momentum ratio reached a critical value of approximately 3.5. This phenomenon appears to be dependent on stack location and upstream conditions and thus may not be typical of cubical buildings. Nevertheless, these results demonstrate the complexity of the flow around the Hall Building and the difficulties in developing generalized dispersion models for estimating diffusion of building exhaust.

4. As a consequence of increasing the stack height, higher rooftop dilution values were obtained near the stack. However, the effect of stack height diminished as the distance from the stack increased. On the other hand, stack locations had little

influence on dilution values. Further investigations on these topics still need to be done. In particular, the experiments should be carried out for a number of wind directions and building shapes.

5. The building configuration should be taken into account when determining the stack design parameters. It was found in the present study that, for the isolated Hall Building model, as the exhaust momentum ratio increases to 4, dilution values decrease at all locations on the rooftop. Only a very slight increase was found when the M-value was raised to 6. Obviously, this fact suggests that, for an isolated cubic-shape building with a flush vent or short stack, increasing the exhaust velocity may not significantly reduce the rooftop contaminant concentrations.

6. The results of flow visualization experiments showed good agreement with previous findings concerning the flow patterns on the rooftop of an isolated cubic-shape building. Plume behavior becomes complicated and unpredictable with the existence of upstream buildings. Digital image analysis could be carried out in the future to provide more detailed information regarding the behavior of plumes emitted from roof top stacks.

REFERENCES

Allwine, K., Meroney, R. and Peterka, J. (1980), "Rancho Seco building wake effects on atmospheric diffusion: simulation in a meteorological wind tunnel", NUREG/CR-1286.

ASHRAE (1993) Chapter 14, Airflow around buildings, *ASHRAE handbook--1993 fundamentals*, American Society of Heating, Refrig. and Air-Cond. Eng., Inc., Atlanta.

ASHRAE (1997) Chapter 15, Airflow around buildings, *ASHRAE handbook--1997 fundamentals*, American Society of Heating, Refrig. and Air-Cond. Eng., Inc., Atlanta.

Bächlin, W., Theurer, W. and Plate, E.J. (1991), "Wind field and dispersion in a built-up area – a comparison between field measurements and wind tunnel data", *Atmospheric Environment*, Vol. 25A, No. 7, pp.1135-1142.

Castro, I.P. and Robins, A.G. (1977) "The flow around a surface-mounted cube in uniform and turbulent streams", *Journal of Fluid Mechanics,* Vol. 79, pp. 307-335.

Georgakis, K., Smith, J., Goodfellow, H. and Pye, J. (1995) "Review and evaluation of models estimating the minimum atmospheric dilution of gases exhausted near buildings", *Journal of the Air & Waste Management Assoc.*, Vol. 45, pp. 722-729.

Halitsky, J. (1963) "Gas diffusion near buildings", *ASHRAE Transactions*, Vol. 69, pp. 464-484.

Halitsky, J. (1990) "Calculation of minimum available atmospheric dilution downwind of building exhausts", *ASHRAE Transactions*, Vol. 96, pp.46-52.

Higson, H. L., Griffiths, R.F., Jones, C.D. and Hall, D.J. (1994) "Concentration measurements around an isolated building: a comparison between wind tunnel and field data", *Atmospheric Environment*, Vol. 28, No. 11, pp. 1827-1836.

Hosker, R.P. (1979) "Empirical estimation of wake cavity size behind block-type structures", *Fouth Symposium on Turbulence, Diffusion and Air Pollution*, Jan.15-18, pp. 603-609.

Huber, A.H. and Snyder, W.H. (1982), "Wind tunnel investigation of the effects of a rectangular-shaped building on dispersion of effluents from short adjacent stacks", *Atmospheric Environment*, Vol. 28, No. 12, pp. 2837-2848.

Hunt, J.C.R., Abell, C.J., Peterka, J.A., Woo, H. (1978), "Kinematical studies of the flows around free or surface-mounted obstacles", *Journal of Fluid Mechanics*, Vol. 86, Part 1, pp. 179-200.

Kot, S.C. (1989), "Numerical modelling of contaminant dispersion around buildings", *Building and Environment*, Vol. 24, No.1, pp. 33-37.

Lamb, B. and Cronn, D. (1986), "Fume hood exhaust reentry into a chemistry building", Journal of the American Industrial Hygiene Association, Vol. 47(2), pp. 115-123.

Lam, K.S., Kot, S.C., Fung, K.W. and Ma, R.Y.P., (1985) "A field validation of roof-top dispersion formula in an urban centre", *Journal of Wind Engineering and Industrial Aerodynamics*, Vol. 21 pp.295-305.

Lam, K.S. and Kot, S.C. (1993) "Field study of roof top dispersion in an urban area", 3rd Asia-Pacific Symposium on Wind Engineering, Dec. 13-15, Hong Kong.

Lee, J.T., Call, D.L., Lawson Jr., R.E., Clements, W.E. and Hoard, D.E. (1988) "A video image analysis system for concentration measurements and flow visualization in building wakes", Progress Report, November, Los Alamos National Laboratory, Los Alamos, USA.

Li, W.W. and Meroney, R.N. (1983) Gas dispersion near a cubical model building", *Journal of Wind Engineering and Ind. Aerodynamics*, Vol. 12, pp. 15-23.

Martin, J.E. (1965), "The correlation of wind tunnel and field measurements of gas diffusion using krypton-85 as a tracer", Ph.D. Thesis, Dept. of Health Sciences, University of Michigan, Ann Arbor, USA.

Martinuzze, R. and Tropea, C. (1993), "The flow around surface-mounted, prismatic obstacles placed in a fully developed channel flow", *Journal of Fluids Engineering*, Vol. 115/85.

Meroney, R.N. (1982), "Turbulent diffusion near buildings", Engineering Meteorology, Elsevier, Amsterdam.

Munn, R.E. and Cole, A.F.W. (1967), "Turbulence and diffusion in the wake of a building", *Atmospheric Environment*, Part 1, pp. 33-43.

Ogawa, Y., Oikawa, S. and Uehara, K., (1983) "Field and wind tunnel study of the flow and diffusion around a model cube, I -- Flow measurements, II -- Nearfield and cube surface flow and concentration patterns", *Atmospheric Environment*, 17, pp. 1145-1171.

Olivari, D. and Babuska, V. (1990), "Use of video camera recording and digital image processing for the analysis of pollutant dispersion in the near wake of a cube", *Journal of Wind Engineering and Industrial Aerodynamics*, 34 (1990) 291-301.

Pasquill F. (1962), Atmospheric Diffusion, The Dispersion of Windborne Material from Industrial and Other Sources, D. Van Nostrand Company, Ltd., London, England.

Perera, M.D., Tull, R.G., White, M.K. and Walker, R.R. (1991), "Assessing Intake contamination from atmospheric dispersion of building exhaust", Proceedings of the 12th AIVC Conference, Ottawa, pp. 347-357.

Petersen, R.L. (1986), "Wind tunnel investigation on the effect of platform-type structures on dispersion of effluents from short stacks", *Journal of the Air Pollution Control Association*, 36, pp. 1347-1352.

Petersen, R.L. and Wilson, D.J. (1989), "Analytical versus wind tunnel determined concentrations due to laboratory exhaust", *ASHRAE Transactions*, 95(2): pp. 729-736.

Petersen, R.L. and Ratcliff, M.A. (1991), "An objective approach to laboratory stack design", *ASHRAE Transactions*, Vol. 97, No. 2.

Ramsdell Jr., J.V. and Fosmire, C.J. (1997), "Estimating concentrations in plumes released in the vicinity of buildings: model development", *Atmospheric Environment*, 32, 1663-1689.

S-2.1, r.15 (1994) "Regulation respecting the quality of the work environment", Quebec.

Saathoff P.J. and Melbourne W.H., (1997) "Effects of free-stream turbulence on surface pressure fluctuations in a separation bubble", *Journal of Fluid Mechanics*, Vol. 337, pp. 1-24.

Saathoff, P.J. and Stathopoulos, T., (1997) "Dispersion of exhaust gases from roof level stacks and vents on a laboratory building--Discussion", *Atmospheric Environment*, 31. 1087-1089.

Saathoff, P.J., Wu, H. and Stathopoulos, T., (1996) "Dilution of exhaust from rooftop stacks -- Comparison of wind tunnel data with full-scale measurements", *Proc. of 9th Joint Conf. On Applications of Air Pollution Meteorology*, Amer. Meteorological Soc. -- Air & Waste Management Assoc., Atlanta 341-345.

Schulman, L.L. and Scire, J.S. (1991), "The effect of stack height exhaust speed, and wind direction on concentrations from a rooftop stack", *ASHRAE Transactions*, Vol. 97, Part 2.

Schuyler, G.D. and Turner, G.G., (1989) "Comparison of wind tunnel test results with empirical exhaust dilution factors", *ASHRAE Transactions*, 95(2): pp. 737-744.

Seinfeld J.H. (1975), Air Pollution, Physical and Chemical Fundamentals, McGraw-Hill, Inc., New York, United States.

Selvam, R.P. and Huber, A.H. (1995), "Computer modelling of pollutant dispersion around buildings: current status", Proceedings of the 9th Int. Conf. On Wind Engrg., New Delhi, India, pp. 594-605.

Start, G., Gate, J., Dickson, C., Ricks, N., Ackerman, G. and Sagendorf, J. (1977), "Rancho Seco building wake effects on atmospheric diffusion", NOAA Tech. Memo. ERL ARL-69.

Thompson, R.S. (1991), "Concentrations from above-roof releases of laboratory exhausts – a wind tunnel study", *ASHRAE Transactions*, Vol. 97, Part 2

Turner, D.B. (1994), Workbook of Atmospheric Dispersion Estimates, 2nd Ed., CRC Press.

Wilson, D.J. (1979), "Flow patterns over flat-roofed buildings and application to exhaust stack design", *ASHRAE Transactions*, Vol. 85, Part 2.

Wilson, D.J. (1983), "A design procedure for estimating air intake contamination from nearby exhaust vents", *ASHRAE Transactions*, Vol. 88, Part 2.

Wilson, D.J. (1997), "Dispersion of exhaust gases from roof level stacks and vents on a laboratory building—Author's Reply", *Atmospheric Environment*, 31, 1091-1093.

Wilson, D.J. and Britter, R.E. (1982), "Estimates of building surface concentrations from nearby sources", *Atmospheric Environment*, 16, No. 11, pp. 2631-2646.

Wilson, D.J. and Winkel, G. (1982), "The effect of varying exhaust stack height on contaminant concentration at roof level", *ASHRAE Transactions*, Vol. 88, Part 1.

Wilson, D.J. and Chui, E. (1985), "Influence of exhaust velocity and wind incidence angle on dilution from roof vents", *ASHRAE Transactions*, 91(2B) 1693-1706.

Wilson, D.J. and Chui, E., (1987) "Effect of Turbulence from Upwind Buildings on Dilution of Exhaust Gases", *ASHRAE Transactions*, 93(2), 2186-2197.

Wilson, D.J. and Lamb, B., (1994) "Dispersion of exhaust gases from roof level stacks and vents on a laboratory building", *Atmospheric Environment*, 28, 3099-3111.

Wilson, D.J. and Chui, E.H. (1994) "Influence of building size on rooftop dispersion of exhaust gas", Atmospheric Environment, Vol. 28, No. 14. pp. 2325-2334.

Wilson, D.J. (1995), Concentration Fluctuations and Averaging Time in Vapor Clouds, Center for Chemical Process Safety of the American Institute of Chemical Engineers, New York, United States.

Wu, G., Higuchi, K. and Meroney, R.N. (1991), "Application of digital image processing in wind engineering", 8th International Conference on Wind Engineering, London, Ontario.

APPENDIX A

DESIGN OF AUTOMATIC AIR SAMPLERS

The automatic air samplers used in the Hall Building field test shown in Figure A1, were designed and fabricated at the Institut de recherche en santé et en sécurité du travail du Québec (IRSST). The basic function of the air sampler is to collect the air samples continuously at predetermined time intervals. The air samples were collected in 1-litre bags (Cali-5-Bond) using a low-flow sampling pump (MSA C-210). The bags were connected with the sampling pump by polyethylene tubes through a distributor. Each bag had a LUER type valve, which is normally closed so that no sample air would be lost if the tube was unintentionally disconnected during the test.

Preliminary tests were carried out to make certain that no sulfur hexafluoride (SF_6) would adhere to the bag material. Furthermore, the bags were evacuated before each test to prevent contamination of the air samples.

Figure A2 shows the manual programming unit, which controlled the samplers by radio signals. It was used to set up the sampling period and waiting time between samples and to start the samplers. The information provided by the programming unit includes: the number of bags being used, the sampling time, the elapsed sampling time and the current drawn by the sampling pump.

The power supply of the air sampler can be either 110/120 V AC or a 12 V gel-acid type rechargeable battery.

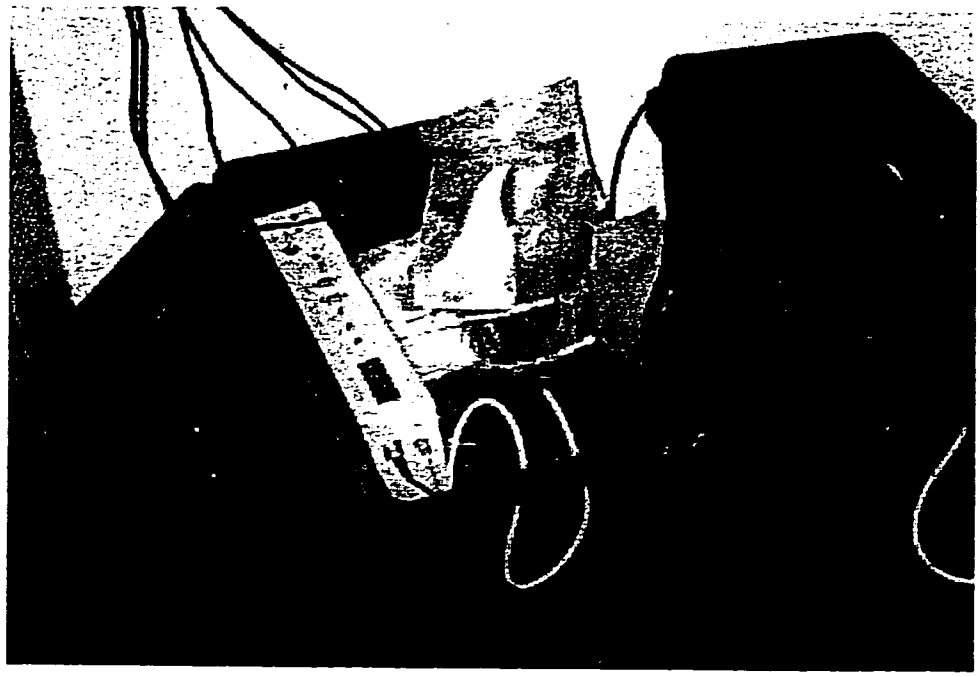

Figure A1 The automatic air samplers with sample bags attached

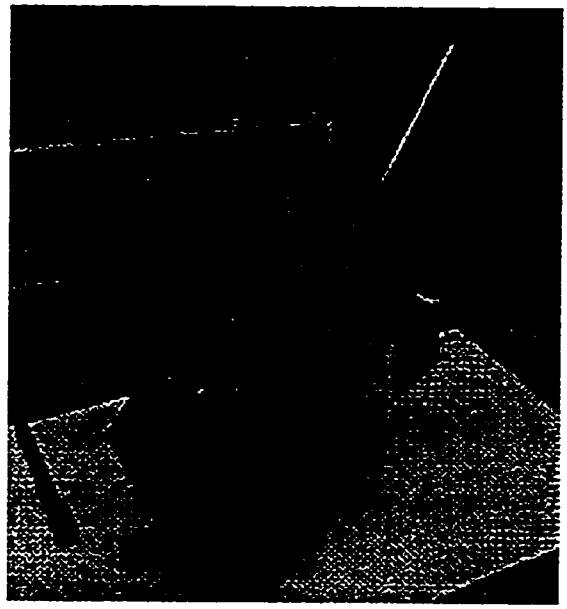

Figure A2 The manual programming unit

APPENDIX B

CALIBRATIONS

The gas chromatograph and flow control meters were calibrated periodically during the present study to ensure the accuracy of experimental data.

1) Flow control meters

Four Matheson flow control meters with different ranges and gas specifications were used in the study:

- 0 – 10 SLPM (liter per minute) for both N2 and SF6;
- 0 – 2 SLPM (liter per minute) for N2;
- 0 – 100 SCCM (cc per minute) for SF6;
- 0 – 1000 SCCM (cc per minute) for N2.

A Hastings Mini-Flo Calibrator Model HBA-1A was employed to calibrate the flow control meters. Figure B1 shows a sample spreadsheet of the flow control meter calibration.

2) Gas chromatograph

Tracer gas concentrations were measured with a Varian Gas Chromatograph (GC). The GC was calibrated approximately every 6 months. A calibration curve showing SF_6 concentration as a function of the GC reading is shown in Figure B2 A wide range of SF_6

concentration was obtained by mixing a flow of a certified SF_6-N_2 mixture (1090 ppb SF_6) with N_2 from another cylinder. The SF6 and N2 were fed into the system through two branches of a Y-shape connector respectively. Since the gases were precisely controlled by the flow control meters, the concentration of the gas mixture could be calculated. A series of different concentration gases were measured.

The GC readings were plotted with the corresponding actual concentration values, as shown in Figure B2 to B4. The calibration curves are actually the trendlines generated using Microsoft Excel on the basis of the calibration data series. Note that no calibration data were obtained within the lower part range (i.e. GC reading less than 3) as shown in Figure B2. More tests were performed afterwards to supplement the calibration data series, as plotted in Figure B3. Figure B4 shows the most recent calibration curve, which is composed of three parts as described below the figure.

0 - 10 SLPM					
Reading 5, V=500cc		Reading 6, V=500cc		Reading 7, V=500cc	
Time (S)	Actual Flow (l/m)	Time (S)	Actual Flow (l/m)	Time (S)	Actual Flow (l/m)
5.78	5.190	5.24	5.725	4.25	7.059
5.88	5.102	5.06	5.929	4.13	7.264
5.87	5.111	5.15	5.825	4.36	6.881
5.8	5.172	5.24	5.725	4.2	7.143
5.97	5.025	4.94	6.073	4.43	6.772
Average=	5.120	Average=	5.855	Average=	7.024
Factor =	1.024	Factor =	0.976	Factor =	1.003

0 - 10 SLPM					
Reading 8, V=800cc		Reading 9, V=800cc		Reading 10, V=800cc	
Time (S)	Actual Flow (l/m)	Time (S)	Actual Flow (l/m)	Time (S)	Actual Flow (l/m)
5.91	8.122	5.25	9.143	4.82	9.959
5.91	8.122	5.25	9.143	4.92	9.756
5.97	8.040	5.31	9.040	4.81	9.979
5.98	8.027	5.27	9.108	4.99	9.619
5.98	8.027	5.31	9.040	4.84	9.917
Average=	8.067	Average=	9.095	Average=	9.846
Factor =	1.008	Factor =	1.011	Factor =	0.985

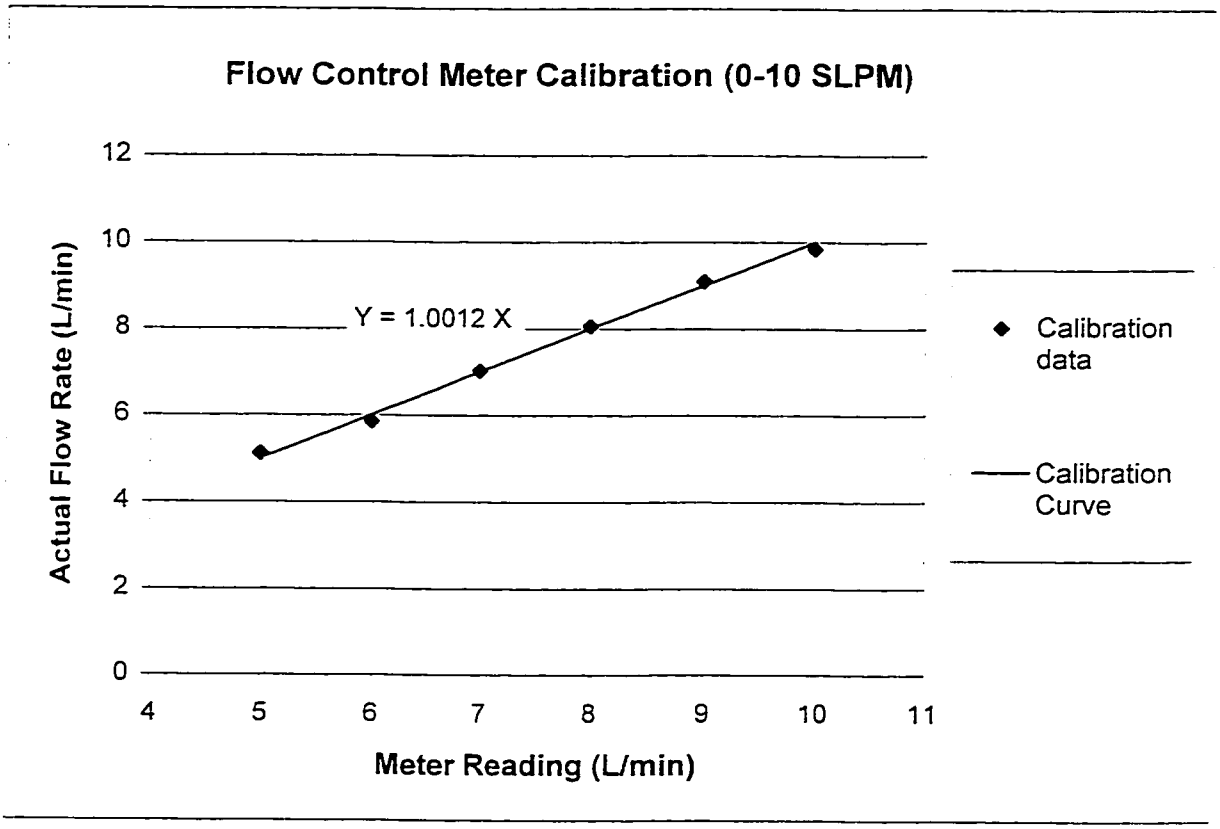

Figure B1 A sample spreadsheet of the flow control meter calibration

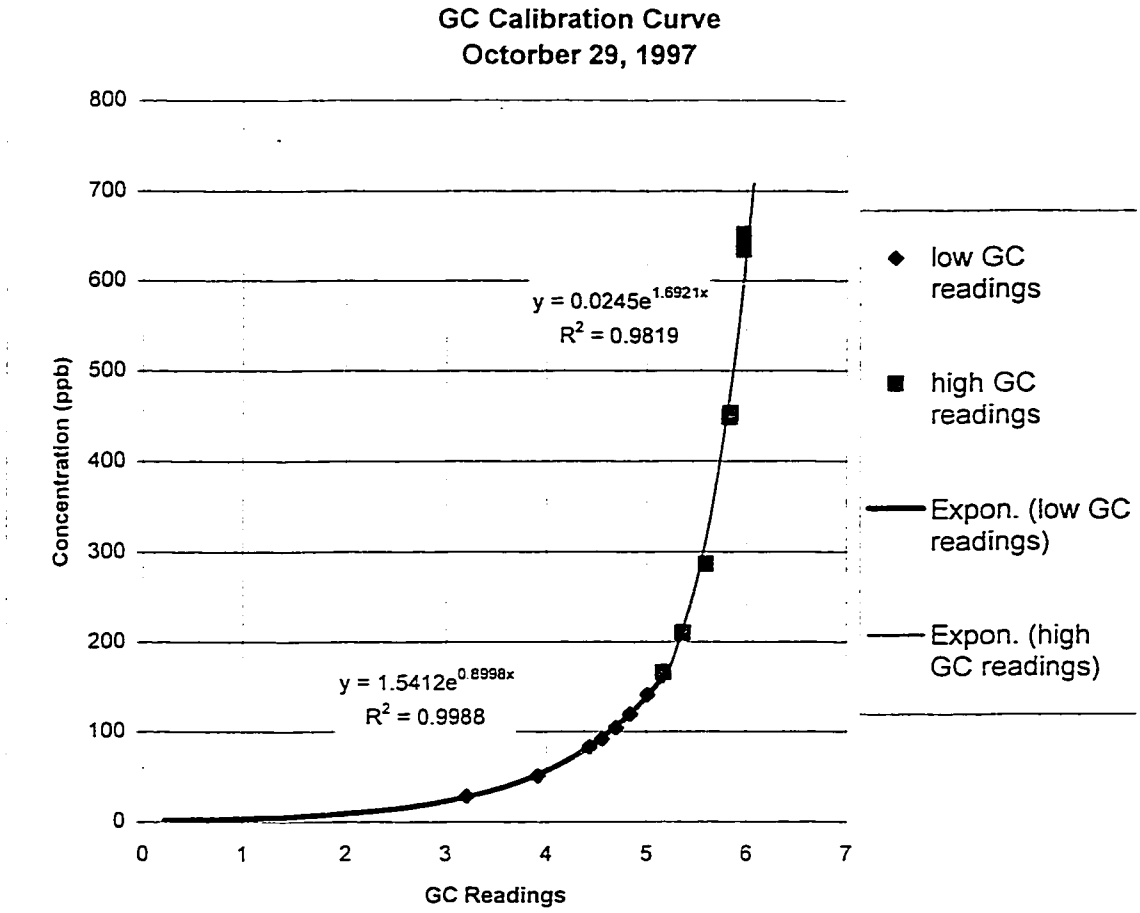

Figure B2 GC calibration curve of October 29, 1997

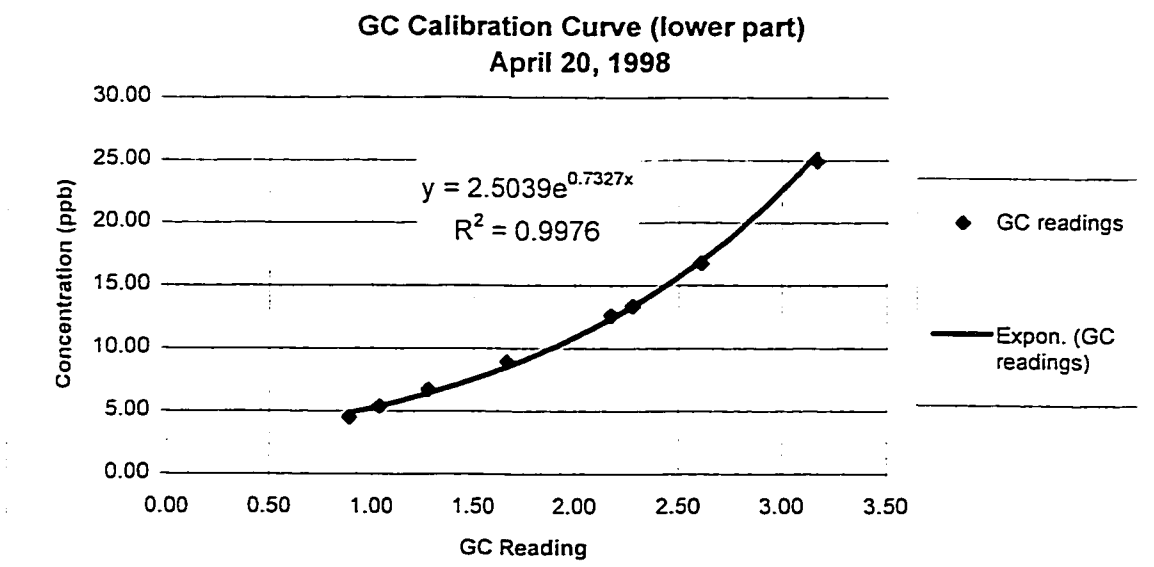

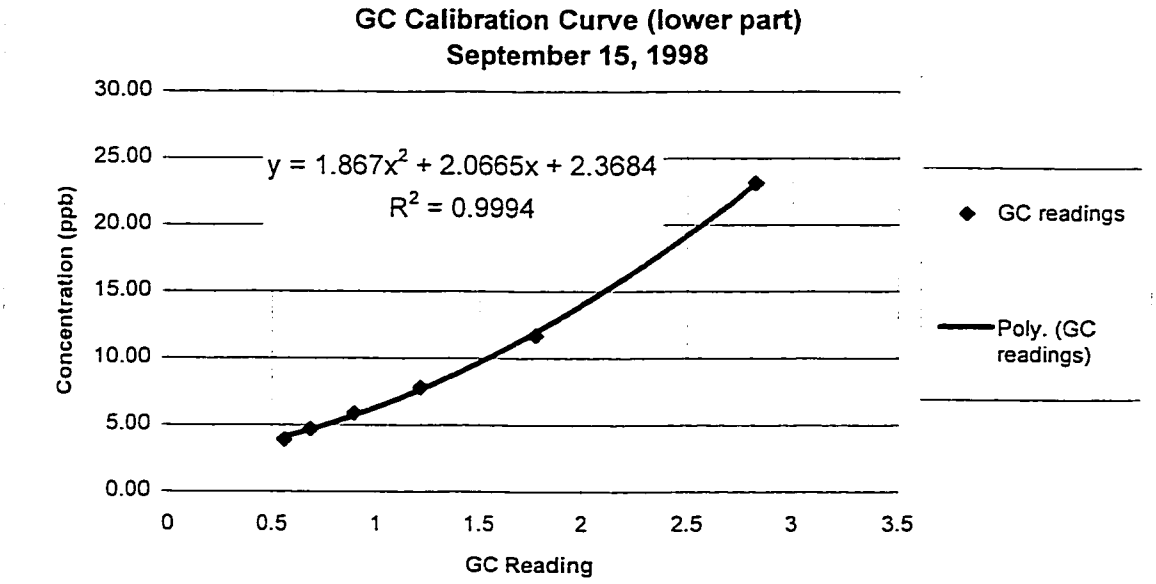

Figure B3 GC calibration curve (lower part) of April 20 and September 15, 1998

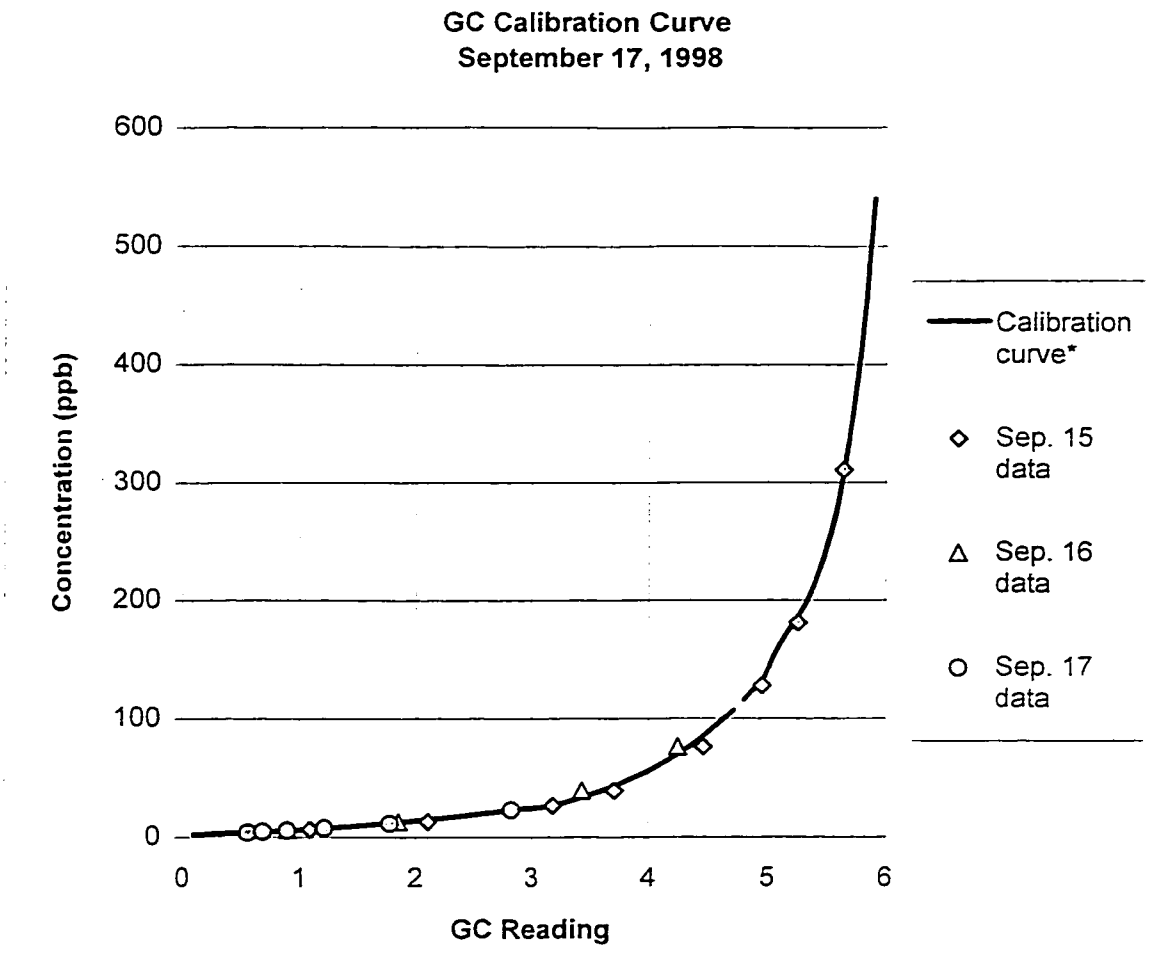

* Note: If $x \leq 3.0$, then $y=1.867x^2+2.0665x+2.3684$;

If $3<x\leq 5$, then $y=1.5412e^{0.8988x}$;

If $x>5.0$, then $y=234846-189450x+57228.6x^2-7673.63x^3+385.665x^4$;

Where x is GC Reading, y is calculated concentration.

Figure B4 GC calibration curve of September 17, 1998